EFFECT OF ALTERNATIVE FUELS ON THE MICROSTRUCTURE AND STRENGTH DEVELOPMENT OF CEMENT PASTE

by

SOROUR SEMSARI PARAPARI

Submitted to the Graduate School of Engineering and Natural Sciences

in partial fulfillment of

the requirements for the degree of

Master of Science

Sabancı University

August 2015

EFFECT OF ALTERNATIVE FUELS ON THE MICROSTRUCTURE AND STRENGTH DEVELOPMENT OF CEMENT PASTE

APPROVED BY:

Prof. Dr. Mehmet Ali Gülgün
(Thesis Supervisor)

Assoc. Prof. Dr. Melih Papila
(Thesis co-advisor)

Assoc. Prof. Dr. Cleva Ow-Yang

Asst. Prof. Dr. Zeynep Başaran Bundur

Assoc. Prof. Dr. Burç Mısırlıoğlu

DATE OF APPROVAL: 29.07.2015

Bütün sevdiklərimə…

EFFECT OF ALTERNATIVE FUELS ON THE MICROSTRUCTURE AND STRENGTH DEVELOPMENT OF CEMENT PASTE

Sorour Semsari Parapari

Materials Science and Nano-Engineering, MSc Thesis, 2015

Supervisor: Prof. Mehmet Ali Gülgün

Keywords: Cement, Alternative Fuels, Phase distribution, Strength development

Abstract

The object of this study was to investigate the effect of using alternative fuels in the cement production process on the microstructure and strength development of the output cement. Five different samples were produced using different alternative fuels in a cement kiln. The samples were prepared respectively with all kinds of alternative fuels (in the dirty kiln), petrocoke (in the clean kiln), waste plastics, a mixture of waste plastics and sewage sludge and lastly sewage sludge.

The microstructure of the cement clinkers was studied with scanning electron microscopy (SEM). The results showed that the distribution of main phases of alite, belite, aluminate and ferrite varies in the samples prepared with different fuels. The alite/belite ratio varied between 5.2 and 1.5 among the samples. The phase distribution measurements using x-ray diffractometry (XRD) showed good agreement with the SEM results. Chemical composition of the clinkers was analyzed using energy dispersive x-ray spectroscopy (EDS) and x-ray fluorescence (XRF) methods. The sulfur and phosphorous amounts were higher in the samples with higher belite content.

Hydrated cement paste samples were prepared with water to cement ratio of 0.3 and 0.5 by mass. The strength of the hydrated cement samples was measured in the compression tests for several curing ages up to 28 days. Results showed that alternative

fuel usage affected the compressive strength values of hydrated cement samples, particularly the sample produced with all alternative fuels. The reactivity of hydrated phases was investigated using SEM and XRD analyses.

ALTERNATIF YAKITLARIN ÇIMENTO PASTASI MIKROYAPISI VE MUKAVEMET GELIŞMESINE ETKILERI

Sorour Semsari Parapari

Malzeme bilimi ve nano-mühendisliği, MSc Tezi, 2015

Danışman: Prof. Mehmet Ali Gülgün

Anahtar kelimeler: Çimento, Alternatif Yakıtlar, Faz Dağıtımı, Mukavemet Gelişmesi

Özet

Bu araştırmanın amacı, çimento üretiminde kullanılan alternatif yakıtların çimento mikroyapısı ve mukavemet gelişmesinde etkilerini incelemekti. Beş numune farklı alternatif yakıtlar kullanılarak çimento fırınında üretilmiştir. Bu numuneler sırasıyla her türlü alternatif yakıt (pis fırın), petrokok (temiz fırın), yalnız plastik atık, plastik atık ve arıtma çamuru karışımı, ve yalnız arıtma çamuru ile pişirilmiştir.

Çimento klinkeri örneklerinin mikroyapısı taramalı elektron mikroskobu (SEM) ile incelenmiştir. Sonuçlar farklı alternatif yakıtla hazırlanan numunelerdeki alit, belit, aluminat ve ferrit ana fazlarının farklı dağılımlarını göstermiştir. Alit/belit oranı 5.2 ve 1.5 arasında değişmektedir. X-ışını difraktometre (XRD) analizi, faz dağıtımı ölçümlerinde SEM ile yakın sonuçlar elde etmiştir. Klinker örneklerinin kimyasal bileşimi enerji dağıtıcı x-ışını spektroskopisi ve x-ışını fluoresans metodları ile incelenmiştir. Sulfur ve fosfor miktarları, belit fazı miktari ile artmıştır.

Hidrasyon deneyleri 0.3 ve 0.5 ağırlıklı su/çimento oranı ile yapılmıştır. Hidrate çimento örneklerinin mukavemetleri basma testleri ile farklı kürlenme zamanları için ölçülmüştür. Alternatif yakıtı kullanımı çimento basma mukavemetinde etki yaratabilmiştir, Özellikle tüm alternatif yakıtlarla üretilen numune daha az mukavemet miktarları göstermiştir. Hidratasyon sonucu oluşan fazlar SEM ve XRD ile incelenmiştir. Fazların yüksek reaktivitesi gösterilmiştir.

ACKNOWLEDGMENTS

First and foremost, I would like to express my deepest appreciation to my supervisor, Professor Mehmet Ali Gülgün. He has supported me thoughout my thesis with his knowledge, patience and kindness. I have always been amazed and motivated by his never-ending enthusiasm to explore and willingness to share his knowledge and experience. I have learned so many things from him in different fields that has helped me broaden my vision not only professionally, but also personally. One simply could not wish for a better or friendlier supervisor. I regard myself truly lucky to be one of Mali hoca's students .

Next, I would like to thank my co-advisor, Dr. Melih Papila, for his continuous support and kindness during my master's studies. I am mostly grateful for his guidance and encouragement throughout this work. I have immensely enjoyed working and interacting with him. It was such a luck for me that he co-advised my thesis project. He motivated me when I was discouraged and guided me with his knowledge and experience whenever I confronted problems. Working under Mali-Melih supervision was the best thing happened to me in my whole educational life.

My sincere thanks go to Dr. Cleva Ow-Yang for her remarkable wisdom and valuable guidance. She has been my role-model in my academic life. I learned the importance of being organized and punctual through her. It was my fortune that she was present in my interview; otherwise I could not catch the chance to be in this position. She has always been kind to me no matter if I disappointed her, just like my mother ☺

I am also thankful for the insightful and constructive comments of my other committee members, Dr. Zeynep Başaran Bundur and Dr. Burç Mısırlıoğlu, which helped me to improve my thesis. Special thanks to Dr. Bundur for allowing me to use the cement testing facilities at their laboratory at Özyeğin University.

I would like to thank AkçanSA company for this amazing project. The financial support and efforts in sample preparation is greatly acknowledged.

I am mostly grateful for the helps of Mr. Turgay Gönül, our laboratory specialist. Turgay abi constantly assists us in our experiments and tests with patience. I have learned many invaluable things from him.

I thank Mr. Pozhhan Mokhtari for XRD analyses and results. I also thank the other colleagues and friends with whom I interacted during my master's studies at Sabanci University. It was such a pleasure to have known them and worked with them.

I do not know how to fully express my gratitude to my lovely parents, my warm-hearted grandparents and my sweet sisters, Sona and Parisa; without the love and support of my family I could not have pursued my education. Without them I could not be where I am and who I am today. They were always there for me with their generous and kind hearts. I love you!

Last but not the least, I want to thank my beloved husband and best friend, Ali Khalili Sadaghiani. It would not be enough to describe the happiness I feel beside him by words. He has been my source of joy and strongest support in the last five years. His love and presence in my life have been and will be an inspiration for every challenge in my life.

TABLE OF CONTENTS

LIST OF TABLES

LIST OF FIGURES

LIST OF ABBREVIATIONS

a/b: alite/belite

AF: Alternative Fuel

BSE: Back-Scattered Electrons

EDS: Energy Dispersive X-ray Spectroscopy

OM: Optical Microscopy

SE: Secondary Electrons

SEM: Scanning Electron Microscopy

UTM: Universal Testing Machine

VLM: Visible Light Microscopy

w/c: water to cement ratio by mass

XRD: X-Ray Diffraction

XRF: X-Ray Fluorescence

NOMENCLATURE

CaO	SiO_2	Al_2O_3	Fe_2O_3	SO_3	MgO	K_2O	Na_2O	H_2O
C	S	A	F	$\bar{S}$	M	K	N	H

mineral name	cement terminology	chemical formula	cement notation
calcium hydroxide	Portlandite	$Ca(OH)_2$	C
calcium silicate hydrate	-	$CaO_x(SiO_2)_y \bullet zH_2O$	C-S-H
calcium sulfate	Gypsum	$CaSO_4 \bullet 2H_2O$	$C\bar{S}H_2$
dicalcium silicate	Belite	Ca_2SiO_4	C_2S
monosulfate calcium aluminate	Monosulfate	$Ca_4Al_2(SO_4)(OH)_{12} \bullet 6H_2O$	AFm
tetracalciumaluminoferrite	Ferrite	$Ca_4Al_2Fe_2O_{10}$	C_4AF
tricalcium aluminate	Aluminate	$Ca_3Al_2O_6$	C_3A
tricalcium silicate	Alite	Ca_3SiO_5	C_3S
trisulfate calcium aluminate	Ettringite	$Ca_6Al_2(SO_4)_3(OH)_{12} \bullet 26H_2O$	AFt

Chapter1: INTRODUCTION

1-1) Cement history

Since early times, there was a need for a material that would bind stones and later on bricks into a solid and formed mass. The Assyrians and Babylonians learned to use clay for this purpose. The Egyptians discovered the potential of calcined lime and gypsum and used them as binding agents for building such structures as the Pyramids. The Greeks were able to make further improvements and the Romans developed cement mortars by adding sand to the calcined lime and constructed structures of remarkable durability. The secret of Roman success in making the cementitious paste was the mixing of slaked lime (chemically calcium hydroxide) with a pozzolana admixture, a volcanic ash widely distributed in the Mediterranean. This process led to the production of cement as a material capable of hardening under water.

However, the first artificial cement was invented in 1824 by Joseph Aspdin. This cement had a color similar to the white-grey limestone found on the Isle of Portland in England and so Aspdin called it 'Portland Cement'. His method, which consisted of a careful preparation of calcareous (limestone) and clayey materials, is still in use and Portland cement has become one of the dominant construction materials [1-3].

Today, nearly 200 years after its discovery, there are about 1,500 cement factories around the world producing Portland cement. Each year, millions of tons of cement are being manufactured, e.g. according to Statistica portal more than 4000 million tons of cement were produced in 2014 worldwide [4].

1-2) Cement definition

Cement may be defined as the bonding material capable of uniting fragments and solid bodies to form compacted assemblies. When mixed with water, cement forms a plastic paste and sets (hardens) upon the chemical reactions called hydration. The term hydraulic cement then describes a substance which reacts with water and develops rigidity with time, but also does not react with water after being set and could be used under water. The strength of the cement paste increases as the hydration duration increases [1, 5].

Cement is made by heating a mixture of calcareous and argillaceous materials to temperatures up to 1450 °C. At these temperatures, the minerals melt and due to the phase changes, new chemical compounds form as calcium silicates and other calcium compounds. Hydraulic properties of cement are primarily due to the hydration of calcium silicates but other chemical compounds may also participate in the hardening process.

The word concrete is usually confused with cement. Concrete is a composite material produced by using cement paste to bind fine and coarse materials like sand, gravel, and rocks and make a dense coherent mass [5, 6].

1-3) Types of cement

There are many types of cement used in the construction industry. By far, the most widely used is Portland cement. Portland cement may be used as pure or alternatively, it may be used as a part of a mixture with other materials that also have cementitious properties, such as blastfurnace slag, fly ash and pozzolana. These cements are called composite cements or blended cements.

Portland cement itself can be divided into a number of different types, each cement having different characteristics. Normal grey cement for general-purpose use is usually referred as Ordinary Portland Cement (OPC). The other variations of Portland cement include white Portland cement, sulfate-resisting Portland cement, rapid-hardening Portland cement and etc.

Different standards are used for classification of Portland cement. The two major standards are the ASTM C150 [7] (American Society for Testing and Materials) used primarily in the USA and European standard EN 197 [8]. EN 197 cement types CEM I, II, III, IV, and V may be similar to the similarly named cement types in ASTM C150, but not necessarily identical. Standard specifications are based partly on chemical composition such as amount of calcium aluminates or physical properties such as specific surface area. Also, they could partly be related to the performance tests, such as setting time or compressive strength developed under standard conditions. The five Portland cement types and white Portland cement as described in ASTM C150 with their general characteristics and application are listed in Table 1.1 [7, 9].

Table 1.1. General features of main Portland cement types as stated in ASTM C150 [9].

	Classification	Characteristics	Applications
Type I	General purpose	Fairly high C_3S content for good early strength development	General construction (most buildings, bridges, pavements, precast units, etc)
Type II	Moderate sulfate resistance	Low C_3A content (<8%)	Structures exposed to soil or water containing sulfate ions
Type III	High early strength	Ground more finely, may have slightly more C_3S	Rapid construction, cold weather concreting
Type IV	Low heat of hydration (slow reacting)	Low content of C_3S (<50%) and C_3A	Massive structures such as dams. Now rare.
Type V	High sulfate resistance	Very low C_3A content (<5%)	Structures exposed to high levels of sulfate ions
White	White color	No C_4AF, low MgO	Decorative (otherwise has properties similar to Type I)

There are also many types of other types of cement that are not based on Portland cement. However, the quantities of these other cements used are small compared with Portland cement and composites of it. A few of these cements can be named as [1, 3, 6, 9]:

- Calcium aluminate cements
- Calcium sulfoaluminate cements
- Lime concrete/mortar
- Expansive cements

Due to the wide usage of Portland cement, the word cement is generally used to describe Portland cement, as it will be used in this study.

1-4) Cement manufacturing process

The manufacturing procedure of cement is schematically presented in Figure 1.1 [10]. As it is seen, cement production includes various steps and processes from preparation of raw materials to obtaining the final product.

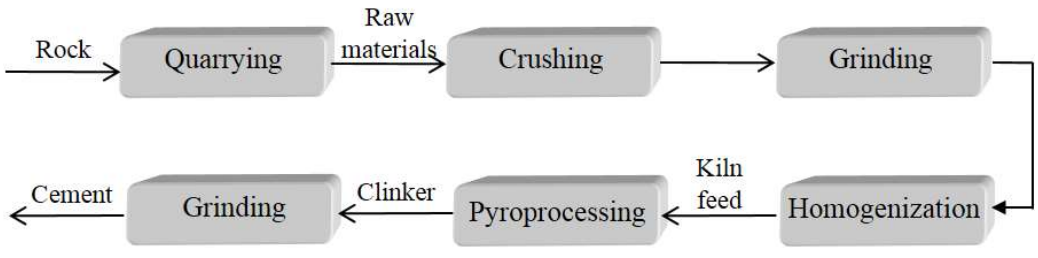

Figure 1.1. Schematic of the cement manufacturing procedure [10].

The first step in the manufacture of cement is to combine a variety of raw ingredients so that the resulting cement will have the desired chemical composition. These ingredients are firstly quarried or mined, usually from a site close to the cement plant. Because the main components in cement are CaO, SiO_2, Al_2O_3 and Fe_2O_3, the raw materials should contain these oxides in high amounts. The common sources of lime (CaO) employed in the manufacture of Portland cement are limestone (calcium carbonate) and chalk, while the main sources of silica (SiO_2) are clays or shales. Clays are aluminum silicates and usually contain some combined iron, too. Clays are also favorable because they are made of fine particles already and thus need little processing prior to use. Other naturally occurring materials like Bauxite and Iron ore or industrially by-products like slag and fly ashes are also used as the raw materials [3, 6, 11].

After the preparation of raw ingredients, crushing and grinding stages take place to obtain a mix which has 85% of the particles less than 90 μm in size. The final preparation of the raw meal before it is sent to the pyroprocess area requires special blending (homogenization). The goal of the blending is to provide the raw meal with an optimum consistency. The kiln feed is the result of a fine grinding of the raw meal, which usually uses heat from the exhaust gases of the kiln and the clinker cooler. The pyroprocessing often takes place in a pre-calciner which is supplied with about half of the total fuel energy. In this step, the raw feed is pre-calcined before entering the kiln. Figure 1.2 shows a cement manufacturing factory presenting the raw feed silo, pre-heater tower, rotary kiln and other parts [6, 12, 13].

Figure 1.2. Cement manufacturing factory [14].

The blended mix is then fed into a cement kiln for sintering. The materials are burned in temperatures as high as 1450 °C and as a result of the partial fusion, nodules of so-called clinkers are formed as the product of the kiln process. Because the raw ingredients are not completely melted, the mix must be agitated to ensure that the clinker forms with a uniform composition. This is accomplished by using a long cylindrical kiln that slopes and rotates slowly. The rotary kiln is a steel tube with a length to diameter (L/D) ratio between 10 and 38, which is usually divided in five or more different stages. The kiln is inclined approximately 2.5 to 4.5%, which mechanically rotates at 0.5 to 4.5 revolutions per minute. To heat the kiln, a mixture of fuel and air is injected into the kiln and burned at the bottom end [9, 13, 15,16]. A variety of fuels can be used in the kiln, from which we will see more in sections 1-8 and 1-9. A schematic of rotary kiln together with the pre-heater tower, clinker cooler and other sections can be seen in Figure 1.3-a [17]. Figure 1.3-b shows one of the rotary kilns of AkçanSA cement factory in Büyükçekmece, Istanbul.

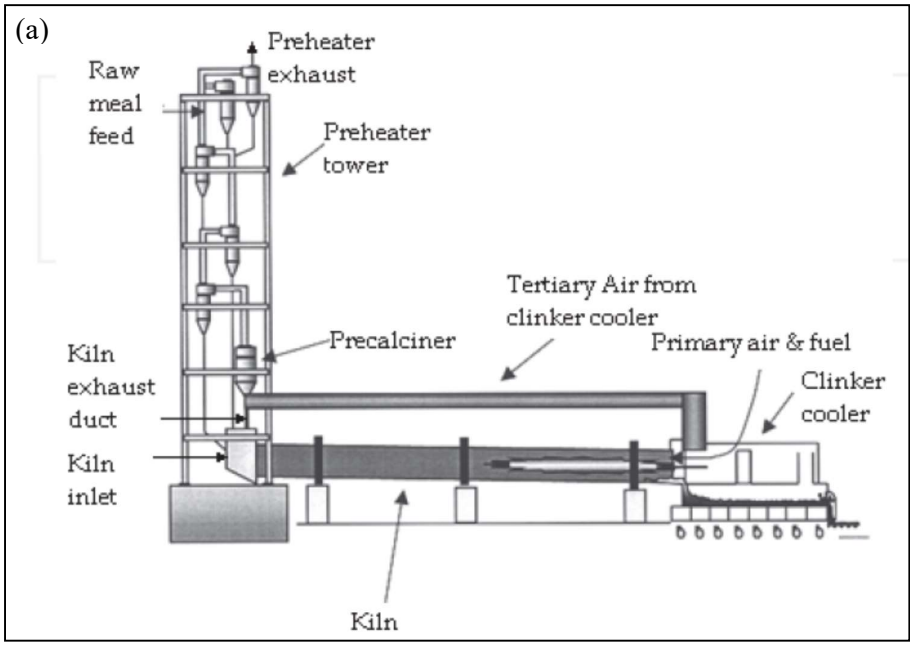

Figure 1.3. a) A schematic of rotary kiln with the pre-heater tower, clinker cooler and other sections [17], b) A rotary kiln in AkçanSA factory, Büyükçekmece, Istanbul.

The raw mix enters at the upper end of the kiln and slowly works its way downward to the hottest area at the bottom over a period of 60-90 minutes, undergoing several different reactions as the temperature increases. It is important that the mix move slowly enough to allow each reaction to be completed at the appropriate temperature. Rotary kiln heats the clinker mainly by radiative heat transfer and this is more efficient at higher temperatures, enabling a more uniform temperature in the burning zone, the hottest part of the kiln. One of the key elements inside the kiln is the use of specialized refractories (heat resistant bricks) that are capable of withstanding the high temperatures. Different stages in the kiln which describe the reaction zones can be listed as below [1, 3, 9]:

1) Dehydration zone (up to ~ 450˚C)

The evaporation and removal of the free water occurs.

2) Calcination zone (450˚C – 900˚C)

At about 600˚C the bound water is driven out of the clays, and by 900˚C the calcium carbonate is decomposed, releasing carbon dioxide and forming CaO.

3) Solid-state reaction zone (900˚ - 1300˚C)

CaO and reactive silica combine to form small crystals of belite, one of the four main cement minerals. In addition, intermediate calcium aluminates and calcium ferrite

compounds form. These play an important role in the clinkering process as fluxing agents and increasing the rate of reaction.

4) Clinkering zone (1300˚C – 1550˚C)

The hottest zone where the formation of the most important cement mineral, alite, occurs. The zone begins as soon as the intermediate calcium aluminate and ferrite phases melt. Inside the liquid phase, alite forms by reaction between belite crystals and CaO. Crystals of solid alite grow within the liquid, while crystals of belite formed earlier grow in size. The clinkering process is complete when all of silica is in the alite and belite crystals and the amount of free lime (CaO) is reduced to a minimal level (<1 wt%).

5) Cooling zone

The temperature drops rapidly and the liquid phase solidifies, forming the other two cement minerals aluminate and ferrite. In addition, alkalis and sulfate dissolved in the liquid combine to form K_2SO_4 and Na_2SO_4. The rate of cooling from the maximum temperature down to about 1100˚C is important, with rapid cooling giving a more reactive cement. This occurs because in this temperature range, the alite can decompose back into belite and CaO, among other reasons.

The nodules are now hard and the resulting product is called cement clinker. Clinker is composed of rounded, dark grey nodules, ranging in size from less than 1 mm to 30 mm or more [3]. Figure 1.4 shows typical cement clinker nodules.

Figure 1.4. Cement clinker nodules. The variation of sizes is observable [18].

The cooled clinker is mixed with a few percent of gypsum, acting as a hydration modifier, and sometimes additional components depending on the type of cement, and is then ground to cement. In this way, a fine powder with particles usually less than 40 μm in diameter is obtained. Clinker grinding is one of the most energy consuming steps in cement production and thus, a vast amount of research has been done to investigate and improve the grindability of clinker. It has been found that crystal size and content of main phases, and amount and distribution of porosity in clinker enormously affect the grindability[19, 20].

1-5) Cement composition

As discussed previously in section 1-4, the first output of the cement kilns is a dark-grey nodular material called clinker. Clinker is a complex system made up of a series of impure chemical compounds. The primary chemical compositions that construct Portland cement clinker are CaO, SiO_2, Al_2O_3, Fe_2O_3, and some small amounts of oxides, such as MgO, K_2O, Na_2O and SO_3. SO_3 also enters the cement composition through gypsum, which is added to clinker during grinding. Table 1.2 presents a typical analysis of a Portland cement clinker. It can be seen that the CaO possess the highest content in the composition, following which are SiO_2, Al_2O_3, Fe_2O_3[3, 6].

Table 1.2. Typical chemical analysis of a Portland cement clinker [3].

Compounds	SiO_2	Al_2O_3	Fe_2O_3	CaO	MgO	K_2O	Na_2O	SO_3	LOI	IR	Total
Content (wt%)	20.7	5.7	2.5	64.0	1.0	0.6	0.2	2.7	1.5	0.5	99.5

Balance is due to minor oxides, typically P_2O_5, TiO_2, etc.
LOI=loss on ignition, IR=insoluble residue

Throughout clinkering (refers to all of the operations before, during and after firing in rotary kilns), these oxides combine to form other compounds that constitute cement clinker. For example, calcium oxide and silicon dioxide combine to form modified forms of calcium silicates. Also, calcium aluminate and calcium aluminoferrite compounds form during clinkerization from calcium oxide, aluminum oxide and iron oxide. These compounds are known as phases in cement notation. A phase in cement chemistry is actually pointing out to the related mineral and is defined

as a part of the system having a uniform chemical and physical characteristics distinguished from other parts of the system.

There are four main phases in clinker composition:

- Tricalcium silicate, known as Alite
- Dicalcium silicate, known as Belite
- Tricalcium aluminate, known as Aluminate
- Tetracalcium aluminoferrite known as Ferrite

The chemical formula, shortened name and approximate percentage weight (ordinary Portland clinker) are shown in Table 1.3. Shortened names like C_3S and C_2S are often used in cement terminology. It can be seen in the table that alite phase with 50-70% wt% and belite phase with 15-30% wt% are the most important phases in the composition of clinker. Aluminate and ferrite phase are often called the matrix phases or the interstitial phases which are the last to form during cooling process of clinkerization. None of these phases are present in their pure form and typically contain ionic substitutions in their crystalline structures. Beside of these major phases, there are also some other minor phases like free lime (CaO), Periclase (MgO) and alkali sulfates. Calcium sulfate dihydrate is added to the clinker before grinding to form cement. Although usually referred to as gypsum, other types of calcium sulfate may also be used [1, 3, 6, 21].

Table 1.3. Typical phase composition of the ordinary Portland clinker [6, 21].

Name	Chemical Formula	Shortened Formula	Content (wt%)
Tricalcium silicate *alite*	$3CaO.SiO_2$	C_3S	50-70
Dicalcium silicate *belite*	$2CaO.SiO_2$	C_2S	15-30
Tricalcium aluminate *aluminate*	$3CaO.Al_2O_3$	C_3A	5-10
Tetracalcium aluminoferrite *ferrite*	$4CaO.Al_2O_3.Fe_2O_3$	C_4AF	5-15
Calcium sulfate dehydrate *gypsum*	$CaSO_4.2H_2O$	$C\underline{S}H_2$	4-6

In general, there is a wide variation in the amount of the main clinker phases in ordinary Portland cements manufactured in different plants. The actual phase composition is dependent on lots of parameters, for example:

- The quantities of each of the main oxides (CaO, SiO_2, Al_2O_3 and Fe_2O_3) in the raw materials.
- The extent to which they have combined to form the main clinker phases.
- The chemical compositions of the phases (including impurities).
- The sintering and subsequent cooling processes.

On the other hand, the amount of these main phases in various types of Portland cement is also different. Table 1.4 presents the typical phase compositions of five Portland cement types (ASTM C150) along with some of their physical properties [22].

Table 1.4. Typical phase compositions and physical properties of five types (ASTM C150) of Portland cement [22].

Compound/ Property	**Type I**	**Type II**	**Type III**	**Type IV**	**Type V**
C_3S (wt%)	58	49	60	25	40
C_2S (wt%)	15	26	15	50	40
C_3A (wt%)	8	6	10	5	4
C_4AF (wt%)	10	10	8	12	10
gypsum (wt%)	5	5	5	4	4
Loss on Ignition	1.7	1.5	0.9	0.9	0.9
Blaine (m^2/kg)	350	350	450	300	350
1-day Strength (psi)	1000	900	2000	450	900
7-day Heat of Hydration (J/g)	330	250	500	210	250

Alite (C_3S) and belite (C_2S) are the primary phases that remain solid throughout the clinkering process. They are the active ingredients of cement, producing strength when hydrated by generating the main hydration product, amorphous calcium silicate hydrate phase, also known as C-S-H. However, the C_3S hydrates much more rapidly than the C_2S, and thus, is responsible for the early strength development. Tricalcium aluminate (C_3A) and tetracalcium aluminoferrite (C_4AF) also hydrate early, but the products that are formed contribute little to the properties of the cement paste and can be even deleterious to some degree. These minerals are present because pure calcium

silicate cements would be virtually impossible to produce economically. Without the liquid from which they form, the clinker cannot be formed at an industrially viable temperature. Figure 1.5 presents a schematic diagram showing the variations in typical contents of phases during the formation of Portland cement clinker [6, 9, 23].

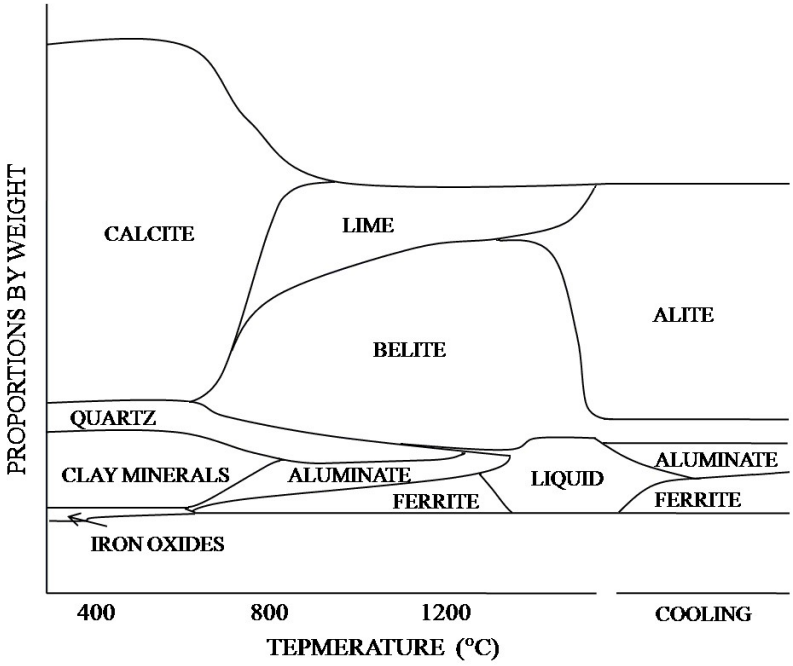

Figure 1.5. Schematic diagram of phase transformations during formation of Portland cement clinker [6].

Cement microstructure can be described as composite grains from ground clinker consisting of domains of crystalline alite and belite partly embedded in frozen liquid phases (interstitials) of aluminate and ferrite. Figure1.6-a and Figure 1.6-b illustrate the microstructure of the polished sections of cement clinker in SEM (BSE) and OM, respectively. The phases are shown on the images. Alite and belite appear as light grey and dark grey in BSE images (the reason will be discussed later in section 1-11), whereas the matrix phases of aluminate and ferrite appear as the darkest and brightest among the main phases. In the OM image, brown crystals are alite, blue crystals are belite and bright interstitial region is mainly ferrite, with small dark inclusions of aluminate. It should be noted that alite is not actually brown and belite is not actually blue, they appear brown and blue because the polished section has been etched with hydrofluoric acid (HF) to show the crystals more clearly. The pores (voids) of clinker are also shown on the images, being the black regions in SEM and grey regions in OM

image. These pores are usually filled with epoxy resin during specimen preparation for microscopy [3, 24, 25].

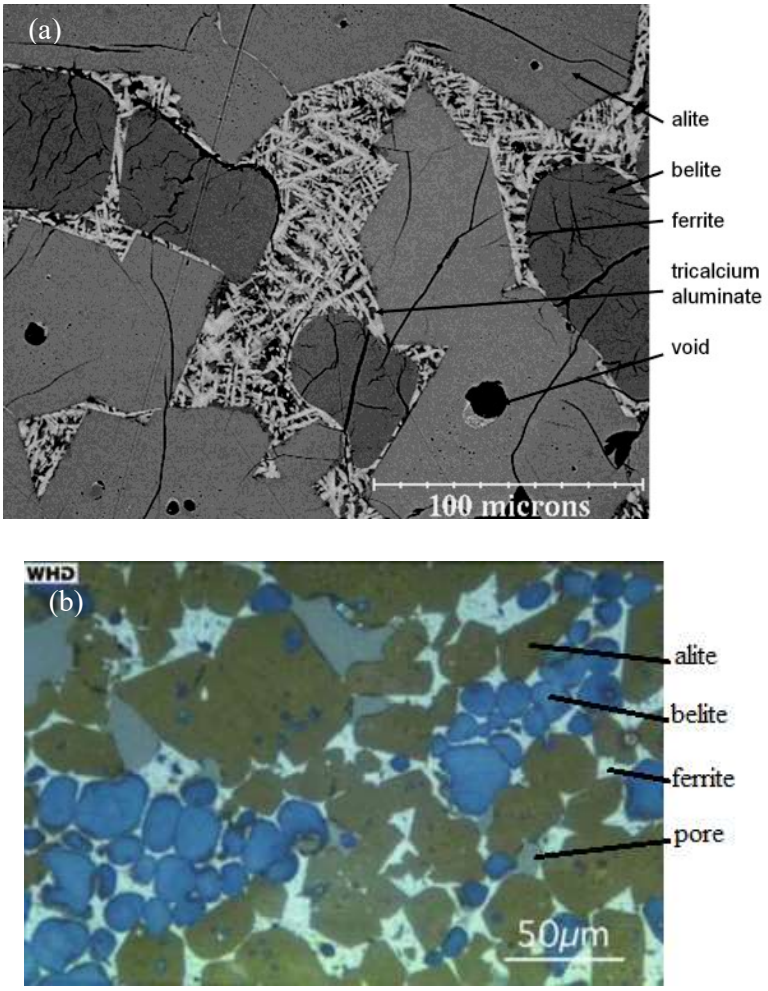

Figure 1.6. The microstructure of clinker in a)SEM (BSE) [25] and b)OM [24]. The phases are shown.

The proportions of each of the main minerals (alite, belite, etc.) are of major importance in determining the properties of the cement produced from the clinker. Some of the aspects that are directly related to the size, shape and distribution of phases and pores in the cement clinker are as follows [1, 26, 27]:

- Prediction of cement performance in the strength development
- Reactivity of the phases in hydration reactions
- Prediction of clinker grindability, since the grinding process consumes a significant amount of energy

- Temperature profile-burning efficiency relationships in the calcining and burning zones of the kiln

The clinker minerals can attain several crystalline modifications. Each of these minerals (phases) will be discussed separately.

1-5-1) Alite

Alite is the most important and abundant constituent of all ordinary Portland cement clinkers, of which it constitutes 50-70% wt%. It is tricalcium silicate (Ca_3SiO_5) modified in composition and crystal structure by ionic substitutions. It reacts relatively quickly with water and so the hydration of C_3S gives cement paste most of its strength, particularly at early times to ages up to 28 days [6].

Alite generally forms hexagonal crystals with crystal sizes up to about 150 μm (Figure 1.6). Pure C_3S can form with three different crystal structures. The equilibrium structure at temperatures below 980˚C is triclinic (T). At temperatures between 980˚C – 1070˚C the structure is monoclinic (M), and above 1070˚C it is rhombohedral (R). In addition, the triclinic and monoclinic structures each have three polymorphs, so there are a total of seven possible structures (Figure 1.7). The pure compound, when cooled to room temperature, is thus T1. In industrial clinkers, due to the incorporation of impurities, the form present at room temperature normally approximates to M1 or M3 or a mixture of these. T2 triclinic form is found rarely. It means that the impurities are able to stabilize the monoclinic structure and prevent the structural transformation from monoclinic to triclinic that would normally occur on cooling.

However, all of these structures are similar and their reactivity has no significant differences. The most important feature of the structure is an asymmetric packing of the calcium and oxygen ions that leaves large “holes” in the crystal lattice. Fundamentally, the ions do not fit together very well, causing the crystal structure to have a high internal energy. As a result, C_3S is highly reactive.

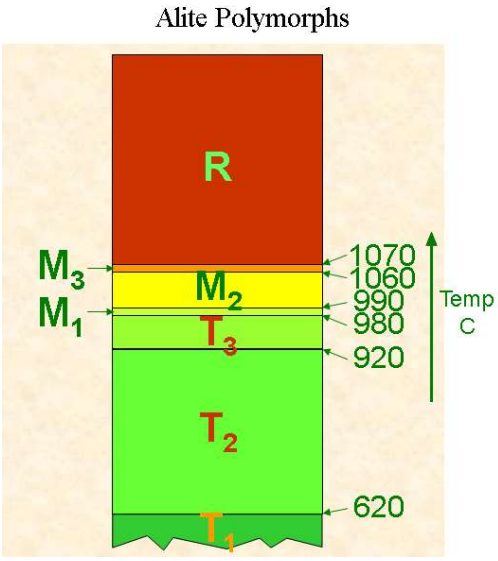

Figure 1.7. Polymorphic phase transitions in C_3S [23].

The C_3S in a cement clinker usually contains about 3-4% of oxides other than CaO and SiO_2. This mineral should therefore be called alite rather than C_3S. In a typical clinker the alite would contain about 1 wt% each of MgO, Al_2O_3, and Fe_2O_3, along with smaller amounts of Na_2O, K_2O, P_2O_5, and SO_3. However, these amounts can differ considerably regarding the composition of the raw materials used to make the cement. Between the three major impurities, Mg and Fe replace Ca, while Al replaces Si. The oxide ions in structure of alite confer on it a high reactivity, which causes it to develop early strength (within the first seven days) [6, 9, 23, 25].

Typical chemical compositions of alite, belite, aluminate and ferrite phases are given in Table 1.5.

Table 1.5. Typical chemical compositions of main phases in clinker [6, 25].

Phase (wt%)	Na_2O	MgO	Al_2O_3	P_2O_5	SO_3	K2O	CaO	TiO_2	Mn_2O_3	Fe_2O_3
Alite	0.1	1.1	1.0	25.2	0.1	0.1	71.6	0.0	0.0	0.7
Belite	0.1	0.5	2.1	31.5	0.1	0.9	63.5	0.2	0.0	0.9
Aluminate (cubic)	1.0	1.4	31.3	3.7	0.0	0.7	56.6	0.2	0.0	5.1
Ferrite	0.1	3.0	21.9	3.6	0.0	0.2	47.5	1.6	0.7	21.4
Aluminate (orthor.)	0.6	1.2	28.9	4.3	0.0	4.0	53.9	0.5	0.0	6.6
Aluminate (low Fe)	0.4	1.0	33.8	4.6	0.0	0.5	58.1	0.6	0.0	1.0
Ferrite (low Al)	0.4	3.7	16.2	5.0	0.0	0.2	47.8	0.6	1.0	25.4

1-5-2) Belite

Belite is the second most abundant phase and composes 15-30% wt% of ordinary Portland cement clinkers. It is dicalcium silicate (Ca_2SiO_4) with some modifications by ionic substitutions. Belite reacts slowly with water and so contributes little to the strength at the beginning of hydration. However, at later ages it substantially takes part in strength increment. After one year of hydration, the strengths of pure alite and pure belite are very close under similar conditions [6].

Belite displays a rounded form with crystal sizes ranging from 5 to 40 μm (Figure 1.6). Similar to C_3S, C_2S can form with different structures (Figure 1.8). The high temperature α structure has three polymorphs, α- C_2S possessing hexagonal structure and α'_H and α'_L possessing orthorhombic structure. The polymorph which is in equilibrium at intermediate temperatures is β and is also orthorhombic. Also, there is a low temperature γ-polymorph with again orthorombic structure. The important aspect of γ-C_2S is that it has a very stable crystal structure that makes it completely unreactive in water. However, the β structure is readily stabilized by the other oxide components of the clinker and thus the γ form is almost never present in Portland cement. The crystal structure of β-polymorph is considerably less irregular than that of C_3S, and this causes the lower reactivity of C_2S. It is claimed that α'-polymorph is more reactive than β-polymorph. Usually the β polymorph is found in clinkers, although smaller amounts of α, α'_H, and α'_1 polymorphs may also occur. Optical microscopy of lamellar structures on etched specimens and X-ray powder diffraction data are useful for distinguishing both alite belite polymorphs.

The C_2S in cement contains slightly higher levels of impurities than C_3S (Table 1.5). According to Taylor, the overall substitution of oxides is 4-6%, with significant amounts of Al_2O_3, Fe_2O_3, and K_2O [6, 9, 23, 25].

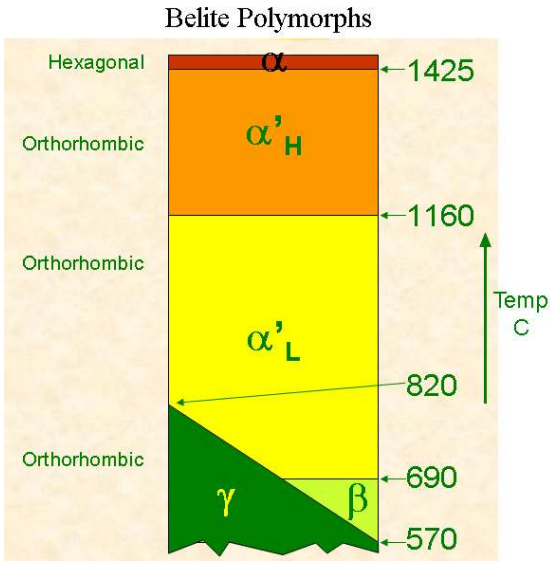

Figure 1.8. Polymorphic phase transitions in C_2S [23].

1-5-3) Aluminate

Portland cement clinkers usually compose of 5-10% wt% of aluminate. It is tricalcium aluminate ($Ca_3Al_2O_6$), highly altered in composition and also in structure by ionic substitutions. Like C_3S, it is highly reactive and reacts rapidly with water, releasing a significant amount of exothermic heat during the early hydration period. Hydration of C_3A can cause undesirably rapid setting unless a set-controlling agent, usually gypsum, is added. Unfortunately, the products of C_3A hydration contribute little to the strength or other engineering properties of cement paste. In some conditions, e.g. the presence of sulfate ions, C_3A and its products can even harm the concrete by participating in expansive reactions that lead to cracking.

Aluminate forms as small 1-60 μm crystals exhibiting irregular to lath-like habit, filling the area between the ferrite crystals. Pure C_3A forms only with a cubic crystal structure. The structure is formed by Ca^{+2} atoms and rings of six AlO_4tetrahedra. Similar to C_3S, the bonds are distorted from their equilibrium positions, causing a high internal energy and a high reactivity.

High amounts of CaO and Al_2O_3 in the C_3A structure can be substituted by other oxides. The high levels of substitution can lead to other crystal structures. The C_3A in Portland clinker, which typically contains about 13% oxide substitution, is primarily cubic, with smaller amounts of orthorhombic C_3A. The C_3A and C_4AF minerals form by

simultaneous precipitation as the liquid phase cools after the clinkering process, and thus these phases are closely intermixed. This makes it difficult to figure out the exact compositions of the two phases. The cubic form usually contains ~4% substitution of SiO_2, ~5% substitution of Fe_2O_3, and about 1% each of Na_2O, K_2O, and MgO. The orthorhombic form has similar amounts of impurities, but with a greater (~5%) substitution of K_2O (Table 1.5) [6, 9, 23, 25].

1-5-4) Ferrite

Ferrite constitutes 5-15% wt% of Portland cement clinkers. It is Tetracalcium aluminoferrite (Ca_2AlFeO_5), highly modified in composition by variation in Al/Fe ratio and ionic substitutions. Ferrite's reaction rate with water is somewhat variable, perhaps due to differences in composition or other characteristics. However, in general, the reactivity is high initially and low or very low at later ages.

Ferrite crystals form as dendritic, prismatic, and massive crystals. Ferrite has one significant property in that nearly all the transition metal ions in the clinker end up in it. The other phases are nearly colorless, but the ferrite has a dark greenish-grey color, and is responsible for the overall color of the clinker. It is for this reason that in making white clinker, the quantity of ferrite is minimized by restricting the amount of transition metals in the raw mix.

A stable compound with any composition between C_2A and C_2F can be formed as C_4AF and it is an approximation that represents the midpoint of this compositional series. The crystal structure is complex, and is believed to be related to the mineral perovskite. The actual composition of C_4AF in cement clinker has generally higher aluminum than iron, and there is considerable substitution of SiO_2 and MgO (Table.1-5). Taylor mentions a typical composition (in normal chemical notation) to be $Ca_2AlFe_{0.6}Mg_{0.2}Si_{0.15}Ti_{0.5}O_5$. However, the composition varies somewhat depending on the overall composition of the cement clinker [6, 9, 23,25].

1-5-5) Free lime and Periclase

Phases in lesser quantities, but still influential to performance, include periclase (MgO) and free lime (CaO). Periclase may exhibit a dendritic or equant crystal habit both within and between the other clinker constituents, ranging in size up to 30 μm.

Free lime may occur as isolated rounded crystals or in masses with variable crystal size. These phases are usually difficult to be revealed in microscopic observations [25, 28].

Free lime and periclase (or magnesia) both has a detrimental effect on cement properties. Therefore, manufacturers minimize the amount produced even that it is not possible to eliminate them completely. Both incline to hydrate when cement mixes with water, and the resulting hydroxide occupies more space than the original, dense oxide. This matter is problematic when the structure has started to form and may case unsoundness in hardened paste.

Free lime exists in the clinker if the finishing reaction of lime with belite to form alite is not completed, if there are large unreactive particles of calcium carbonate in the raw mix, or if the mix contained too much lime. The limit for the presence of free lime in the clinker composition is usually said to be 3%. Periclase dissolves in all the four main phases (and particularly the ferrite) to a limited extent. Once this limit (which may be in the range 1.5-3.0%) is exceeded, periclase starts to form as a separate phase. The magnesia is somewhat more soluble in the clinker melt than in the solid minerals, and so periclase tends to crystallize out. According to Hewlet, periclase should not exceed 6% in the composition of clinker [1, 6, 23].

1-5-6) Alkali sulfates and calcium sulfates

These minor compounds may also occur in clinker and are significant because they have been found to affect hydration rates and strength development. Alkali (usually K and Na) sulfates should be limited to less than 3% incorporating all of their compounds. Increased alkali levels in clinker are considered potentially detrimental. However, sulfate is beneficial in the kiln process because it promotes reactions by acting as a flux. These phases form late in the clinkering process and generally are found along crystal perimeters within the pores.

The most found alkali sulfates in cement compounds include arcanite (K_2SO_4), aphthitalite ($(Na,K)_2SO_4$), calcium langbeinite ($K_2SO_4 \cdot 2CaSO_4$). One or more forms of calcium sulfate are added during clinker grinding to control setting. However, the clinker alkali sulfate phases may also contribute to setting and the alkalis and sulfates should be considered together [1, 3, 25, 29, 30].

1-5-7) Pores

Clinker is a highly porous material. Although porosity is not actually considered as a phase, but it is present as one of the major parts in cement clinkers. Porosity is almost always present in clinkers and determines how easy or difficult it is to grind the clinker. Since grinding is one of the most energy-consuming steps in cement manufacturing, porosity analysis is of utmost importance particularly in reducing costs [20, 27]. Although porosity content has a major role in the grindability of clinker [31], it has also been stated that porosity is only a factor in coarse grinding and not influential when grinding to ordinary cement fineness [32].

The content, shape and size of the pores may give an idea of sintering grades in the kiln [33]. Low sintering grades of clinker may result in high porosity amount [34], whereas hard burning tends to cause low clinker porosity and often contributes to production of dust instead of good, nodular clinker. It also slows down the cooling process, both because the maximum temperature is higher, and because the low-porosity clinker is more difficult to cool [35].

1-6) Hydration of cement

1-6-1) Hydration process

Cement reacts with water in a process called hydration. During hydration, the clinker compounds react with water simultaneously and at different rates, giving insoluble hydration products. In the cement paste which is a mixture of cement powder and water, hydration products gradually replace the water in the spaces between the cement grains and this way, hydration proceeds. The reaction products, called hydrates, are responsible for cement hardening and strength development and they give cement its binding properties.

Hydration includes all ongoing chemical and physical processes in the cement-water system. The three main processes are:

1. Dissolution of clinker phases: releasing ions to water (pore solution forms)
2. Precipitation: formation of hydrate phases
3. Diffusion: processes at later hydration times

The pore solution is highly alkaline (pH > 13) due to dissolution of Na and K salts and also formation of CH (calcium hydroxide). The solid phases that are formed during precipitation are thermodynamically more stable than the pore solution, so the tendency

to approach equilibrium is the driving force for hydration. During the hydration of cement, phases are converted into other phases with lower free energy and thus these reactions are exothermic. This release of excess energy in the form of heat is called heat of hydration [1, 3, 9].

The hydration of cementitious systems is strongly time dependent and can be divided in five major stages, as shown in Figure 1.9 (Rate of heat evolution as a function of time). These stages are:

(1) Initial hydration (minutes): Mainly dissolution of aluminate-rich phases (e.g. C_3A) and precipitation of calciumaluminate sulfate hydrates (e.g. ettringite)

(2) Induction or dormant period (up to 2-4 hours): The hydration reactions are slowed and relatively low heat evolves. The nature of this period is still in debate.

(3) Main hydration or acceleration period (up to 24-48 hours): The rate of reaction is accelerated and dissolution of tricalcium silicate results in precipitation of calcium silicate hydrates (C-S-H) and calcium hydroxides (Portlandite) into the capillary porosity (originally occupied by water). This causes a large decrease in the total pore volume and a concurrent increase in strength. At the end of Stage 3 about 30% of the initial cement has hydrated, and the paste has undergone both initial and final set. Both the reaction rate and the duration depend strongly on the temperature and on the average particle size of the cement.

(4) Deceleration period (in the order of days): The hydration rate decreases as the hydrated material covers the cement particles.

(5) Diffusion-limited reactions (days to years): Hydration continues with a slow rate. It proceeds with the outward diffusion of dissolved ions from the cement particles or inward diffusion of water to reach the unreacted cement cores. The products precipitate into the capillary pores. These diffusion processes become slower and slower as the layer of hydration product around the cement particles becomes thicker and thicker [9, 36-39].

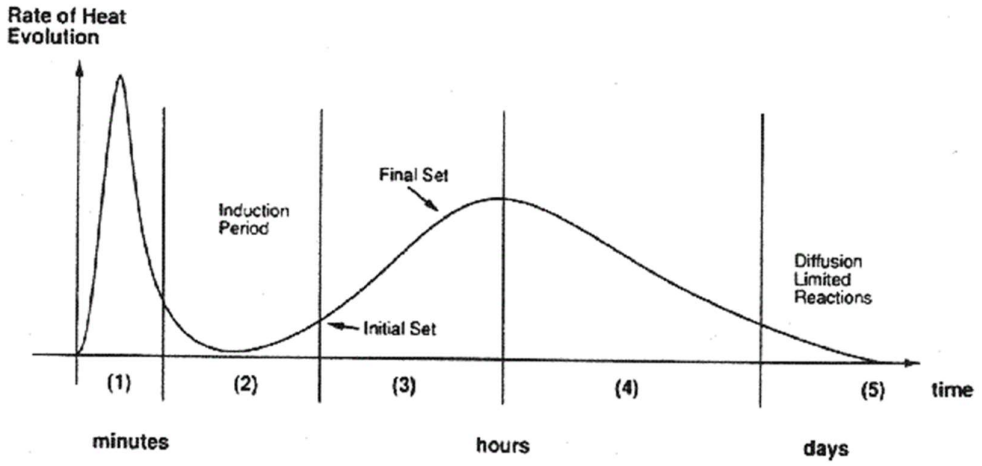

Figure 1.9. Stages in the hydration of cement [36].

Figure 1.10 presents the conversion stages of cement particles to hardened cement paste. The hydration starts at the surface of the particles and develops into the particles by time. The particles grow smaller and the capillary pores are filled with hydration products [40].

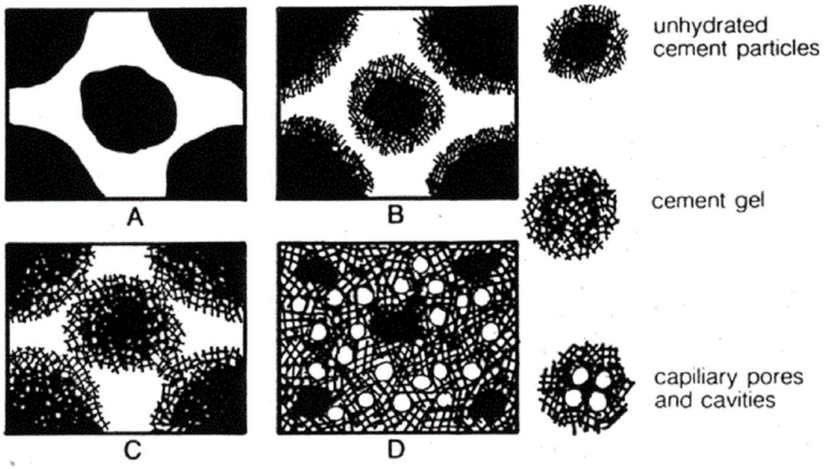

Figure 1.10. The progress of hydration reactions on cement particles [40].

There are lots of factors which could affect the kinetics of the hydration process and the structure of the hydration products, like:

1. the phase composition of the clinker and the quality and quantity of foreign ions incorporated in the crystalline lattices of the individual clinker minerals
2. the quantity and form of calcium sulfate or other admixtures
3. the particle size and distribution
4. curing conditions (air or water curing) and hydration temperature

5. the water/cement ratio of the mix.

Figure 1.11 shows how the w/c ratio could affect the hydration process and evolution of porosity, which eventually determine the cement strength. A higher w/c ratio means higher porosity in the paste and lower strength, but higher workability. For complete hydration of cement, usually a water/cement ratio of 0.25 is needed. If a lower amount is used, some cement may remain unhydrated. If a greater amount is used, the excess water may remain in the capillary pores [1, 41,42].

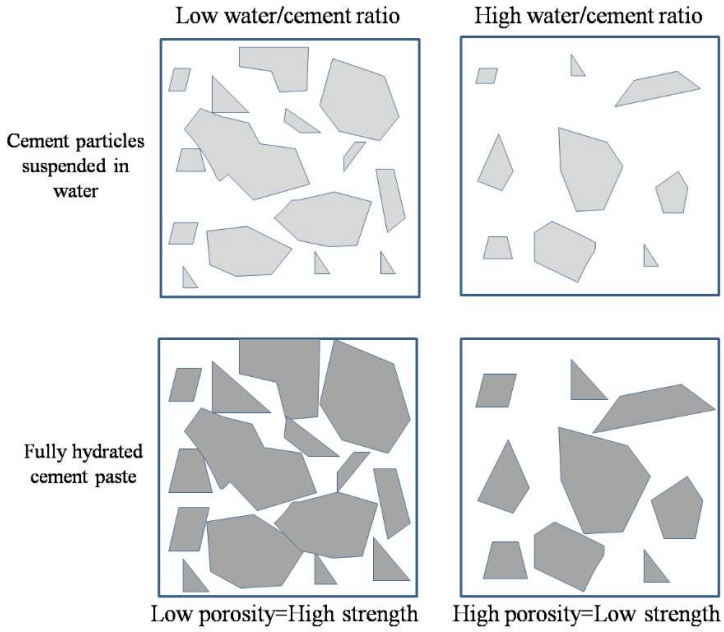

Figure 1.11. Effect of water/cement ratio on the porosity content and strength of cement [41].

1-6-2) Hydration products

Hydration begins as soon as cement comes in contact with water and continues as long as favorable moisture and temperature conditions exist and space for hydration products is available. Within a few hours of mixing with water, cement paste starts to gain in stiffness and strength, going from a viscous fluid to a plastic solid to finally a stiff solid. This change happens because the hydration products have a larger density than the anhydrous phases and occupy more space, filling most of the space created by the consumption of water and increasing the solid volume.

Clinker phases (alite, belite, aluminate and ferrite) all react with water, but the degree of reaction is different for each of them. Figure 1.12 shows that around 70% of

C_3S reacts within 7 days, in which only 25% of C_2S reacts. This shows how C_3S provides the early strength and C_2S provides the late strength. The assumption that the cement compounds are hydrating independently is not entirely true. An example for the compound interaction is a faster hydration of C_2S in the presence of C_3S due to changes in the concentrations of Ca^{2+} and OH^- in solution, which also will affect the hydration of C_3A and C_4AF. The more reactive C_3A is expected to consume more sulfate ions than C_4AF, increasing the reactivity of C_4AF by formation of less ettringite than expected. The initial hydration of C_3A contributes to the activation of the hydrations of the other clinker minerals. An increase in the amount of free lime may shorten the dormant period due to earlier precipitation of $Ca(OH)_2$[1, 42-44].

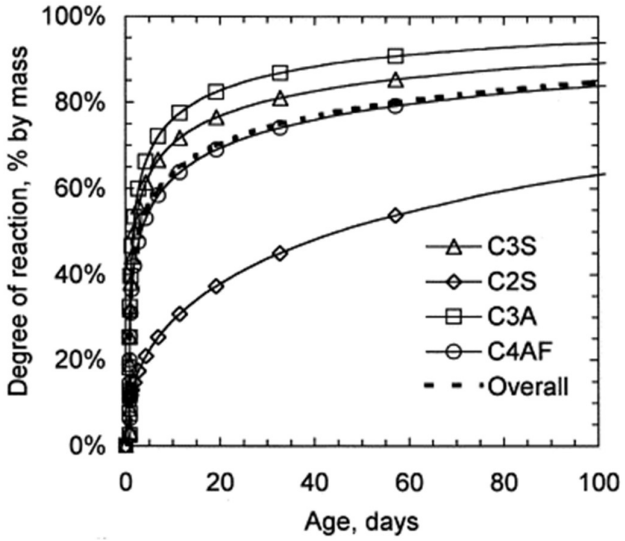

Figure 1.12. The percentage of reaction of the individual compounds of clinker [43].

Upon hydration, calcium silicates (C_2S and C_3S) undergo hydrolysis producing well-crystallized calcium hydroxide (CH) and a gel-like near amorphous calcium silicate hydrates (C-S-H) (Eq.1.1 and Eq.1.2).

$$2C_3S + 6H \rightarrow C_3S_2H_3 + 3CH \quad \text{(Eq.1.1)}$$

$$2\ C_2S + 4H \rightarrow C_3S_2H_3 + CH \quad \text{(Eq.1.2)}$$

The hydration of tricalcium aluminate (C_3A) in the presence of gypsum produces needle like crystals of a high sulfate calcium sulfoaluminate called ettringite (Eq.1.3). This ettringite continues to form until all the sulfate ions have been removed at which point further hydration of C_3A results in the conversion of the ettringite into a low sulfate sulfoaluminate referred to as monosulfate (Eq.1.4).

$C_3A + 3C\bar{S}H_2 + 26H \rightarrow C_6A\bar{S}_3H_{32}$ (ettringite) (Eq.1.3)

$2C_3A + C_6A\bar{S}_3H_{32} + 4H \rightarrow 3C_4A\bar{S}H_{12}$ (monosulfate) (Eq.1.4)

The ferrite phase (C_4AF) reacts in a similar way to the C_3A (Eq.1.5 and Eq.1.6), but more slowly. One important difference is that some of the aluminum in the reaction products is substituted for iron. A convenient way to show these reactions is:

$C_4AF + 3C\bar{S}H_2 + 21H \rightarrow C_6(A,F)\bar{S}_3H_{32} + (F,A)H_3$ (Eq.1.5)

$C_4AF + C_6(A,F)\bar{S}_3H_{32} + 7H \rightarrow 3C_4(A,F)\bar{S}H_{12} + (F,A)H_3$ (Eq.1.6)

where (A,F) indicates aluminum with variable substitution of iron, and (F,A) indicates iron with variable substitution of aluminum. The $(F,A)H_3$ is an amorphous phase that forms in small amounts to maintain the correct reaction stoichiometry. Although the main reaction products of ferrite phase are not pure ettringite and monosulfoaluminate, they have the same crystal structure and they belong to AFt and AFm group.

Also other minor constituents may form upon hydration reactions [9, 37].

Figure 1.13 shows the state transition diagram for cement hydration reactions. Arrow patterns denote the collision of species to form hydration products [45].

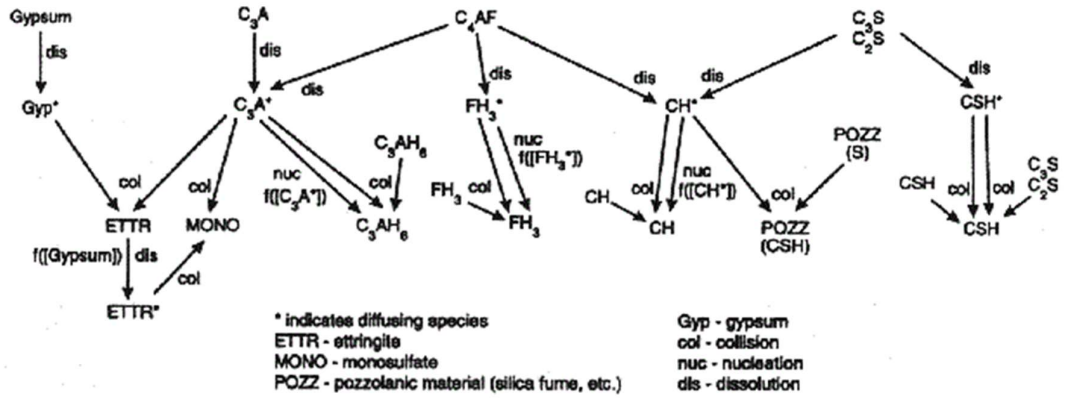

Figure 1.13. State transition diagram of cement hydration. The abbreviations are explained on the figure [45].

The structure of hardened cement paste is highly heterogeneous consisting mainly of amorphous C-S-H gel (Ca 70% by mass), CH crystals (Ca 20% by mass), calcium sulfoaluminates, unhydrated cement grains and porosity containing either water or air. The main hydration phases are discussed below with more detail.

1-6-2-1) Calcium silicate hydrate

This is the main reaction product. The generic form is $xCaO \cdot SiO_2 \cdot yH_2O$ and it is often abbreviated, using cement chemists' notation to C-S-H, the dashes indicating that no strict ratio of SiO_2 to CaO is inferred. The Si/Ca ratio is somewhat variable but typically approximately 0.45-0.50 in hydrated Portland cement. The amorphous C-S-H gel is the principle product of Portland cement hydration and forms the main binding agent between the unhydrated particles of cement and other crystalline products of hydration. C-S-H is primarily responsible for some of cement's principal properties such as strength, shrinkage, and durability.

The structure of this calcium silicate hydrate has been object of extensive studies. However, knowledge of the atomic structure of this chemical phase is still undetailed.

1-6-2-2) Calcium hydroxide(Portlandite)

The formula is $Ca(OH)_2$, which is often abbreviated to CH. CH is formed mainly from alite hydration (in smaller amounts from belite hydration). Alite has a Ca:Si ratio of 3:1 and C-S-H has a Ca/Si ratio of approximately 2:1, so excess lime is available to produce CH. Portlandite is crystalline in nature and has a well-defined composition. It is known to grow either as irregular crystals or as hexagonal platelets.

1-6-2-3) AFm and AFt phases

These are two groups of minerals that occur in cement. AFm and AFt are shorthand for a family of hydrated calcium aluminate hydrate phases, aluminate-ferrite-monosubstituent and aluminate-ferrite-monosubstituent, respectively. One of the most common AFm phases in hydrated cement is monosulfate and by far the most common AFt phase is ettringite. The general definitions of these phases are somewhat technical. For example, ettringite is an AFt phase because it contains three (t-tri) molecules of anhydrite written as $C_3A.3CaSO_4.32H_2O$.Monosulfate is an AFm phase because it contains one (m-mono) molecule of anhydrite written as $C_3A.CaSO_4.12H_2O$. The aluminum can be partly-replaced by iron in both AFm and AFt phases. AFm and AFt compounds are typically needle-shaped.

- Ettringite

Ettringite is present as rod-like crystals of sub-micrometer diameter and 10-20 μm length, in the early stages of reaction or sometimes as massive growths filling pores or cracks in mature cement or concrete. The chemical formula for ettringite is $[Ca_3Al(OH)_6.12H_2O]_2.2H_2O]$ or, mixing notations, $C_3A.3CaSO_4.32H_2O$.

- Monosulfate

Monosulfate occurs in the later stages of hydration, 1-2 days after mixing. The chemical formula for monosulfate is $C_3A.CaSO_4.12H_2O$. Both ettringite and monosulfate are compounds of C_3A, $CaSO_4$ (anhydrite) and water, in different proportions. Monosulfate crystals are also needle-like, but are about two and a half time smaller than ettringite crystals.

Ettringite forms early after the cement and water are mixed, but it is gradually replaced by monosulfate. This is because the ratio of available alumina to sulfate increases with continued cement hydration; on first contact with water, most of the sulfate is available to dissolve, but much of the C_3A is contained inside cement particles with no initial access to water. Continued hydration gradually releases alumina and the proportion of ettringite decreases as that of monosulfate increases [1, 3, 6].

The relative volumes of each of the phases in a typical Portland cement paste can be calculated and plotted as a function of the curing age and the degree of hydration of the paste, as shown in Figure 1.14-a and 1.14-b, respectively [46].

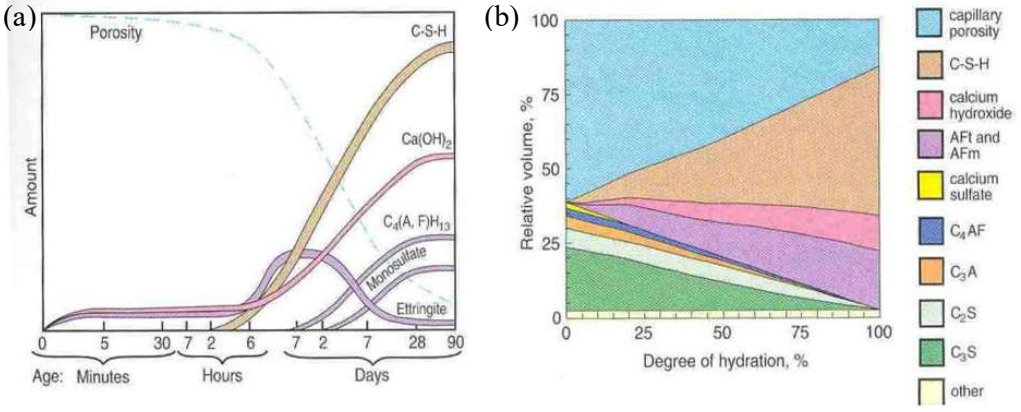

Figure 1.14. Relative content of the phases during hydration of cement as a function of a)curing time and b)degree of hydration [46].

1-6-3) Evolution of hydration products

The hydration process of cement is substantially complicated. This process cannot be considered as the sum of hydration reactions of the cement phases, individually. Figure 1.15 illustrates a schematic of hydration process of anhydrous cement at (a) beginning and after (b) 10 minutes, (c) 10 hours, (d) 18 hours, (e) 1–3 days, and (f) 2 weeks. A cement grain is typically illustrated as larger silicate particles surrounded by smaller C_3A and C_4AF crystals. The reactive phases of aluminate and ferrite react first with gypsum. This results in formation of an amorphous gel at the surface of the cement particles and growing of short rods of ettringite. After this initial reactivity span, cement hydration slows down and the induction period starts. After this period, the acceleration occurs. In between 3 to 24 hours after hydration begins, about 30% of cement reacts to form calcium hydroxide and C-S-H. The development of C-S-H in the acceleration period takes place in two levels. After about 10 hours of hydration (Figurec), C_3S forms "outer C-S-H," which instead of the surface of the C_3S crystals, grows out indirectly from the ettringite needles. Thus, in the beginning phase of the reaction, the silicate ions must move through the aluminum and iron rich phase to form the C-S-H. After 18 hours of hydration, C_3A continues to react with gypsum forming longer ettringite rods as the second phase of acceleration period (Figured). The ettringite and C-S-H particles appears to form a hydrating layer about 1 μm from the surface of anhydrous C_3S crystals. A small amount of "inner C-S-H" forms inside this layer. The deceleration period begins after 1–3 days of hydration, when the reactions slow down (Figure e). Some C_3A reacts with ettringite to form monosulfate. "Inner C-S-H" continues to enlarge near the C_3S surface, making the 1 μm gap narrower between the hydrating layer and anhydrous C_3S. The rate of hydration generally depends on the diffusion rate of water or ions to the anhydrous surface. After 2 weeks of hydration (Figure f), the gap is completely filled with C-S-H. The original, "outer C-S-H" becomes more fibrous by time [47].

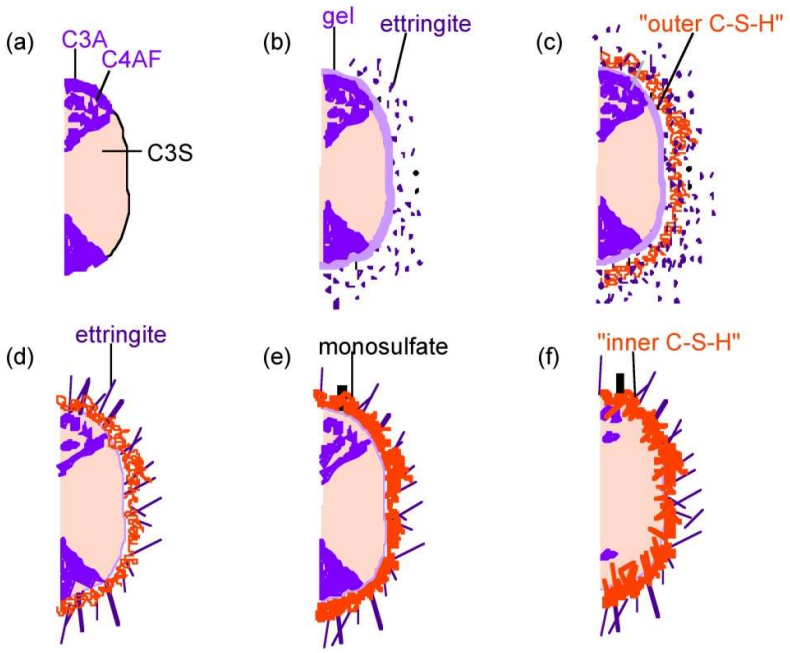

Figure 1.15. Schematic representation of the hydration process of anhydrous cement (a) at beginning and after (b) 10 minutes, (c) 10 hours, (d) 18 hours, (e) 1–3 days, and (f) 2 weeks [47].

SEM images of hydrated cement paste showing needle-like ettringite, and CH platelets and fibrous C-S-H can be seen in Figure 1.16-a and Figure 1.16-b, respectively [48].

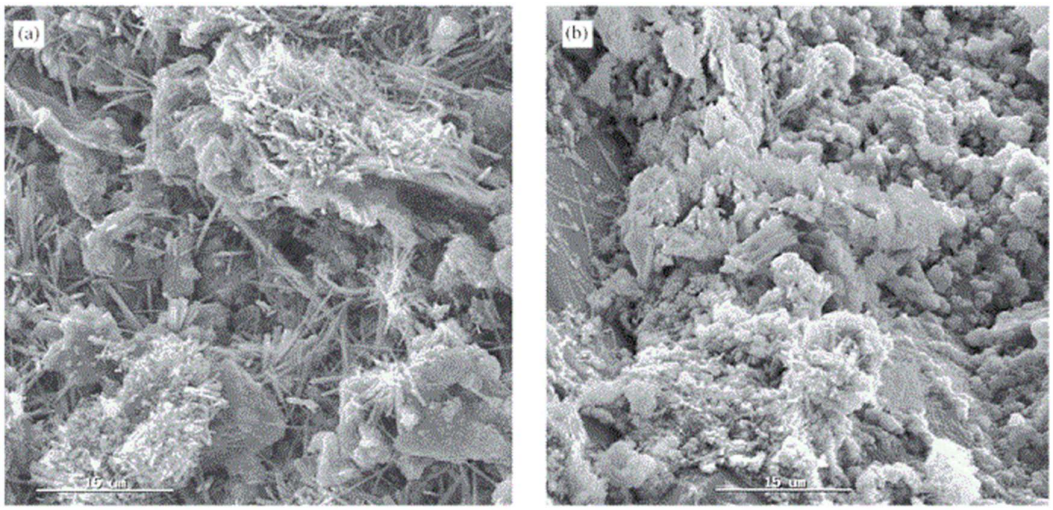

Figure 1.16. SEM SE images of hydrated cement paste showing a) ettringite-formed region and b) CH and C-S-H-formed regions [48].

1-6-4) Hardening and strength development

Hydration of cement results in hardening of cement paste. The conditions of this hydration play an integral role in the physical and chemical properties of the hardened paste.

Hardening is the process of strength gain, and is often confused with setting (curing) which is the stiffening of the cement after it has been mixed with water. As hydration continues, cement becomes harder and stronger. Most of the hydration and strength development take place within the first month, but then continues, though more slowly, for a long time with adequate moisture and temperature. Figure 1.17 shows that at the 7th day of hydration, ~75% of total (28th day) strength is achieved for standard type I cement (ASTM C150). This figure also shows that there is a relative difference in the strength development of different cement types, which is mainly due to their chemistry and composition [23, 42, 49, 50].

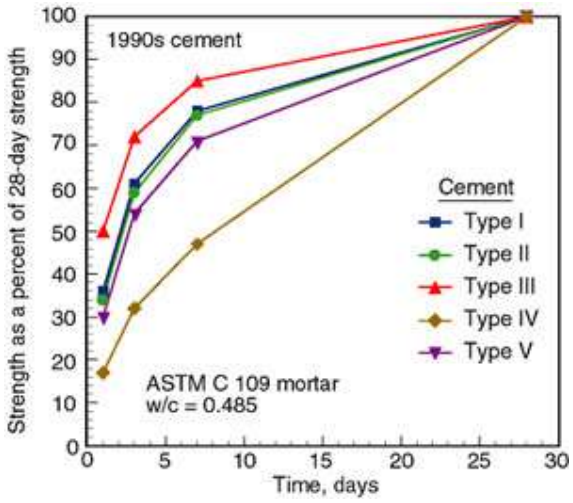

Figure 1.17. Strength development graphs of five cement types (ASTM C150) with w/c=0.485 [49].

Not all of the clinker minerals contribute to the strength development to the same extent. Figure 1.18 illustrates the strength development of four different phases in clinker. Alite and belite phases are the main strength-giving phases due to their hydration, which results in C-S-H gel formation. C_3S is most reactive, giving early strength, but C_2S also has a significant longer term contribution. The C-S-H produced is the principal binding phase in Portland cements and is quantitatively the most important

hydration product. The C_3A and C_4AF reactions are fast but give little contribution to strength [23, 51].

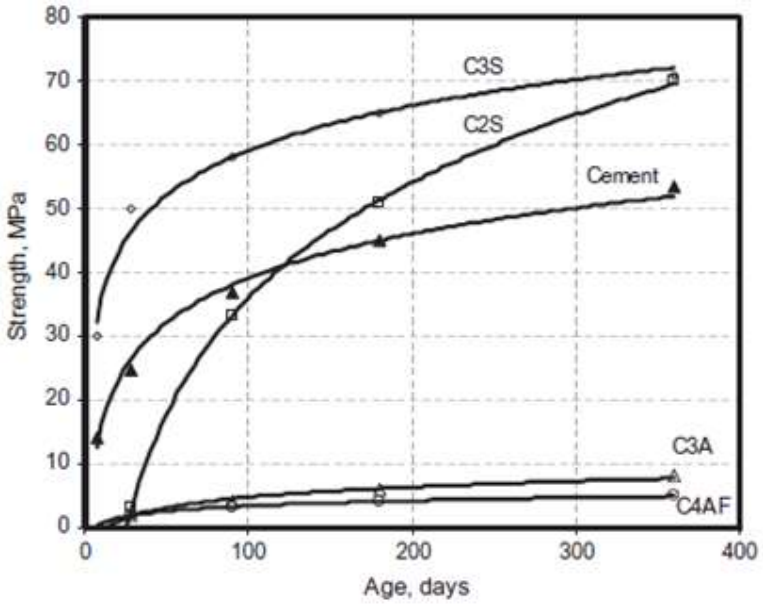

Figure 1.18. The compressive strength development of cement phases [51].

1-7) Fuel usage in cement manufacturing

The cement industry consumes a significant amount of natural resources and energy. The clinker production itself is one of the most energy-intensive processes which expends thermal energy of 3-6 GJ/tonne of clinker produced. Providing this much of thermal energy requires the consumption of a huge amount of fuels [52, 53]. Coal, gas, oil, liquid and solid waste materials, petroleum coke and other energy resources have all been successfully used as fuels for burning cement in kilns, either solely or in various combinations. Selecting the fuel is a very important step and a large number of parameters have to be taken into account. Since fuel costs can amount to as much as 43 per cent of the manufacturing costs, the selection is primarily governed by the cost [1].

The manufacturing of cement is not an environmentally friendly process. Beside of wasting a tremendous amount of natural resources, either as the raw materials or fossil fuels, airborne pollution in the form of dusts and gases is a major concern. Cement production is responsible for about 5% of global man-made CO_2 emissions. The amount of CO_2 emitted by the cement industry is nearly 900kg of CO_2 for every 1000kg of cement produced [54].

Two major sources of CO_2 emissions can be identified in the cement industry. The first source is due to the fuel combustion for burning the clinker, the pre-heaters and other operations (around 40%). The second source is the natural release of CO_2 during the de-carbonation of limestone (around50%) [55-57].

Therefore, the kiln process is the largest source of air emissions in cement manufacturing. However, there are also some minor sources during the whole production process. As illustrated in Figure 1.19, some lower amounts of CO_2 are produced during other stages, like the quarrying and transportation of raw materials and grinding and packing of the product. This Figure also shows the proportional magnitude of contribution to CO_2 emissions by the widths of the arrows [58, 59].

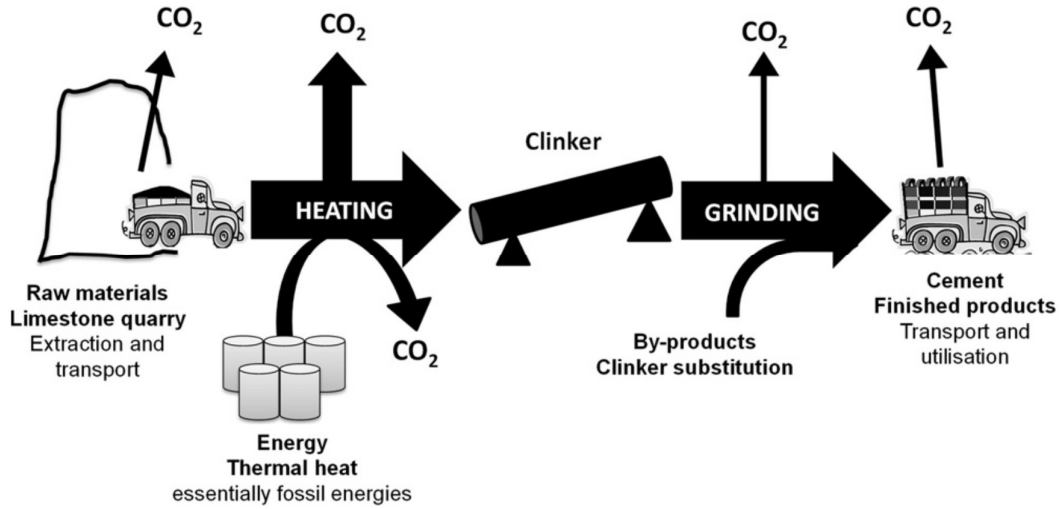

Figure 1.19. Simplified cement production process and related CO_2 emission sources. The magnitude of each source is identified by the width of the relative arrow [58]

In addition, combustion products are generated inside the kiln, and are released in the form of gas. Nitrogen oxides (NO_x), sulfur oxides (SO_x), carbon monoxide (CO) and organic emissions (i.e., acid gases and volatile organic compounds) are all the result of the fuel firing inside the kiln and the high temperatures of the process. The cement manufacturing industry is under utmost pressure to reduce these emissions [55, 56, 60, 61].

There are also lots of other important parameters in the fuel selection procedure. One of them is the least affection of produced clinkers by the fired fuels. In other words, attention has to be paid not to incorporate hazardous elements or compounds in the

clinker chemistry through the fuels, which could influence its properties adversely. The other factors could be named like the flame shape, burning degree, ease of flame feeding, design of the kiln and the availability of the fuel [62, 63].

Natural gas is one of the important fuels to be used in cement kilns. Although it cannot be considered as the cheapest one, it is the simplest fuel to use since its feeding does not create a problem in the kiln and it introduces no components which can interfere with the chemistry of the materials. The low flame emissivity may not be such a problem in cement kilns as has been suggested; however, the additional gas volume produced as a result of combustion can lead to a lower unit output.

From economic considerations it is useful to use heavy fuel oil in cement kilns. However, the disadvantage is that the sulfur content of up to 4% could be introduced to the system, the effect of which will be discussed later.

At the present time pulverized coal and petroleum coke are extensively consumed with regard to their cost. The composition of the different coals used to fire cement kilns can vary considerably, but in most kiln systems the coal ash is incorporated into the feed materials, and in so doing changes the compound composition of the product. The absorption of 2% coal ash from a 100% coal is shown to reduce the tricalcium silicate content from 76 to 64%. This could have the effect of lowering the 28-day strength by 4-5 MPa. Coarse coal ash particles and those projected insufficiently far into the kiln can fail to combine, giving higher levels of free lime and additional quality problems. This problem can be solved by appropriate grinding of coal. It should also be taken into account that the ignition temperatures of the different forms of coal could be significantly different. For example, lignite can ignite at around 400°C, whereas the anthracitic types of coal need ignition temperatures of 700°C. This also reflects the precautions which must be taken in handling these materials [1, 64].

Modern kilns have a multi-fuel capacity in order to respond to the constant variation of fuel prices and availability. These kilns are supplied with multi-fuel burners [65]. Figure 1.20 presents a retired multi-fuel burner as it was used in a modern rotary kiln at AkçanSA factory. The outlets of different fuels are indicated on the image.

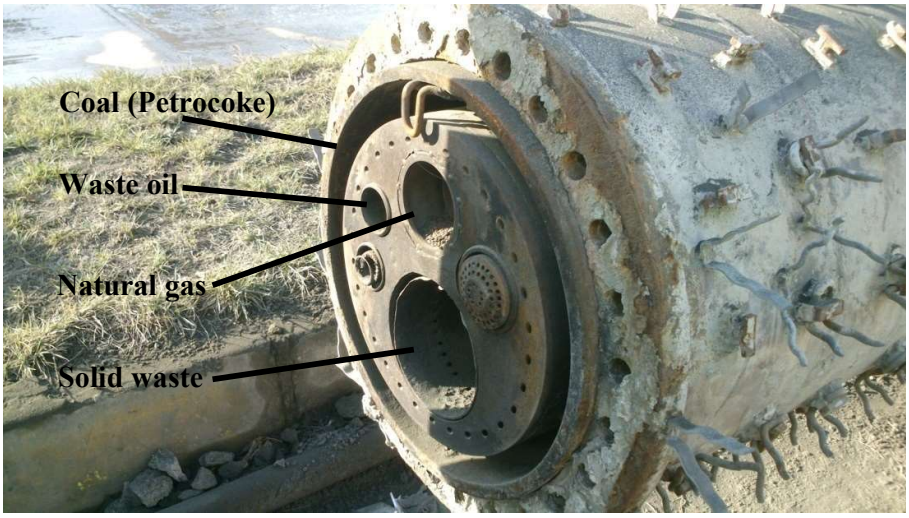

Figure 1.20. A retired multi-fuel burner as it was used in a modern rotary kiln at AkçanSA factory. The outlets of different fuels are indicated.

An improvement in the environmental performance of cement kilns in terms of optimizing the fuel consumption and energy resources as well as a reduction in the emission of gaseous pollutants is a goal for the cement industry. This goal could be obtained through two main methods; the use of alternative fuels or the use of supplementary materials like pozollans in order to reduce the amount of clinker in cement [17, 59, 65, 66].

1-8) Usage of alternative fuels

The cement industry has been steadily exploring the potential development and technological evolution in the last decades. One of the significant techniques that can be studied as a possible potential with a wide application is the use of alternative fuels. This technique provides a numerous amount of benefits among which are the reduction of environmental impact of wastes, reduction of CO_2 emissions, decrement of the waste handling costs, saving the natural fuel resources and reduction of fuel costs for the cement industry. Since alternative fuels are often cheaper than conventional fuels, the possibility of a competitive edge is generated. Nowadays, the utilization of alternative fuels is a reality for many cement plants worldwide, including the ones in Turkey. The use of alternative fuels in European cement kilns saves fossil fuels equivalent to 2.5 million tonnes of coal per year [13, 17, 59, 62, 63, 65, 67-70].

In many plants, fossil fuels used in the cement kiln firing are partly replaced by alternative fuels. This has been conducted usually with usage of a defined mixture of fossil fuels like pulverized coal or natural gas (65-85%) and alternative fuels like chopped tires and waste plastic (15-35%). However, studies are being conducted to develop the capability of kilns in using a higher amount of alternative fuels [13, 71].

But, how is it possible to use other fuels rather than natural fuels in cement facilities? The answer lies in the favorable conditions of clinker producing process in kiln systems. These conditions include high temperatures, long residence times, an oxidizing atmosphere, alkaline environment, ash retention in clinker, and high thermal inertness. These suitable circumstances ensure that the fuel's organic part is burned out and the inorganic part, involving heavy metals is trapped and combined in the product. This leads for potential combustion of all kinds of substances inside the kiln [17, 59].

Candidate materials for the alternative fuels/waste derived fuels are too many to list and they are various in kind. Table 1.6 presents a number of potential materials and wastes to be used as alternative fuels in cement kilns. It can be seen that these materials are available as gas, liquid and solid forms. They include almost every residue from industrial or commercial operations. Sewage sludge, waste plastics, used car tires, spent solvents, used oils and refuse derived fuels (RDF) are just a few to mention. The list of candidate materials for use as alternative waste fuels continues to expand. Regulatory pressures, economic considerations, diminishing traditional solid waste disposal capabilities, and a number of similar factors are causing the constant change of the candidate waste fuels [17, 62, 72].

Table 1.6. Potential types of materials as alternative fuels in cement kilns [17].

Category	Fuels
Gaseous fuels	Refinery waste gas, landfill gas, pyrolysis gas, natural gas
Liquid fuels	Tar, chemical wastes, distillation residues, waste solvents, used oils, was suspensions, petrochemical waste, asphalt slutty, paint waste, oil sludge
Solid fuels	Petroleum coke, paper waste, rubber residues, pulp sludge, sewage sludge, used tires, battery cases, plastics residues, wood waste, domestic refuse, rice husks, refuse derived fuel, nut shells, oil-bearing soils, diapers, etc.

The alternative fuels may differ from fossil fuels in some characteristics like heating value, shape and size of the fuels and the amount of ash. Thus, knowledge of their composition is important in order to use them in cement manufacturing. Almost all of the alternative fuels have some calorific value which could be exploited in kilns. However, in order to make their usage economically feasible, they must possess a number of criteria like the ones listed below [60, 63]:

- Availability and cost.
- Physical state of the fuel (solid, liquid, gaseous).
- Content of circulating elements (Na, K, Cl, S).
- Toxicity (organic compounds, heavy metals).
- Composition and content of ash.
- Content of volatiles.
- Calorific value (typically over 8 MJ/kg is required).
- Physical properties (scrap size, density, homogeneity).
- Grinding properties.
- Humidity content.

Therefore, it is obvious that the selection of the proper type of fuel is vital for optimum efficiency in kilns. A comparison of coal as a fossil fuel with some of the most common alternative fuels used in cement kiln systems is presented in Table 1.7 [17].

As mentioned previously, the use of alternative fuels in cement manufacturing, do not only result in a energy cost reduction, but it also has significant ecological impacts like conservation of non-renewable resources, reduction of waste disposal requirements and reduction of emissions. The combustion of wastes in the cement kiln systems results in an increased net global reduction in CO_2 emissions as opposed to dedicated incinerators. The reduction of NO_x emissions is also obtained by use of low-grade alternative fuels in kiln systems due to reburn reactions.

Table 1.7. Analysis of coal and some common alternative fuels used in cement kilns [17].

	Coal	Petcoke, (Kääntee et al., 2004)	Predried Sewage sludge (Winter et al., 1997)	Meat and bone-meal (Kääntee et al., 2004)	Tyre
Proximate analysis (wt. percent)					
			As received (wt. percent)		
Moisture (wt. percent)	9.20	1.50	7.00	8.09	0.6
Ash (db)	8.85	0.90	26.70	28.30	19.1
Volatiles (daf)	36.22	11.80	60.60	56.41	56.6
C - fixed	45.63	85.80	5.70	7.20	23.7
Ultimate analysis (wt. percent daf)			As received (wt. percent)		
C	68.6	89.50	37.20	42.10	71.85
H	3.05	3.08	4.29	5.83	6.07
N	1.3	1.71	4.18	7.52	0.20
S	0.49	4.00	0.53	0.38	1.06
O	8.51[7]	1.11	20.10	15.30	1.12
Ash	7.0	0.90	26.70	28.30	19.1
LHV (MJ/kg)	27.89	33.7	14.8	16.2	31
Density (kg/m³)	1300	2023	1140	720	1179

Although the advantages of consuming alternative fuels at cement plants are numerous, the contrary is also possible. It is likely that the poor designs result in projects where cement kilns have higher emissions or the conditions could be in a way that the alternative fuels are not put to their best value use. It is important that the negative effects of pollution on the environment and human health be prevented or kept at a minimum [17, 63].

On the other hand, the clinker must not be used as a sink for heavy metals, as it can harm the product quality. The quality of the produced clinker is highly affected by the quality, type and quantity of the utilized fuel. Some components are likely to be introduced to the product through the used fuel. These components can interfere with the chemistry of the cement materials. In addition, the operation of the kiln system can be affected by the combustion of the fuel used [5, 69]. Poor heat distribution, unstable pre-calciner operation, blockages in the preheater cyclones, buildups in the kiln riser ducts, higher SO_2, NO_x, and CO emissions, and dusty kilns are some of the major challenges for switching from conventional fuels to alternatives fuels. These challenges must be considered in order to achieve successful application [17, 73, 74].

Three common alternative fuels, petroleum coke, sewage sludge and waste plastics will be discussed more thoroughly in this section. As it will be discussed in the following chapters, these fuels have been used to investigate the effect of alternative fuels on cement in this study.

1-8-1) Petroleum coke

Petroleum coke (petrocoke, petcoke) is the solid residual that remains after extraction of all valuable components from crude oil or petroleum. Petrocoke (Figure 1.21) is mainly composed of carbon, but it also contains high sulfur amount and some amounts of heavy metals like vanadium and nickel. The fixed carbon in petrocoke is usually in the range of 80 - 92 percent [17, 75, 76]. Petrocoke often has higher calorific value than coal itself regardless of the coking process, with an LHV (lower heating value) of about 32.5-35 MJ/kg. Also, petrocoke is a low-volatile fuel. Its volatile content range is typically 5-15 percent, depending on the coking process [73, 77].

Figure 1.21. Petrocoke [78].

Petrocoke is widely used in cement kilns as a fuel. The new plants are specifically being designed to enable the 100 percent petrocoke usage, as well as pre-calciners which are being retrofitted to enable petrocoke firing. Although this material is considered to be a by-product, its high application as fuel in cement plants has made it not to be considered as an alternative fuel anymore. Therefore, in this study, petrocoke will not be treated as an alternative fuel but as a main fuel [17, 62].

However, the use of petrocoke as fuel could bring some challenges because of the high sulfur content, poor ignition and burnout characteristics because of its low volatile content. In addition, although petrocoke has higher energy content, it emits around 30

percent more CO_2 than coal per unit of weight. Also, as the sulfur content of petrocoke is several times higher than that of coal, it is expected that combustion of petrocoke will result in higher emissions of SO_2 [79].

Petrocoke has low ash content (Table 1.7) which easily fuses in the cement clinker. Vanadium pentoxide is the minor component with the highest content in petrocoke, the effect of which will be investigated in following sections (section 1-10). However, due to low ash content of petrocoke such high contents of vanadium in cement are unlikely to be present [17, 76].

1-8-2) Sewage sludge

Sewage sludge is the semi-solid material formed during wastewater treatment. Wastewater is a combination of the any liquid or water-carried wastes which have been poured or dumped in to the sewer system of residential, commercial and industrial establishments [17, 80]. Figure 1.22 shows sewage sludge after the drying (dewatering) treatments.

Figure 1.22. Dried (dewatered) sewage sludge [81].

A huge amount of sewage sludge is produced worldwide every day. There are some conventional disposal methods including landfill, sea disposal and land spreading (use in agriculture as organic fertilizer and soil conditioner). Figure 1.23 compares the sewage sludge disposal ways in European Union and North America in 2011.

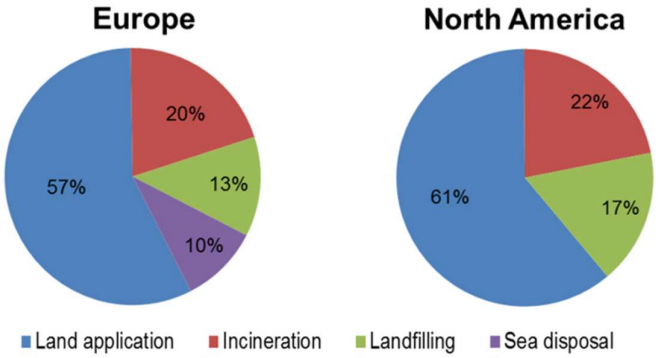

Figure 1.23. Comparison of sewage sludge disposal ways in European Union and North America in 2011 [82].

However, there are economical and ecological restrictions to these methods. Considering these factors, the thermal utilization of sewage sludge seems an attractive means of its management. In many countries, like Japan, USA, Denmark, Netherlands, Switzerland and Belgium sewage sludge is utilized as an alternative fuel in cement manufacturing plants. In cement production, sludge is usually co-combusted with coal (or petrocoke) in predried form. Using the predried sludge makes its storage, transportation and feed easier. This material is dried, pulverized and pneumatically fed to the burners during the co-firing. The environmental concerns of sewage incineration are decreased significantly when sewage sludge is used as fuel in cement kilns. During the firing, the organic part of the sludge is destroyed and the inorganic part, including heavy metals, is trapped and combined in the product [13, 17, 62, 80].

There are however concerns related to the usage of sewage sludge as a fuel in cement kilns. Similar to all other fuels, the calorific value, feeding process, etc. should be taken into account. The investigations show that the calorific value of sewage sludge (~8300 kJ/kg) makes it viable as a supplementary fuel in cement kilns. Also, it is shown that the usage of this material as fuel does not affect the raw material composition dramatically because of the law ash content [83-88]. However, opposite findings are also present in which incorporation of minor elements into clinker was unfavorable. It has also been stated that sewage sludge is prone to affect the phase distribution of clinker [80, 83-85,89-91]. The chemical composition of sewage sludge is of utmost importance while using in clinker kilns and it should be controlled constantly. The investigations have shown that the sewage sludge ash has a high content of SiO_2, Al_2O_3 and Fe_2O_3. These compounds are prone to affect the quality and properties of cement if excess amounts of sewage sludge are used [17, 80]. Rodriguez et al. [85], Lin. et al. [83,

84] and Kwon et al. [91] have shown that the C_2S phase formation is increased, i.e. the belite phase is stabilized and alite crystallization is delayed, with the usage of sewage sludge. These effects are attributed to the minor elements, especially Phosphorous in the composition of sewage sludge. Rodriguez et al. [85] has proved that there is 5% P in belite and 2.2% P in alite of the sample prepared with 15% of sewage sludge ash. It is suggested that P stabilizes the belite crystal lattices. Also, Lin et al. [83] has found 0.75% P_2O_5 in their sludge ash-produced samples, whereas the typical amount of P_2O_5 in Portland cement can be as high as 0.46. In the same study, the formation of α -C_2S was observed. Figure 1.24 shows XRD patterns of 4 clinker samples, OPC related to the standard sample and ECO-A, ECO-B and ECO-C related to three clinkers produced with same amounts of different sewage sludge compounds. It can be seen that α-C_2S formation is increased in ECO-B and ECO-C samples in comparison with OPC sample [83].

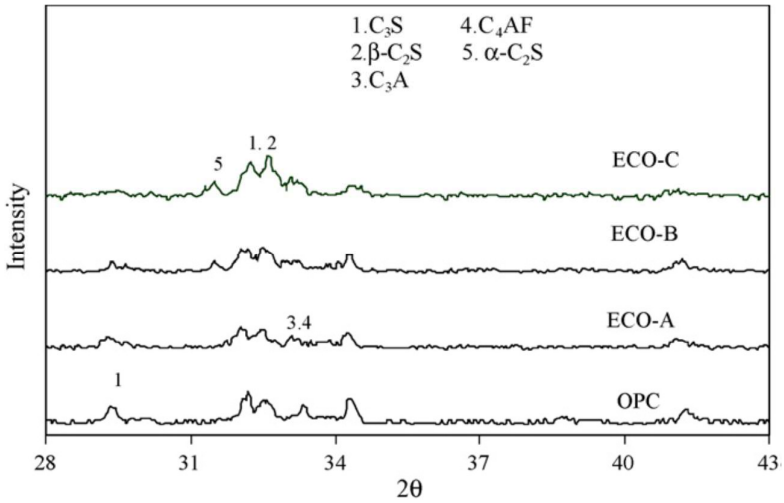

Figure 1.24. XRD patterns of four clinker samples. OPC:standard Portland sample, ECO-A, ECO-B and ECO-C:samples produced with different sewage sludge compositions [83].

One other effect is the increment in alite and belite crystal sizes because of a reduction in the viscosity of interstitial phase [85]. Also, the porosity content of the clinkers increases by using sewage sludge [84]. One of the other significant effects that was observed is the decrement in free lime amount [85], which is in contrast with the previous findings that Phosphorous increases the free lime amount [1, 91]. Kwon et al. [91] has shown that the free lime reduction is attributed to the presence of chlorine in sewage sludge, although Cl compounds are known to affect more in the kiln process

than the quality of clinker. Lin et al. [84] also showed that the concentrations of Ti, Ba, Zn, Cr, Cu, Ni and Pb in the clinkers increase with adding the sewage sludge ash into the raw meals, while those of Mg and Sr obviously decrease, and those of Al, Fe and Mn slightly decrease.

The other studies on sludge ash addition in cement have shown an increment in the setting time of cement, i.e. a delayed early and final setting time [87, 92,93]. In addition, the compressive strength of the cement has been found to be influenced by substituting the sludge ash in the composition [83, 84,94]. Figure 1.25 shows the compressive strength development graphs of four samples in the work by Lin. et al. [83]. It is seen that the compressive strength of samples prepared with sewage sludge (ECO-B and ECO-C) is developed more slowly than the standard sample. This could be because of the increased α –C2S content of these samples.

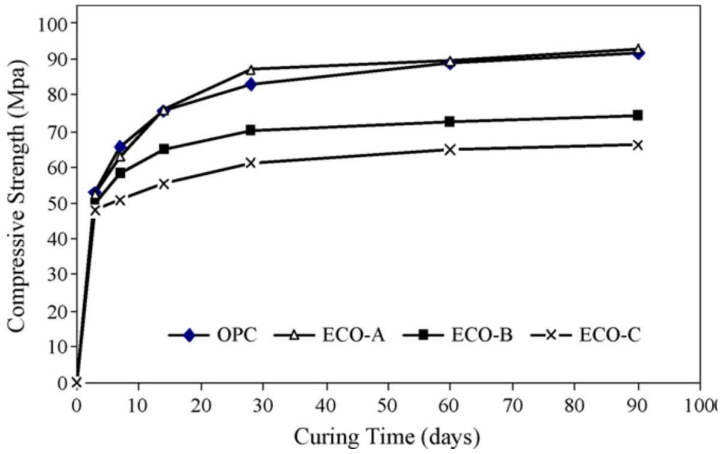

Figure 1.25. The compressive strength development graphs of four samples, OPC: ordinary Portland sample, ECO-A, ECO-B and ECO-C:samples produced with different sewage sludge compositions [83].

However, in the later studies [84], it is shown that although the strength may be affected slightly in early ages, the influence is decreased in later curing ages (Table 1.8). This might be attributed to the increased amounts of C_2S in the clinkers produced with sewage sludge and the minor elements carried with it.

Table 1.8. Flexural strength and compressive strength of cement samples prepared with sewage sludge ash contents as raw meals [84].

Sewage sludge content (%)	Flexural strength (MPa)			Compressive strength (MPa)		
	Curing time (days)					
	3	7	28	3	7	28
0	6.02	7.56	9.65	31.42	45.27	63.15
0.5	5.98	7.55	9.62	30.28	44.79	62.56
1.0	5.75	7.62	9.67	32.59	43.66	64.01
1.5	5.74	7.69	9.59	32.63	42.55	61.72
2.0	5.65	7.59	9.62	31.78	43.51	65.44
2.5	5.43	7.53	9.62	28.07	43.33	63.52
3.0	5.41	7.51	9.65	30.02	42.58	63.48
5.0	5.22	7.52	9.56	31.25	43.21	62.58
8.0	5.21	7.56	9.61	30.02	41.85	61.95
10.0	5.16	7.35	9.49	29.95	42.68	60.64
12.0	5.08	7.16	9.45	29.86	40.28	60.98
15.0	4.98	7.02	9.55	28.64	39.33	60.48

All of these findings show that the examination of the influence of the alternative fuels on the products could be of high significance.

Usage of sewage sludge in cement manufacturing could also cause some problems to the kiln systems. For example, a chlorine content of the sludge of more than 0.2 - 0.5 percent may cause clogging in the cyclone preheaters. To restrict the hazardous oxide contents, it is suggested the maximum sewage sludge feed rate to be no more than 5 percent of the clinker production capacity of the cement plant unless the sludge is conditioned and stabilized by lime, normally 0.3 – 0.5 kg CaO/kg dry sludge [80].

1-8-3) Waste plastics

Waste plastics (or plastic wastes) are generated from municipal solid waste (MSW) and other similar sources. These materials usually include either plastic scrap from manufacturing processes or post-consumer plastics obtained from MSW recycling programs. Figure 1.26 shows waste plastics as packaged form. In recent years, several cement plants have reported establishing use of plastics as an alternative fuel. The interest to use these materials as fuel is increasing and investigations are being conducted in making their use feasible [95, 96].

Figure 1.26. Waste plastics, packaged to be recycled as fuel [97].

Technical reports of cement manufacturing indicates that the principal issues regarding the use of plastics include identifying (generating) an adequate long-term supply of the material. In addition, it is important to be ensured that the material is clean and not contaminated with the other MSW contents (non-plastic materials). It is reported that waste plastics possess a calorific value similar to that of coal (approximately 8-10 kJ/kg depending on the type of waste plastics). The availability of these materials for use as alternative fuel is also dependent on the relative cost of disposal in landfills and/or the relative cost of alternative beneficial uses. Alternative fuel suppliers have reported that the available supply of plastics may be limited because MSW recycling agencies may be more interested to use post-consumer plastics as recycled raw materials, rather than to use in cement kilns or other facilities for energy recovery.

It is of utmost importance that the plastic materials be adequately separated from the general solid waste stream to facilitate material handling and usage. On the other hand, chlorinated plastics (e.g., polyvinyl chloride) must be segregated from other plastics because cement kilns need to limit the amount of chlorine feed to the kiln to ensure clinker quality. The chlorine in the plastic can generate air emissions (e.g., chlorinated dioxins) if it is in excess of the permitted limits. Also, the chlorine content can affect the quality of the clinker produced. However, cement plants in different regions may have different tolerances for the amount of chlorine, depending on the alkali content of the raw materials and other parameters [67, 95, 96].

1-9) Minor components in cement

The use of waste materials or industrial by-products as alternative fuels or raw materials in cement production is gaining worldwide interest. However, beside of the beneficial impacts of their use, there are also deleterious effects. Apart from the potential detrimental environmental implications (e.g. emission of hazardous materials), some of them may introduce elements which have not traditionally been found in significant quantities in Portland cement clinker. As a consequence, cement chemistry and the ease of combination of the clinker raw feed constituents in the kiln, which both influence the clinker quality, are influenced [22, 98-100].

Common examples of these elements would be phosphorous from sewage sludge used as alternative fuel, magnesium from blast-furnace slag used as an alternative raw material and manganese from various waste streams derived from steel manufacture. A number of these elements are regarded as problematic due to their ability to form stable compounds or solid solutions with C_2S, thereby preventing combination in the kiln and leading to high free lime contents and poor quality cement. This list would include strontium, boron and phosphorous. Sulfate could also be included because at moderate concentrations it has been reported as restricting or preventing the formation of C_3S [98]. Silicate and calcium aluminate networks retain large amounts of Cd [101], Pb, Cr and Zn, but modify their behavior during hydration [102]; Cd and Zn delay setting and diminish strength [103], while Cr shortens setting time and increases early strength [104]. Odler and Schmidt [105] performed a careful study on the effect of ZnO on the Portland cement structure. They found that the amount of C_3S and C_4AF formed increases significantly, while C_2S and C_3A decrease due to this addition. The influence of oxides of Mo, Nb, W and Zr[106] was also studied and it was found that they affect the microstructure and properties of clinker. For instance, the Mo and the W produce a viscosity decrease of molten product formed during clinkering; consequently there is an increase of diffusion rate of solids and bigger alite crystals were obtained. Results must be interpreted with caution and it is important to consider the magnitude of addition, because the fixation efficiency depends on the addition level compared with saturation level and with the thermal effect (calcination temperature, residence time, partial gas pressure, etc.).

Usually the economic benefits for using alternative materials containing these elements is overwhelmingly high; and in many cases a fall in quality is regarded as an acceptable price to pay. However, in many cases there are solutions available which will

compensate for the quality loss when using waste streams. For example it has been well documented that the use of fluorine as a mineraliser in the case of high levels of sulfate can facilitate the lower temperature formation of C_3S and produce a cement of higher quality than without these two components [98].

The effect of minor elements is largely dependent on the type of elements and their concentration levels. On the other hand, the level of application and amount of substitution of alternative fuels in cement kilns are closely related to their composition and concentration of minor elements. Therefore, a thorough understanding of effect of minor elements in cement composition is of great significance. In this section, cement elements will be classified according to their presence in the composition and the impact of important ones will be discussed separately. Bhatty has categorized cement elements into four parts as major, lesser, minor and trace elements [22].

- **Major Elements**

The elements that are more abundantly present (>5wt%) in cement clinker are the major elements. These are calcium (Ca), silicon (Si), aluminum (Al), iron (Fe), and oxygen (O). These elements compose the main minerals in clinker, which were discussed in section 1-5, in depth.

- **Lesser Elements**

Four lesser elements are alkali elements of sodium (Na) and potassium (K), magnesium (Mg), and sulfur (S), which appear in virtually all commercial clinkers at l-5 wt% concentration, are represented in chemical analyses as oxides like Na_2O, K_2O, MgO, and SO_2.

- **Minor Elements**

Elements other than the major and the lesser may be considered as minor elements. The concentration levels of minor elements in the clinker are almost always less than 1 wt% and are generally categorized on the basis of the frequency with which they occur in the raw material mix. Manganese (Mn), phosphorous (P), chlorine (Cl), titanium (Ti), fluoride (F) and barium (Ba) are classified as minor elements in cement chemistry.

- **Trace Elements**

The elements occurring at less than 0.02% or 100 ppm are classified as the “trace” elements. Nickel (Ni), cobalt (Co), molybdenum (Mb), zinc (Zn) and vanadium (V) are some of the trace elements in cement composition. Due to their extremely small concentration levels, it seems unlikely that the presence of trace elements will have any significant effects on cement manufacturing. However, their effects on clinker can significantly change if concentrations are increased beyond certain levels [22].

Table 1.9 contains a list of minor constituents (including lesser, minor and trace elements) with their average quantities in OPC clinkers.

Table 1.9. Minor compounds and their quantities in OPC clinkers[22].

Minor Compounds	Mean Value (%)
MgO	1.48
K_2O	0.73
SO_3	0.80
Na_2O	0.16
TiO_2	0.27
Mn_2O_3	0.06
P_2O_5	0.10
SrO	0.09
Minor Compounds	**Mean Value (ppm)**
ZnO	120
Cr_2O_3	103
V_2O_5	100
Cl	90
As_2O_3	56
CuO	55
PbO	16
CdO	0.5
Tl_2O	0.3

In cement manufacturing care is taken to avoid constituents which, even when present in small amounts (< 1%), may have adverse effect upon the performance of the product and/or the production process [1].The role of some of minor and trace elements in the formation of clinker and their effect on cement properties are discussed in this section.

- Alkalis

Potassium (K) and sodium (Na) are the most common alkalis found in cement. According to Table 1.9 K_2O and Na_2O are found with 0.7 and 0.15 wt% quantities in OPCs. Since sodium and potassium occur together in raw feed and because of their

similarities in their behavior in cement, it is appropriate to discuss them together. The alkali content of cements usually come from the raw materials and can be maintained at a given level with a careful selection of materials and control of high-alkali dusts from the kiln system [1, 22].

The alkali metals have a very strong affinity for SO_3 and where there is sufficient sulfate, the alkalis are normally present as compounds of sulfates such as K_2SO_4 (arcanite), Na_2SO_4 (thenardite), $Na_2SO_4 \cdot 3K_2SO_4$ (aphthilalite) and calcium langbeinite $2CaSO_4 \cdot 4K_2SO_4$. If their amount is more than the required stoichiometric balance, the excess will be dissolved in the silicates, aluminates, and ferrites. Table 1.10 shows the alkali ranges in the main phases as reported by Lea. The Na_2O is considered to mostly enter the C_3A where it normally increases the reactivity. The K_2O mostly enters the C_2S (C_3A as well) where it again enhances the reactivity to water, but may inhibit its conversion to C_3S and thus lower the overall reactivity. Therefore, high alkali levels affect the setting behavior of cement. If present in excess, alkalis often lead to higher pH and better early strength, but lower 28 day strengths [1, 17, 22, 107].

Table 1.10. Range of alkali distribution in main phases [22].

Clinker Phase	Na_2O (wt%)	K_2O (wt%)
C_3S	0.1-0.3	0.1-0.3
C_2S	0.2-1.0	0.3-1.0
C_3A	0.3-1.7	0.4-1.1
C_4AF	0.0-0.5	0.0-0.1

Where the alkalis are present as their sulfates, the viscosity of liquid phase is decreased, thus promoting the formation of C_3S and increasing its crystal size to a point where its hydraulic activity is inhibited. If the alkalis are not there as their sulfates, the liquid phase viscosity is increased and the formation of C_3S inhibited.

In addition, because of the alkali-silica reactions, high alkali amounts can be problematic in the presence of moisture, in which it cause expansive reactions with certain types of aggregates and gives rise to cracking in concretes and mortars [1, 22].

- Sulfur

Sulfur incorporates into the clinker composition as sulfur oxide in average amounts of ~1 wt% (Table 1.9). Since sulfur is introduced into the system through the fuel (mostly coal and petrocoke) as well as the raw materials, the sulfur content of the fuel can become an important factor in kiln system operation [17, 22].

As stated for alkalis, sulfur and alkalis have an interest to form alkali sulfates, with mentioning that it is unlikely that the proportions of both would be always in right amounts to form only them. Some sulfur (sulfate) also enters into the structure of the main clinker phases, particularly C_2S (up to 0.5 wt% SO_3). Belite also may contain small inclusions of alkali sulfate. Belite sulfate contents generally increase as the total clinker sulfate increases [3, 108,109].

It has been reported that increasing sulfate amounts decreases alite, increases belite and the aluminate and ferrite contents are not affected distinctly (Figure 1.27), especially in low silica modules (SM). Increment of sulfate contents also results in alite crystals growing larger. The crystal sizes of aluminate and ferrite phases are on the other hand significantly reduced [110, 111].

Gies et al. [112, 113] has reported that a belite-rich cement could be produced by using increased sulfate contents in alkali free raw materials with reasonable hydraulic activity. This was related to the presence of 0.6-0.8 wt% sulfate in belite.

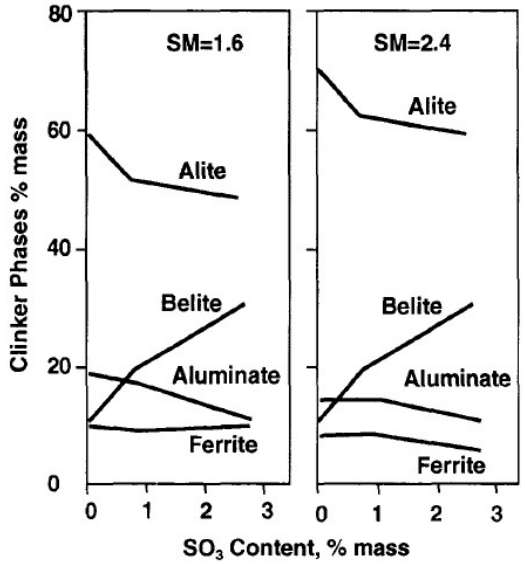

Figure 1.27. Phase contents of clinkers as a function of SO_3 amount, for two SMs[110].

It is normally more beneficial for the clinkering process that there is an excess of sulfur over alkalis [110].

If the clinker sulfate content is gradually increased (perhaps by burning a higher-sulfur fuel like petrocoke), there will be less alkali in aluminate and belite and more alkali sulfate as arcancite. This causes better combinability and cement performance improves. If the sulfate amount is increased further, the excess sulfate combines with calcium to form double sulfate calcium langbeinite, which is useful as set controller [3]. However, Gartner's research [114, 115] has shown that sulfate compounds in clinker are rather unreactive and do not contribute much to set control or to the hardening of paste. So, even a high sulfate clinker needs additional sulfate, which generally comes from gypsum to achieve enough set control. This, however, depends upon the C_3A content, and sulfate should not exceed the maximum limit specified by ASTM C150 without the sulfate expansion test. It might be noted that excessive sulfate in cement can lead to expansion problems in concrete [22].

The fact that sulfate compounds would form, is the reason why it is generally possible to use fuels with high sulfur content in the cement industry without significantly harmful consequences to the cement and also to environment [17, 116].

Oxidizing conditions in the kiln system are particularly important if sulfur is to be maintained in the clinker in order to combine with the alkalis. However, care has to be taken because an excess of sulfate will result in the formation of low-melting-point eutectics based upon alkali sulfates and calcium sulfates and therefore lead to build-up and blockages in the kiln[1, 17].

- Magnesia (MgO)

According to Table 1.9 the average amount of MgO in clinker composition is ~1.5 wt%. Magnesium (Mg) in Portland cement is mainly coming from magnesium carbonates present in the limestone, although smaller amounts are derived from clay and shale [22].

Small amounts of magnesium can replace calcium in four main phases, but if these phases cannot accommodate all of Mg within their crystal structure, the excess will be formed as large periclase crystals. The soluble amount is related to the cooling rate of clinker. When clinker is rapidly cooled, it retains most of MgO in aluminate and

ferrite phases and some content in alite. This amount decreases with cooling rate. Periclase was discussed previously in section1-5-5, too.

Small amounts of periclase are not problematic and may improve burnability; however large amounts are unfavorable, since the conversion of magnesium oxide to magnesium hydroxide is an expansive reaction and cause unsoundness in concrete. Therefore, standards usually impose a maximum limit of 5 wt% in MgO content in cement [1, 3, 22].

- Carbon

Carbon (C) is a major component of fuels (particularly fossil fuels and petrocoke). It is also present as carbonate in the limestone. Carbon as CO_2 is extensively present in cement kiln systems, but is not present in any significant levels in clinker [22].

As discussed in section 1-9, one of the problems associated with the usage of alternative fuels instead of conventional fuels is the incomplete combustion in the kiln. Incomplete combustion gives rise in the carbon content in the product. This is undesirable for the following reasons. First, high carbon content accelerates corrosion of steel in concretes. Secondly, the carbon absorbs water reducing the quantity available for hydration reaction. Thirdly, the alkalinity of the cement is affected. Finally, high carbon content ash darkens the concrete reducing its aesthetic appeal and leading to inaccurate prejudgments of the concrete quality [17, 117].

- Manganese

Manganese (Mn) is usually present in cement clinkers in the order of 0.02-0.14 wt% as Mn_2O_3. This element usually comes through raw materials like limestone and shale.

Manganese substitutes for ferric oxide in the flux and where this occurs, viscosity is decreased. This can lead to the formation of excessively large alite crystals and free lime which are not useful with respect to strength development. If the Mn_2O_3 content increases up to 0.5 wt% or above, reductions in the early strength-giving properties of the cement can be expected. The polymorphism of silicates in clinker may also be affected by the presence of manganese oxides in the raw material [1, 22].

Figure 1.28 shows distribution of some of elements (transition metals) in the main clinker minerals as determined by Hornain [118].

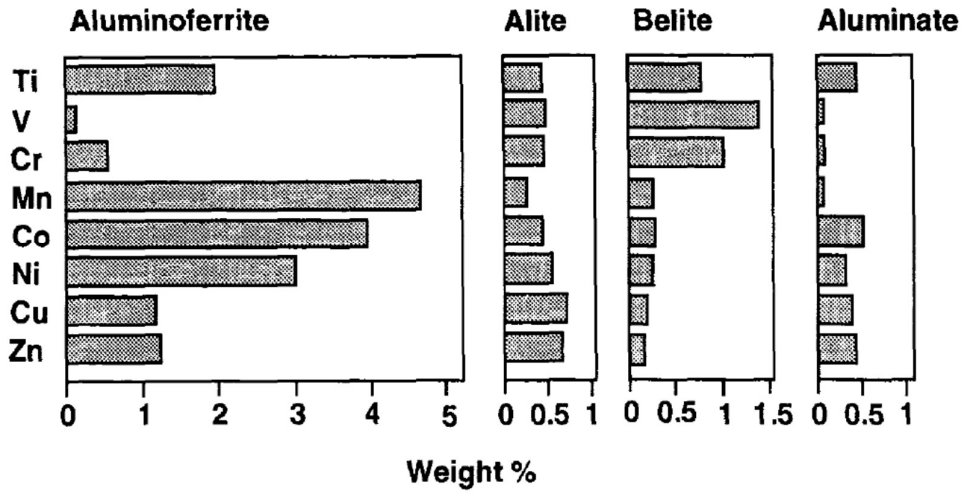

Figure 1.28. Distribution of transition elements in main clinker minerals [118].

- Titanium

The titanium is present as oxide ($Ti0_2$) in cement and its content is generally within the range of 0.14-0.43 wt%. TiO_2 is a refractory material (boiling point: 2500-3000 °C) and could be essentially important in clinker manufacturing.

Hornain [118] has reported that TiO_2 is preferentially distributed in ferrite phase (Figure 1.28). It was observed that a sharp reduction in alite with equal gain in the belite phase occurs when $Ti0_2$ is increased in the raw mix. Alite crystal size increased progressively with 0.2 and 0.4 per cent $Ti0_2$additions, suggesting mineraliser characteristics.

At low contents the effects of Ti on the cement strength is insignificant, however higher levels up to 1 wt% of TiO_2 can inhibit early (1-2 days) strength development, but may improve strengths at ages in excess of 3 days.

It was also reported that about 1 wt% TiO_2 addition in the raw mix reduces the melt temperature by 50-100 °C, probably because of a favorable relationship between ionic potentials and the melt viscosities [1, 22].

- Vanadium

Vanadium is present as V_2O_5 in cement clinker and it usually occurs in the order of 100 ppm. Although it can come from raw materials, it is also prone to be derived from fuels like petroleum coke. In one study, Weisweiler et al. [119] has reported nearly 800 ppm vanadium in petrocoke. Petrocoke ash contains very high levels of V_2O_5 (up to 60 wt%), although due to a low overall ash content, Moir et al. [120] found no more than 0.08 wt% V_2O_5 in clinker produced in cement kiln that used 50% petrocoke as an alternative fuel. Vanadium, if present, tends to be found in the alite, the crystal size of which increases with additions up to 0.4 wt%. However, according to Hornain (Figure 1.28) vanadium also could concentrate in belite. Odler et al. [121] reported that l wt% V_2O_5 can significantly reduce the free lime in clinker when fired at 1200°C.

Presence of vanadium oxide is reported to increase hydraulicity of alite, however a 0.2 wt% addition has lead to a 10% reduction in 28-day strength and this could possibly be associated with the increase in crystal size. High concentrations could also adversely affect the grindability of resulting clinkers.

There have been suggestions that the presence of low levels of vanadium compounds (the use of petrocoke as a fuel can contribute) could lead to a shorter refractory lining life. V_2O_5 is unlikely to vaporize at normal kiln temperatures. On the other hand, vanadium present in fuel may not have adequate contact with the reacting mass in the kiln and largely ends up in the kiln dust as suggested by data from Weisweiler et al. [119].

- Chromium

The chromium content in Portland cement clinkers is normally in the range 0.002-0.02 wt%. Most of this chromium is derived from the feedstock, from the fuel and in some cases from the refractory bricks. In some countries, cements are required to have hexavalent chromium contents less than 2ppm because of the health issue.

Nearly half of the chromium in clinkers has been found to reside in alite. Since increasing additions within the range 0-0.4 wt% increase the crystal size of both alite and belite, it may be considered to have some mineralizing effect. The presence of Cr in raw materials is known to reduce the viscosity of clinker melt due to its high ionic charge. Chromium is known to accelerate the hydration of paste and improve the early strength, and has thus been used to develop high strength cements. A 0.4 wt% Cr

content in the clinker has been reported to give a 10% increase in 28 day strength, which is probably associated with a reduction in the free lime [1, 22].

- Zinc

Zinc is a trace element in cement composition. Beside of the raw materials, it is shown that the usage of used oils and scrap tires could also bring zinc to the composition of clinker.

Zinc in clinker is preferentially retained in ferrite followed by alite, aluminate, and belite (Figure 1.28). ZnO additions accelerate the clinker formation. Alite formations increase at the expense of belite and C_3A due to ZnO. Up to 1 wt% ZnO in the raw mix decreases free lime considerably and retards the hydration. Although additions in excess of 1 wt% could reduce the early strength, late strength has been shown to increase.

The zinc content in tires is, from cement quality point of view, the main constraint in the use of scrap tire as an alternative fuel [22, 105].

- Phosphorous

Phosphorus (P) as phosphates is present in limestone and shale as raw materials. However, P is also found in sewage sludge (one of the major alternative fuels) and thus is important to be investigated. A thorough explanation for the effects of phosphorous in phase formation was given in section 1-9-2, with regards to its presence in sewage sludge.

Cement clinkers contain typically around 0.2 wt% P_2O_5. A high P_2O_5 concentration decomposes C_3S to C_2S and free lime. When higher amounts of P_2O_5 are present, the C_2S is stabilized to an extent that the conversion to C_3S is inhibited. The addition of small amounts of fluorine-containing compounds prevents this effect and permits the formation of C_3S to proceed. When the amount of P_2O_5 present exceeds 1 per cent, it has been reported that 10 per cent of C_3S is lost for each additional 1 per cent of P_2O_5 added. The electron microanalysis results by Ifka et al. [122] have shown that belite and alite accommodate nearly all the phosphorus in the clinker.

It has been stated that an appropriate level of P_2O_5 in clinker reduces the negative effects of alkali on the strength properties of cements. It has also been suggested that P_2O_5 improves the hydraulic properties of belite [1, 22].

- Chlorine

Chlorine is a trace element in clinker composition; however like other halogens it is found frequently in raw materials and fuels. Therefore its role is important. Coal as a primary fuel as well as used oils and scrap tires as secondary fuels can contain high amounts of chlorine up to 0.3 wt%.

The chlorides easily volatilize in the burning zone and condense in the heat exchanger to combine with alkalis to form low-melting-point mixtures. Their effect on the operation of kilns with cyclone preheaters and gate preheaters is very serious. However, since most of the chlorides are volatile, the amount retained in clinker is extremely small (<0.03 wt%). Volatile chlorides react readily with alkalis, so that the alkali level in the clinker is often reduced when chloride is present (sometimes Cl is added deliberately to control the amount of alkalis).

Chlorides, particularly $CaCl_2$, accelerate the hydration and hardening of cement paste and increase the very early strength. At the same time, chloride ions are also known to promote corrosion of steel reinforcing bars in concrete and are detrimental, so most standards for cements restrict the amount of chloride to 0.10 wt%.

In waste-derived fuels such as waste-oils contaminated with chlorides, polyvinylchloride (PVC), chlorinated hydrocarbons and scrap tires, the chlorides would occur in different compounds at much higher concentrations (Akstinat et al., 1988), and cause serious problems. Therefore, care has to be taken in order to make their use feasible [1, 22, 123, 124].

- Fluorine

Fluorine (F) is one of the other halogen elements that its role is significant in cement. Although it enters in small amounts through raw materials, it is frequently added deliberately as CaF_2 to the raw mix. CaF_2 acts as a mineralizer and flux to lower the burning temperature to accelerate the formation of C_3S and reduce fuel consumption [22, 125]. However care has to be taken not to use fluoride beyond 0.25 to avoid adverse effects on clinker behavior by selectively incorporating it into the aluminates or silicate phases at certain burning temperatures. Gartner [114] reported that the presence of fluorides beyond 0.5 wt% can cause both operational and quality control problems, which, under certain situations, can be controlled by P_2O_5 addition.

The presence of F beyond the threshold level stabilizes rhombohedral C_3S crystal structure, which is associated with improved hydraulic properties. Moir [126] demonstrated that by optimizing the levels of F, alumina, alkalis, and sulfates, the C_3S crystallization could be increased. On the other hand, fluorides addition results in formation of calcium langbeinite which increases the setting times and reduces early strengths.

There are indications that the use of fluorine as a mineralizer may give rise to the build-up of excessive coating in the kiln and that this may be due to the formation of additional spurrite [1, 22].

- Lead

Lead (Pb) can be present in trace amounts in raw materials, but it also may be present at some levels in fuels like coal, petrocoke, used oils and scrap tires. Lead tends to vaporize in the kiln and be collected in the kiln dust. There is also evidence that some lead can still be retained in the clinker (0.001-0.02 wt% as PbO). However, Pb has been shown to have no adverse effect on cement properties if present below 70 ppm. The studies on hydration behavior have shown that the initial setting time is increased with a consequent loss in early strength with Pb. However, the 28- and 90-day strengths are comparable to or higher than those of the control [1, 22].

- Molybdenum

Molybdenum (Mo) is one of the other trace elements in cement composition. Molybdenum, having small radius and a high charge number, is an effective reducer of the clinker melt viscosity. The formation of large round alite crystals in clinker prepared with up to 1.5 wt% MoO_3 addition with some modifications in belite has been reported. However, cement pastes prepared from these clinkers exhibited no adverse effects on the engineering properties. The 28-day strengths increased to a maximum with up to 0.5 wt% molybdenum, but were significantly reduced when 3 wt% was incorporated [1, 22, 127].

1-10) Quality control in cement manufacturing

Like all kinds of materials, cement's properties are also directly related to its chemistry and microstructure. Therefore, it is very important to characterize these features to have an understanding of the physical, chemical and mechanical properties

of the cement. Among the many methods, there are a few which are mostly used in the cement studies and manufacturing processes. In this section, some of these methods will be described.

1-10-1) XRF analysis

Currently, in most of the cement manufacturing processes, X-ray fluorescence analysis (XRF) is used to determine the chemical composition of the raw materials and clinkers. The phase composition is computed from the chemical composition by Bogue's calculation. As discussed previously, the proportions of each of the main phases (alite, belite, etc.) are of major significance in determining the properties of the cement produced from the clinker. The Bogue calculation is a very useful method of approximating the quantities of the main minerals in the clinker or cement. If we know the oxide values from the XRF analysis, we can calculate how much of each mineral is present. In principal, this method is calculating the potential phase composition based on some simplifying assumptions, like ignoring the extent to which the oxides have truly combined.

Respectively, alite (Eq. 1.7), belite (Eq. 1.8), aluminate (Eq. 1.9) and ferrite (Eq. 1.10) phase amounts are calculated through the following equations:

$$C_3S = 4.071CaO - 7.6024SiO_2 - 6.7187Al_2O_3 - 1.4297Fe_2O_3 \quad \text{(Eq. 1.7)}$$

$$C_2S = -3.0710CaO + 8.6024SiO_2 + 5.0683Al_2O_3 + 1.0785Fe_2O_3$$

$$= 2.8675SiO_2 - 07544C_3S \quad \text{(Eq. 1.8)}$$

$$C_3A = 2.6504Al_2O_3 - 1.6920Fe_2O_3 \quad \text{(Eq. 1.9)}$$

$$C_4AF = 3.0432Fe_2O_3 \quad \text{(Eq. 1.10)}$$

It can be understood that the mineral proportions computed with the Bogue method, would only be expected if everything were to combine and all the chemical reactions reached equilibrium as the clinker cooled [1, 3, 6, 16, 128]. Studies have been done to modify and improve the Bogue's calculations [129-131].

The actual phase composition is not easy to calculate without additional information, in particular, the true compositions of the minerals. These data can be determined by SEM and x-ray microanalysis.

1-10-2) Microscopical analysis

Analysis by microscopy reveals the microstructure and therefore it is capable of providing an in-depth understanding of the cement properties. Optical microscopy (OM) and scanning electron microscopy (SEM) can be utilized to characterize the mineralogy and microstructure of both clinker and hydrated cement. The microscopical analysis is an indispensable laboratory tool which is capable of providing important information on so many aspects e.g. the shape and size of phases, homogeneity of the mix and phase distribution and equally important, the porosity distribution. Each of these features is of tremendous importance in the quality control of cement manufacturing. The types of characterization performed on clinker by OM and SEM can be named as the quantification of the amounts of alite, belite and the matrix phase, and the crystal size distribution of alite and belite. Qualitative characterization could be the shape of the clinker phases (both SEM and OM) indicating the cooling conditions, the reactivity of alite and belite indicated by color (OM) and the birefringence of alite (OM) indicating the changes in the structure of alite [25-28, 132, 133].

On the other hand, analyzing the microstructure and morphology of the phases after the hydration reaction is also significant in characterizing the cement properties. The amount of the hydrated and unhydrated phases indicating the hydration development, the amount of ettringite and monosulfate during the hydration time and the shape of hydration products are just a few aspects to name.

An important part of the microscopic examination is the preparation of the clinker samples. A frequently used technique of preparation is embedding either the whole or crushed nodules of clinker or hydrated paste in epoxy resin. After that, the samples are cut, ground and polished. Figure 1.29 shows clinker samples prepared for microscopy analysis. For the case of OM, these samples have to be etched. Etching is a technique of imparting color to various crystalline phases in clinker. Certain phases can be resolved in the reflected light. On the other hand, in SEM samples have to be coated with a conductive layer of carbon or gold prior to the examination.

Figure 1.29. Clinker samples embedded in epoxy resin and polished to be used in microscopical analysis [28].

In SEM, the electrons of the high-energy beam interact with the atoms of the sample, thus producing signals that contain important information. The signals produced include secondary electrons (SE), back-scattered electrons (BSE) and characteristic x-rays. The low-energy secondary electrons are best for imaging the surface topography and morphology of the phases. More energetic back-scattered electrons are capable of providing compositional contrast images. Heavy elements (high atomic number) scatter the electrons backwards more strongly than light elements (low atomic number), and appear brighter in the image [134, 135]. Therefore, the cement phases with different average atomic weights appear in various grey scales. For example, among the four main phases in clinker, ferrite, alite, belite and aluminate appear as the brightest to darkest in the microstructure possessing the highest to lowest average atomic weight (Figure 1.6-a). This makes the phase detection and thus quantitative analysis feasible. The same routine works for distinguishing the phases in hydrated cement. The incorporation of water during hydration leads to hydrates. These hydrates have much lower average atomic values than the unhydrated (anhydrous) materials, and therefore strong contrast is obtained between these two regions. There is weaker, but still discernable, contrast among the unhydrated phases, themselves. Within the hydrates, Portlandite (CH) is significantly brighter than the other hydrates. However, it is not possible to differentiate on the basis of grey level alone between the other hydrates (C-S-H, ettringite, etc.).

SE mode provides a better spatial resolution and is useful to investigate the fracture surfaces. Therefore, for analyzing the hydrated phases it is best to use SE [3, 25, 133, 135].

The other important signal produced in the electron-atom interaction is the characteristic x-rays. Characterizing these signals through the energy dispersive X-ray

spectroscopy (EDS) makes the identification of component or elemental composition of a point or an area possible. Using this method, it is possible to determine the exact composition of various phases with a 0.1 wt% precision[26, 134, 135].

1-10-3) XRD analysis

To enable design and manufacture of cement with a wide range of properties, a more thorough characterization of the cement may be needed. In addition to chemical composition and phase composition analysis with the previously mentioned methods, the information about the cement minerals, analyzed by X-ray diffraction analysis (XRD) could be very useful. Powder XRD is used to identify the minerals and characterize their crystallographic structure in clinker or hydrated cement as well. The X-ray diffraction of powder samples results in a pattern characterized by reflexes as peaks in intensity at certain positions. The height, width and position of these reflections can be used to determine many aspects of the material structure [6, 136, 137]. The XRD patterns are recorded. Then Rietveld analysis is usually used to determine the mineral composition. The method is able to deal reliably with overlapping reflections [138]. In this method, a least squares approach is utilized to refine a theoretical pattern until it matches the measured pattern. Figure 1.30 shows an example of a Rietveld analysis of a cement powder. The relative inaccuracy of the amount of a mineral determined by Rietveld's, increases with decreasing amount of the mineral [139-142].

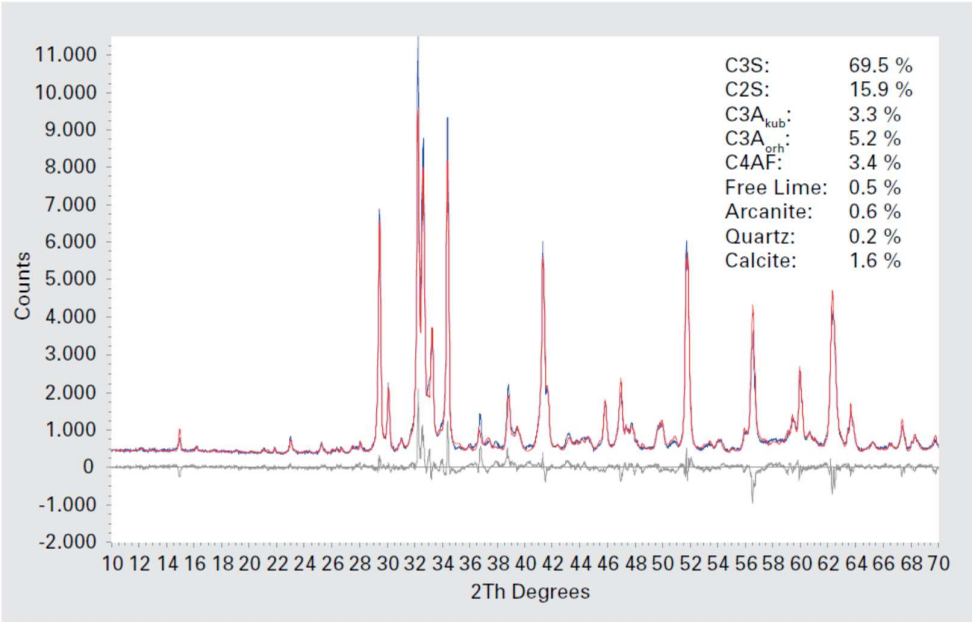

Figure 1.30. Rietveld analysis of a cement powder sample [141].

According to Taylor [6], the potential use of XRD powder diffraction in the study of clinker or hydrated cement includes the qualitative and quantitative determination of polymorphic modifications, state of crystallinity and other features of individual phases. Due to the lack of adequate reference data, Taylor considers XRD to be generally less satisfactory for examining the clinker phases than SEM and x-ray microanalysis. Nevertheless, in the experiments carried out by Stutzman and Leigh [143], XRD and OM methods were compared and the XRD data agreed with the OM data with the exception of aluminate. The XRD data showed greater precision than similar measurements by microscopy.

1-10-4) Other analysis methods

In addition to the described analysis methods, there are lots of other methods to characterize the properties of cement.

The quality of cement during the grinding process is controlled by measurement of fineness, sieve residues, amount of tri-sulfur oxide and loss on ignition. The particle size distribution will further explain the variation in properties at early ages compared to a simple measurement of specific surface by Blaine's method.

Some of the cement samples from the cement mills are tested with respect to setting and strength, and their relative chemical composition is analyzed. The properties being tested in the samples are compressive strength up to 28 days, amount of water required to achieve standard consistency and the setting time.

The amounts of di- and hemihydrate of gypsum could be determined by differential scanning calorimetric (DSC) analysis or thermogravimetric analysis (TGA) [5, 6].

Chapter2: EXPERIMENTAL WORKS

2-1) Hydrated cement tests with commercial OPC

In the course of becoming familiar with cement and its properties, a 50kg packed commercial type IV pozzolanic cement (32.5 MPa) was provided.

The first experiments were done with this cement to obtain the optimum w/c ratio. 4 different w/c weight ratios used to prepare cement pastes: 0.3, 0.35, 0.42 and 0.5. The samples were prepared by mixing the cement powder with the related amount of water (tap water) using a kitchen mixer. After mixing, the pastes were jolted by 50 times hitting on a table. These pastes were poured in round-shaped moulds. After 24 hours, the samples were taken out of the moulds and kept in moist environment. The samples were then cut by a cutting saw in the cubic form of 4*4*4cm prior to the compression test. Compressive strength tests of the samples were carried out on the 14^{th} day of hydration using a Zwick-RoellZ-100 UTM machine. The graph related to the results of this experiment will be shown in the results section.

In the second part of the experiments using the commercial cement powder, hydrated samples were produced to obtain the strength development graph. Appropriate mould was prepared to manufacture the specimens. The stainless steel mould consisted overall of 9 parts as of a 3*3 order.

A water to cement (w/c) ratio of 0.3 was chosen to prepare hydrated cement samples due to the optimized strength and workability. A 6*3 set of samples were prepared and kept under water until strength test time. According to the EN 196-1 standard, hydrated cement pastes should be kept under the water. This is due to the continuation of the hydration in the outer surface as well as the inner parts of the samples. The samples were tested for the compressive strength with the same UTM machine at 1, 2, 4, 7, 14 and 28^{th} day of the hydration.

2-2) Sample production

Clinker and cement samples were produced in the AkçanSA company.

In the first part of the project, 5 different clinker samples were manufactured in the cement firing kilns. The raw materials, heating and cooling conditions of these

samples was tried to be kept constant. On the other hand, the fuels which were used to burn the samples were different. Each of these clinker samples were produced by different combinations of alternative fuels. One of the clinker samples was made in the dirty kiln using a combination of all different kinds of alternative fuels. The word dirty is describing the condition of the kiln after one year of functioning prior to restoration. One other sample was prepared in the clean kiln (right after the restoration of the kiln) using only petrocoke as the firing fuel.

The other three samples were manufactured using petrocoke and one of the plastic waste, sewage sludge and the mix of plastic waste and sewage sludge as the alternative fuels. The detailed production information of the clinker samples with their identification is provided in Table2.1.

Table 2.1. Production conditions and fuels used for burning clinker samples.

sample ID	kiln condition	fuel	alternative fuel	AF amount
clinker#1	post-restoration (clean)	petrocoke	-	-
clinker#2	pre-restoration (dirty)	petrocoke	all alternatives	-
clinker#3	post-restoration	petrocoke	waste plastics	1500kg
clinker#4	post-restoration	petrocoke	waste plastics sewage sludge	1500kg (PW) 2000kg (SS)
clinker#5	post-restoration	petrocoke	sewage sludge	2000kg

AF:alternative fuel- PW:waste plastics- SS:sewage sludge

Although the chemical analysis of the consumed fuels is not available, the analysis of their ashes after the firing could also help to reveal the chemical composition of these fuels. This data is shown in Table2.2 for petrocoke, waste plastics and sewage sludge.

Table 2.2. Chemical analysis of ashes of fuels used for firing the clinker samples.

fuel	% ash	H_2O (%)	SiO_2	Al_2O_3	Fe_2O_3	CaO	MgO	SO_3	Cl^-	Na_2O	K_2O	total
petro coke	6,44	-	22,1	12,9	5,1	36,8	1,3	19,9	0,06	0,6	0,9	99,7
waste plastics	8,63	20,0	27,1	8,1	12,5	38,1	0,1	8,2	3,16	1,9	0,7	99,9
sewage sludge	-	-	41,3	13,9	8,2	25,7	4,1	2,2	0,08	1,6	2,1	99,6

In the second part of the project, clinker samples were grinded with the standard OPC grinding conditions to the Blaine fineness of ~3000 cm^2/g and were added with 3-4 % gypsum. All of the cement powder samples were prepared with the same procedure from the related clinker samples.

In the third part of the project, the clinker#4 was prepared again twice for controlling the truthiness of the results collected at the prior parts of the project.

2-3) Characterization of the clinker samples

The clinker samples which were produced by the AkçanSA company (Figure 2.1) were analyzed by different characterization methods. The microstructure of the samples was analyzed by VLM and SEM. The chemical analysis was done by XRF and EDS, whereas the phase analysis was done by XRD.

Figure 2.1. Clinker nodules in various sizes, manufactured at AkçanSAcompany.

2-3-1) Microscopical analysis

The microstructure of the clinker specimens was investigated using VLM and SEM. Prior to the microstructural analysis, the preparation of specimens was done. A cold-setting epoxy was used to immerse the clinker nodules in the 4cm-diameter moulds. The epoxy was prepared by mixing a liquid and a powder as the hardener with the prescribed proportions. The epoxy was poured in the mould and the clinker nodules with different sizes were put in the mould one by one. The rest of the epoxy was used to fill out the mould and then it was left to set. The cold-mounted specimen hardened completely after ~5 hours. After taking out the specimen from the moulds, they were grinded and polished carefully. As the polishing-aid fluid, instead of water, ethylene

glycol was used to prevent excess heating and also carrying the polishing debris. The sandpapers which were used for grinding were in the order of 50, 100, 200, 400, 600, 800 and 1000 grits. Then the specimens were continued to get polishing with 1200, 2000 and 4000 grits. In the final fine-polishing level, 6 μ, 3 μ and 1 μ polishing clothes along with their relative diamond pastes were used to prepare mirror-like surfaces on the specimens. It is worth mentioning that after each step of polishing, the specimens were washed with an ethanol-jet. In the final step, the specimens were washed thoroughly with ethanol using a sonicator for 20 min.

The SEM samples were coated with a thin Carbon layer (~30nm) to provide a conductive surface for the imaging. It has been proven that Carbon is the ideal coating for the cement microstructural analysis [135]. A JEOL JSM 6010SEM was used to observe the microstructure in both SE and BSE mode. The image of the prepared samples (epoxy-impregnated clinkers) is shown in Figure 2.2.

Figure 2.2. Polished epoxy-impregnated clinker nodules.

2-3-2) EDS analysis

The EDS was conducted to acquire chemical analysis data from the clinker samples. The analysis was carried out along with the SEM observations using an Oxford spectrometer mounted on the JEOL JSM 6010 SEM.

2-3-3) XRF analysis

The XRF measurements were carried out for each of the clinker samples to obtain the chemical analysis. The XRF analyses were carried out in the AkçanSA company.

2-3-4) XRD analysis

The phase analysis of the clinker samples was done with the XRD analysis. The specimen preparation was performed by selecting a few clinker nodules of each sample and grinding them with a pestle and mortar. Appropriate amount of grinding is necessary in order to acquire the accurate results from the XRD measurements. Thus, the grinding continued until the clinker powder achieved a particle size of less than 10 μ. The pulverized sample was then loaded into the sample holder and compacted with a glass slide to remove the excess powder. Figure 2.3 presents the sample holder of the XRD machine and the compaction method of the powder using the glass slide.

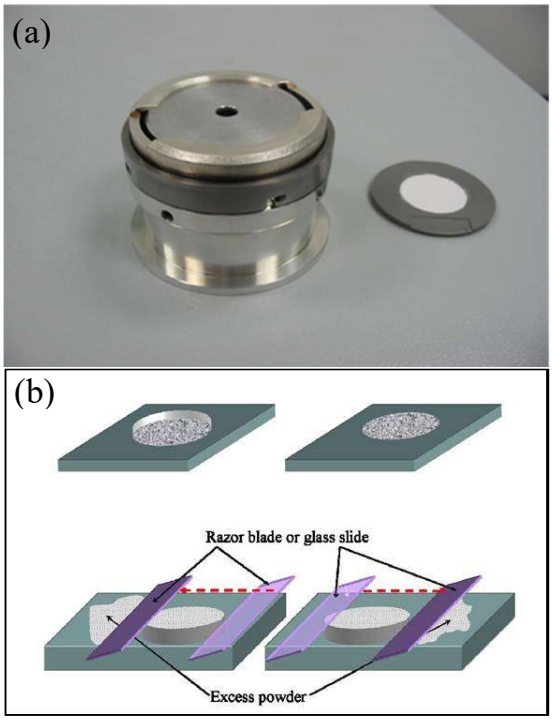

Figure 2.3. The sample holder of the XRD machine (a) and the compaction method of the powder using the glass slide (b).

The characterization was carried out using a Bruker D-8 Advance X-ray powder diffractometer using filtered Cu Ka radiation (λ=0.1542 nm). The measurements were done in the range of 5-90 and with a step size of 0.02. As a result, the diffraction spectrums were obtained in a time period of ~100 min. The raw data was used to identify all phases of the specimen, including calcium silicates, calcium aluminates and etc. The drawback of the conventional powder diffraction method, as was mentioned in chapter1, is that the peaks heavily overlap and therefore prevent the appropriate determination of the structure. The "Rietveld Method" creates an effective separation of

these overlapping peaks, thereby allowing a more precise determination[144].Therefore, the Rietveld method was utilized to quantify the phases identified using diffraction peaks.

2-4) Hydrated cement paste preparation

The cement powders for the hydration tests were provided by the AkçanSA company. The powders were prepared by grinding the clinker pellets (nodules)to the Blaine fineness of ~3000 cm^2/g and mixing with ~3-4% Gypsum, like the standard OPC powders. The cement powder samples were kept under isolation from the environment to prevent exposure to moisture.

The experiments were carried out according to the EN 196-1 (European Standard).

A w/c ratio by mass of 0.3 and 0.5 was used to manufacture the cement pastes. The water (distilled water) and cement were mixed using an automatic UTEST UTCM-0085 model mixing apparatus. According to the EN 196-1 standard, the mixer worked for 90s (60s low speed+30s high speed), stopped to recenter the cement paste in the container and continued mixing for another 60s in high speed. The half of the mix then poured in a 9-eye (4*4*4cm each) stainless steel mould. The ingredients of the mould were compacted by hitting on a jolting table (UTEST UTCM-0090 model) for 60 times. The rest of the paste was poured into the mould and another 60 times jolting was carried out to compact and extract the bubbles out of the paste. The falling height is 15 mm conforming to EN 196-1. At the end, the top surface of the mould was smoothened using a cement trowel.

The paste containing moulds were stored under moist conditions for 24 hours. The samples then were taken out from the moulds and kept curing in a water bath (20±1°C) until strength testing. The hardened cement paste sample can be seen in Figure 2.4.

Figure 2.4. The 4*4*4cm hydrated cement sample.

The stainless steel moulds were cleaned carefully and lubricated with olive oil to prevent corrosion.

2-5) Characterization of the hydrated cement samples

A few characterization methods were utilized to investigate the properties of the hydrated samples. Compressive strength test was carried out to investigate the mechanical properties. SEM was used to analyze the microstructure and XRD was used to perform the phase analysis of the hydrated cement samples.

2-5-1) Compression tests

In order to investigate the mechanical properties of the hydrated cement samples compression tests were performed. For each set of tests, 3 samples were prepared to obey the international standards and to acquire the deviance parameter. The compressive strength tests were carried out first with a Zwick-Roell Z-100 model UTM machine. Because the 100kN force was not enough to break our samples, it was tried to make smaller surface areas using 2 pieces of 2*2*0.5cm stainless steel slabs. However, in order to make the experiments more reliable, a cement compressive strength testing machine, UTEST UTC-4720 model with 2000kN force was utilized for testing all of the samples.

The samples which were produced using w/c:0.3, were tested at the 1, 2, 3, 7, 14 and 28th day of hydration, whereas the samples which were produced using w/c:0.5 were tested at 2, 7 and 28th day of hydration.

2-5-2) SEM analysis

After breaking the samples in the compression test, pieces of the samples were taken to observe the microstructure. These specimens were washed out with ethanol for 10 min and rested inside of an exicator for 2 hours to stop the hydration at the surface. The hydration samples were investigated in two different forms. In the first form, the samples were investigated for the morphology of the hydration products. For this reason, the broken surfaces of the samples were observed without any further treatment. However, in the second form, the surface of the samples was polished to reveal the phase distribution in the microstructure (Figure 2.5).

Figure 2.5. The hydrated samples after preparation for microscopy.

For preparing the second form specimens, 3 different methods were tried. First, the samples were impregnated into the epoxy, as the same method of observing clinkers. Second, the proper pieces of the samples were polished without impregnation. Third, the cement paste was prepared and poured into the epoxy-setting mould. All of the methods were investigated and it was concluded that the best method is the second one. Using this method, the sample preparation can be done in the minimum time. This fact was mostly important for the specimens which were going to be observed in the first few days of hydration.

All of the samples were coated with a thin layer of carbon prior to SEM observations.

2-5-3) XRD analysis

For characterizing the phase distribution in the hydrated samples, XRD was used. For this reason, the broken pieces of the cement samples after the compression test were taken and grinded using a pestle and a mortar. The pulverized samples were loaded on the sample holder and the X-ray diffraction analysis was done on them. The same

procedure as the clinker specimens' investigation was performed on the hydrated cement powders.

2-6) Control cement sample preparation

As the last part of the project, it was aimed to check the results obtained from the samples produced with different alternative fuels. For this reason, two sets of new cement samples were manufactured at two different days with the usage of a mix of waste plastics and sewage sludge as the fuel. Therefore, these new samples were the control samples of sample#4. The new samples were received as cement powders.

2-7) Characterization of the control samples

The new cement powders were characterized using SEM and XRD. Also, these cements were used to prepare hydration samples. The new cement paste samples were analyzed using compression test and XRD.

2-7-1) SEM of cement powders

In order to investigate the microstructure of the new cement powders, microscopy samples were prepared. The powders were mixed with epoxy and after the setting (hardening), the samples were grinded and polished. Before the SEM observations, samples were coated with a thin layer of carbon for providing the conduction.

2-7-2) XRD of cement powders

The phase analysis of the new cement powders was performed using x-ray diffractometry. The Rietveld method was utilized to calculate the phase values.

2-7-3) Compression test of hydrated samples

The compression test was used to analyze the mechanical properties of the hydrated cement samples. The cement pastes were prepared with the same method used for the previous cement samples. The compressive strength of the samples was tested in various days of hydration.

2-7-4) XRD of hydrated samples

After the compression tests, fractured pieces were collected and pulverized for the use in XRD analysis. The XRD measurements were carried out in several days of hydration and the quantity of the phases were calculated by using the Rietveld method.

Chapter3: RESULTS

3-1) First experiments with commercial OPC

As it was mentioned in the experimental section, the very first experiments of the project included preparation of hydrated cement samples from a commercial pozzolanic Portland cement powder. Figure 3.1 shows the compression test data obtained using different w/c ratios at the 14th hydration day. It is obvious that increasing the w/c ratio results in decreasing the compressive strength of the cement. It should be mentioned that with a w/c:0.3, the cement paste was still workable. Using this graph, it was decided to use 0.3 and 0.5 as the w/c ratios throughout the project.

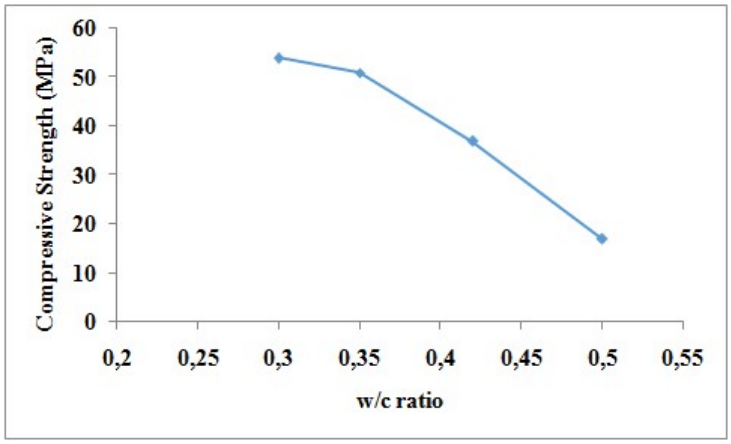

Figure 3.1. Compression test results for the commercial cement for different w/c ratios.

Using w/c:0.3, new hydration samples were prepared and tested for their compressive strength at various hydration days. Figure 3.2 presents the strength development graph of these samples showing the average amount for three samples with the error bars. It can be seen that the strength increases as the days of the hydration increases.

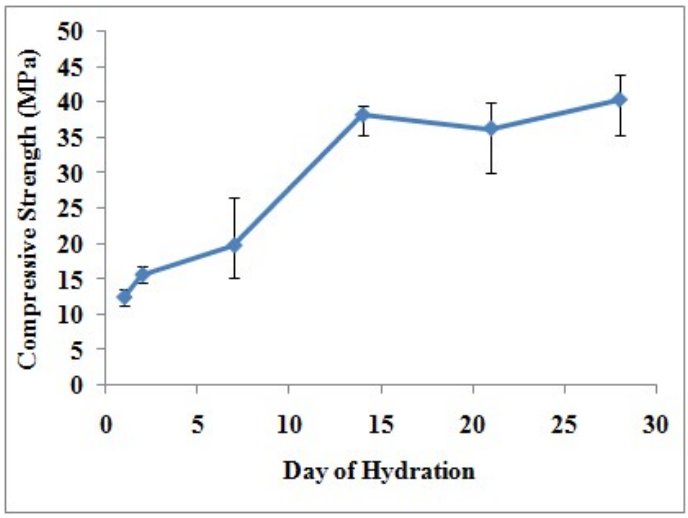

Figure 3.2. Compressive strength development of commercial cement samples during the hydration period.

3-2) Clinker analysis

3-2-1) SEM analysis

3-2-1-1) Imaging

The epoxy-impregnated clinker nodules of all the samples were investigated using a scanning electron microscope. Due to the ability to reveal the phase distribution of the clinkers by different average atomic weights of cement phases, BSE mode was used. Contrary to the SE mode which is suitable for investigating the topographical features on the surface of the samples, BSE mode is useful because of the capability to show the compositional contrast. In other words, the difference in the average atomic weight of the phases in the microstructure appears as the different shades of the grey color. As the atomic weight of the phases increases, the number of the back-scattered electrons from that region increases. This increment in the number of the electrons, i.e. signals, results in a brighter appearance in the SEM image.

For each of the clinker samples which were produced using different alternative fuels, at least 5 nodules preferably of various sizes were investigated. In Figure 3.3, a clinker nodule is shown at a low magnification as imaged in SE mode. The diameter of this nodule was approximately 4 mm.

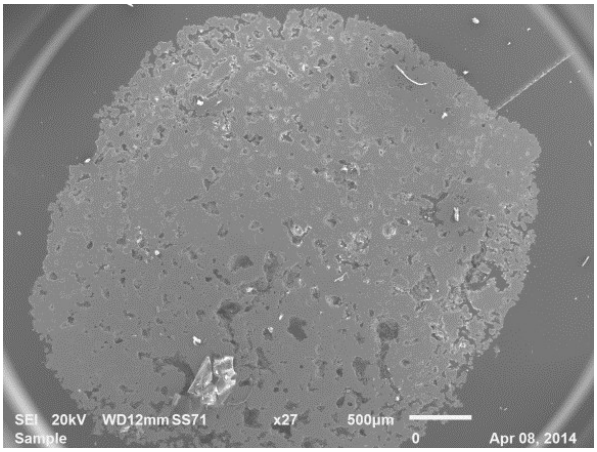

Figure 3.3. SEM image of a clinker nodule in low magnification in SE mode.

Figure 3.4 shows an SEM image taken with the BSEs to show the different phases revealed in the microstructure. Alite phase has an average atomic weight of 15.06 while belite phase has an average atomic weight of 14.56. Considering values, alite particles would appear brighter in comparison to the belite particles; which is illustrated in Figure 3.4. Aluminate and Ferrite phases, on the other hand, possess average atomic weights of 14.34 and 16.65, respectively. In BSE images, ferrite, alite, belite and aluminate will appear from the brightest to darkest contrast in this order as the main phases in clinkers. As discussed previously in chapter1, alite crystals had morphology of pseudohexagonally-shaped particles, whereas belite appeared as roundish-shaped particles in the structure of clinker. Matrix (liquid) phase of the clinker which comprises aluminate and ferrite phases usually solidify as a dendritic interstitial phase which appear in between the alite and belite particles. Also, the pores which are one of the main parts of the clinkers can be seen in Figure 3.5 as the darkest regions. Some of the pores have been filled with epoxy during the mounting process.

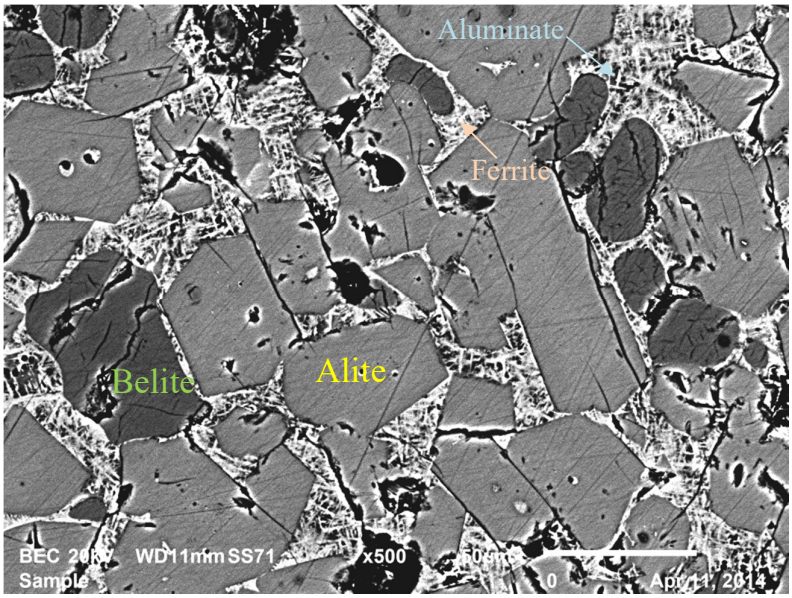

Figure 3.4. SEM BSE image of a clinker nodule presenting the main phases. Ferrite, alite, belite and aluminate appear as the brightest to darkest contrast.

To be able to study and quantify all of the phases along with their distribution in the microstructure, the SEM pictures were taken at 5 different magnifications in all nodules. Figure 3.5 shows the microstructure of one nodule of clinker#1, which were taken at 5 magnifications of 50,100,200,500 and 1000x. Figure 3.5 shows that the distribution of the major phases like alite, belite and pores are quantifiable much better in the lower magnifications like 50 and 100x.On the other hand, at higher magnifications, i.e. 200-500x, the matrix phase and the structure of all phases are revealed more precisely. The matrix phase can be quantified best using 500x magnification image.

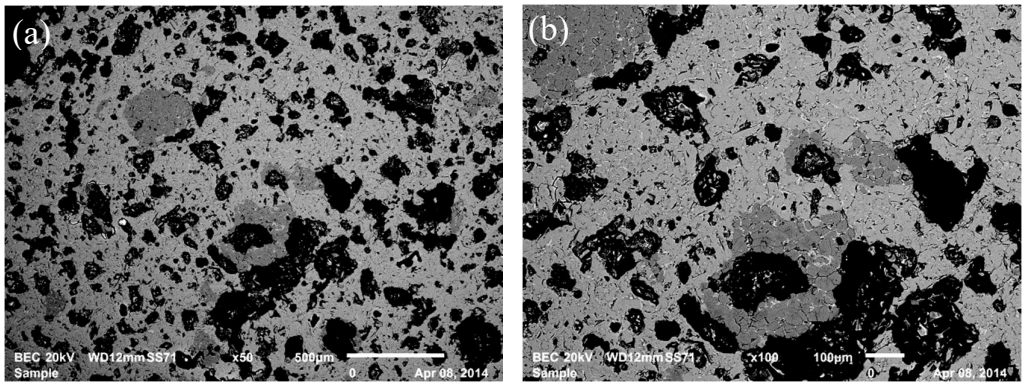

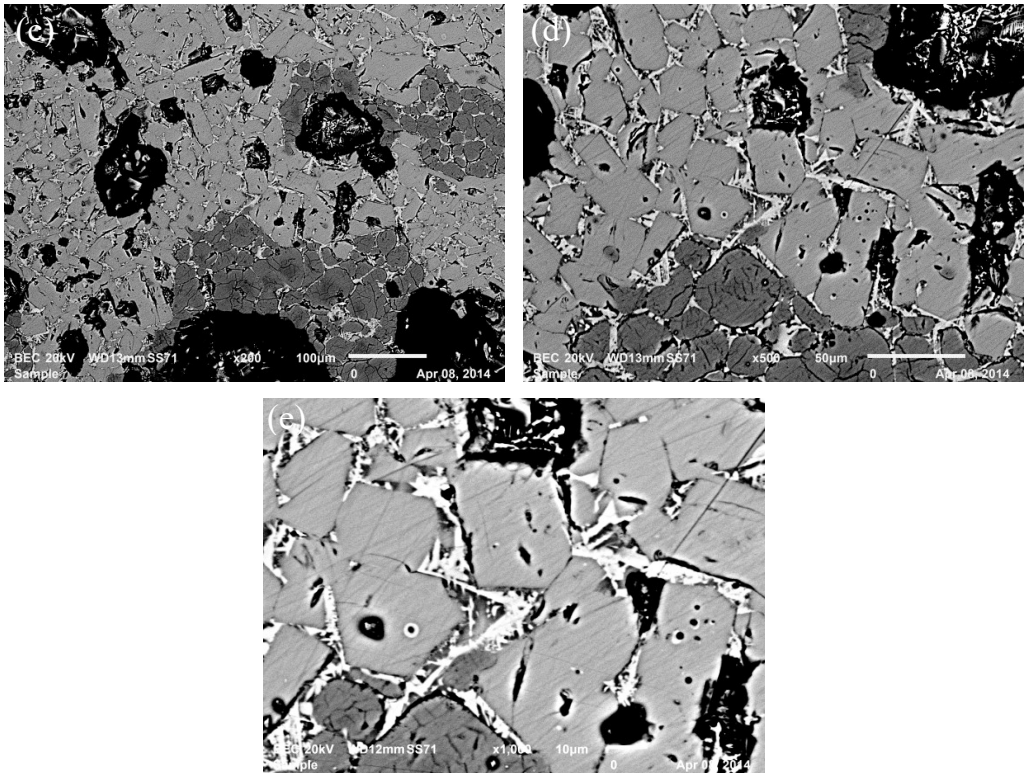

Figure 3.5. SEM BSE images of clinker#1 which were taken in 5 different magnifications: a)50x, b)100x, c)200x, d)500x and e)1000x.

To compare the phase distribution in the 5 clinker samples which were manufactured using different alternative fuels, SEM images are shown at two different magnifications. Figure 3.6 presents the images taken at 50x magnification. The distribution of alite and belite phases throughout the microstructure of the nodule was clearly visible, although the interstitial phases could not be seen. Also, the pore quantity is also measurable using these images. By comparing the images of different clinkers, it is visible that there were some differences in their phase distribution. Clinker#1 (3.6-a) and clinker#4 (3.6-d) possessed a higher amount of alite phase, whereas clinker#2 (3.6-b) and clinker#5 (3.6-e) had more belite phase particles. On the other hand, clinker#3 (3.6-c) contained a moderate amount of alite and belite particles. But, the distribution of the phases also differed in the clinkers. For example, in clinker#3, belite particles were spread nicely throughout the microstructure along with alite particles. However, the belite particles in clinker#2 and #5 were strongly clustered in certain regions.

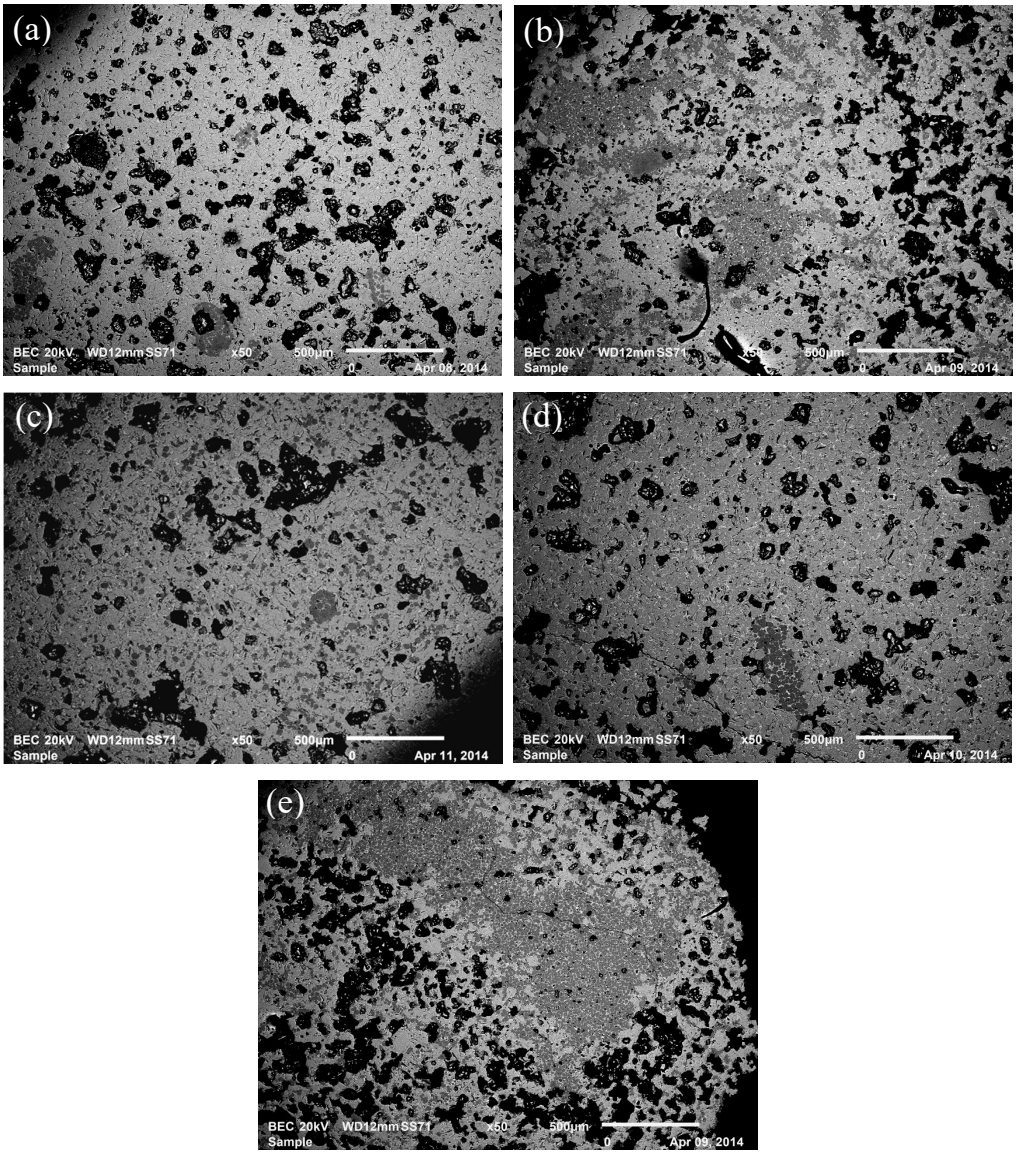

Figure 3.6. SEM images of 5 clinker samples prepared with different alternative fuels at 50x magnification: a)clinker#1,b)clinker#2,c)clinker#3,d)clinker#4 and e)clinker#5.

Figure 3.7 shows the SEM images of the clinkers taken at 500x magnification. The microstructure of the phases could be investigated more precisely in these pictures, compared to the lower magnification images. Moreover, the matrix phase consisting of aluminate and ferrite phases could be seen and quantified. The even distribution of belite among alite particles in clinker#3 was more obvious in this magnification. Nevertheless, this magnification is not proper for quantifying the alite and belite values in the microstructure because of heterogeneity in the microstructure and hence the distribution of the phases in hundreds of micrometers.

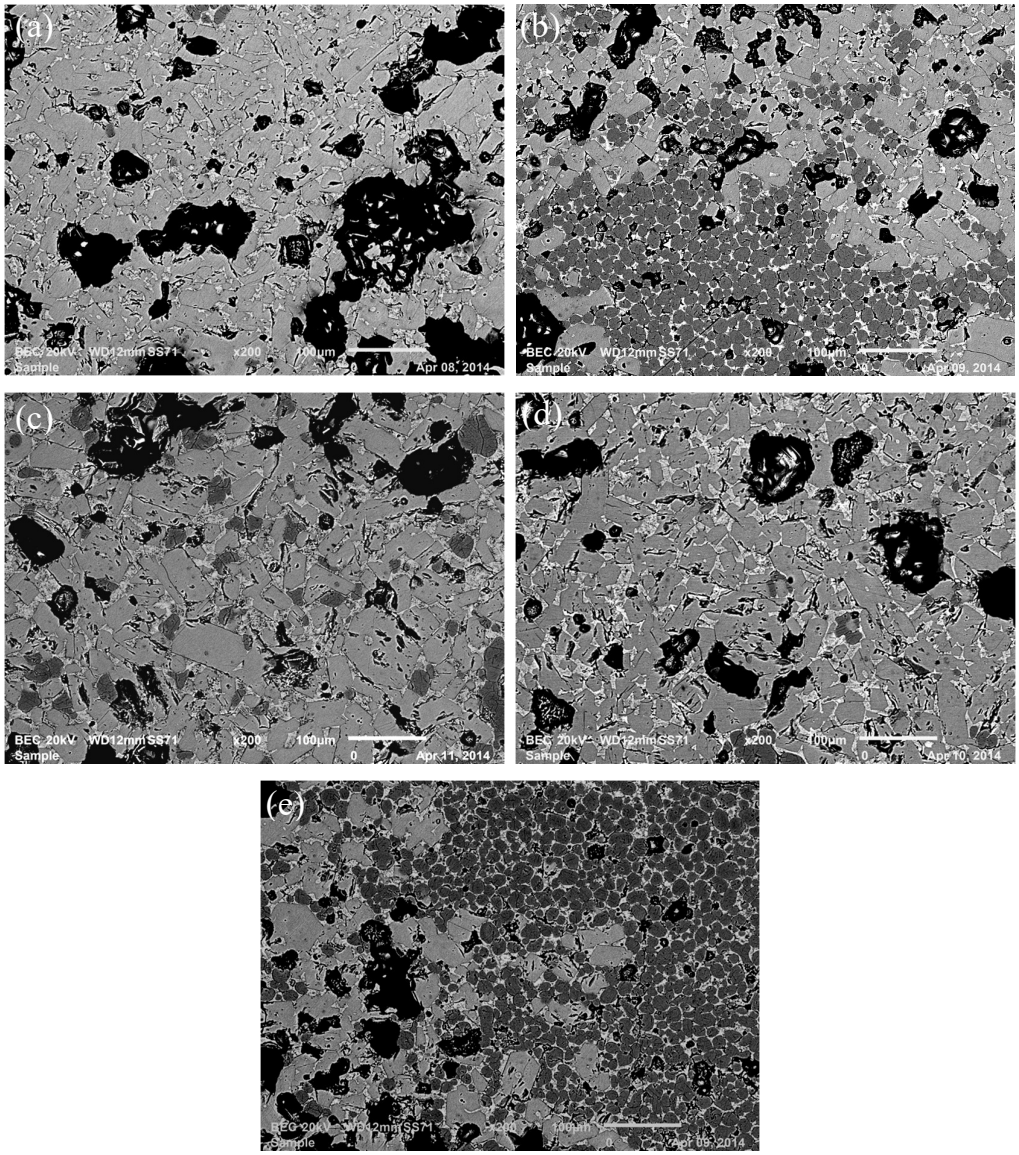

Figure 3.7. SEM images of 5 clinker samples prepared with different alternative fuels at 500x magnification: a)clinker#1, b)clinker#2, c)clinker#3, d)clinker#4 and e)clinker#5.

As it was mentioned earlier in chapter1, clinker cooling has a substantial effect on the formation of the phases, especially on the stability of alite [6, 24]. For example, as the clinker is cooled slower, the probability of transforming alite into belite and free lime (CaO) increases. Heat transfer plays a major role in this process and it is possible that the core of the clinker nodule cannot be cooled with the same speed of the outer regions. To investigate the influence of cooling and the probable differences of calcium silicate phases in inner and outer regions of the nodules, both parts were observed in SEM. Figure 3.8shows SEM images of a nodule of clinker#3, (a) presenting the inner

region and (b) presenting the outer region. Even though the distinction is not much, there still is some difference in the alite/belite ratio, as it is lower in the inner part.

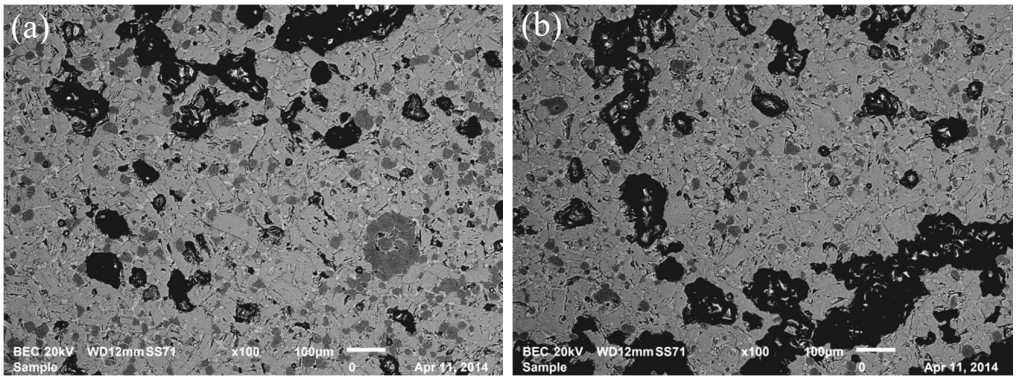

Figure 3.8. SEM image of clinker#3 recorded from a)inner and b)outer part of the nodule.

3-2-1-2) Quantification of the phases

As it is important to compare the microstructure of the clinkers prepared with different alternative fuels, it is as much essential to quantify the phase amounts acquired through microscopic pictures. To fulfill this task, a commercial image analysis software, ImageJ, was utilized. Using this program, it is possible to measure the surface areas of the phases, either by the color contrast or by drawing geometric shapes. These values show the surface area amounts, however it has been proven that in polycrystalline ceramic microstructures, 2D areal density values can be in equipoise with volumetric density values [135, 145]. The volumetric values can then be converted to weight values using average atomic weights.

The first quantification was carried out on alite and belite phases to calculate the alite/belite ratios in clinker samples. Figure 3.9 shows how the different contrast of the phases in BSE images can be used to measure their values. The thresholded images show the complementary alite (3.9-a) and belite (3.9-b) containing regions in the microstructure.

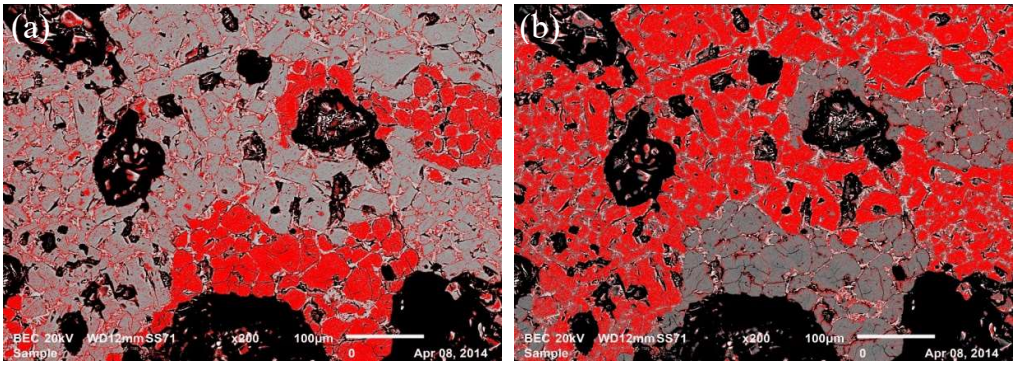

Figure 3.9. Color-thresholded SEM images, presenting a)alite b)belite regions in the pictures.

This procedure was done for all of the clinker samples in 3 nodules and 5 images taken in various magnifications. Figure 3.10 presents the alite/belite (a/b) ratios of one nodule of clinker#1 calculated for 5 magnifications. As it can be seen, as the magnification increases, the probability to obtain false values increases because of sampling of too-small of an area on the nodule. It was determined that the best magnifications for quantification were 50x and 100x, although the calculations were done for all of the images.

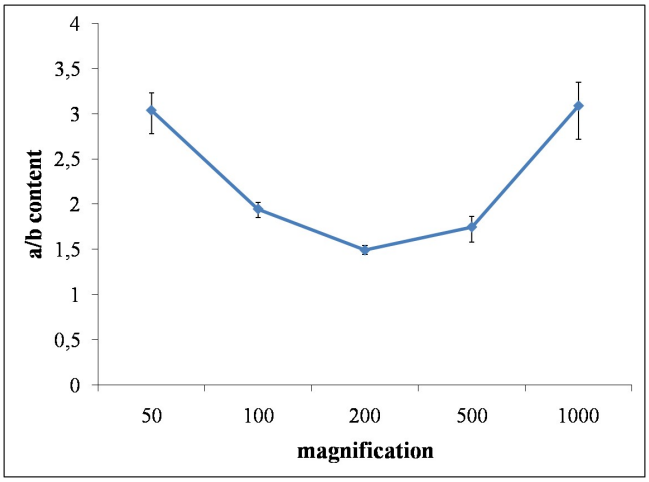

Figure 3.10. The alite/belite ratio of a nodule of clinker#1 quantified using image analysis program for various magnifications.

The same measurements were performed on three nodules of each clinker. Figure 3.11 shows the a/b ratios of the inner and outer regions of clinker#1 nodules in 5 magnifications. The values related to inner and outer regions are distinguished by blue and red colors, respectively. This graph also shows that increasing the magnification

results in scattering away from the realistic values. Moreover, it can be seen that in outer regions the a/b ratios mostly are higher than the inner regions and this could be an indication of the cooling effect.

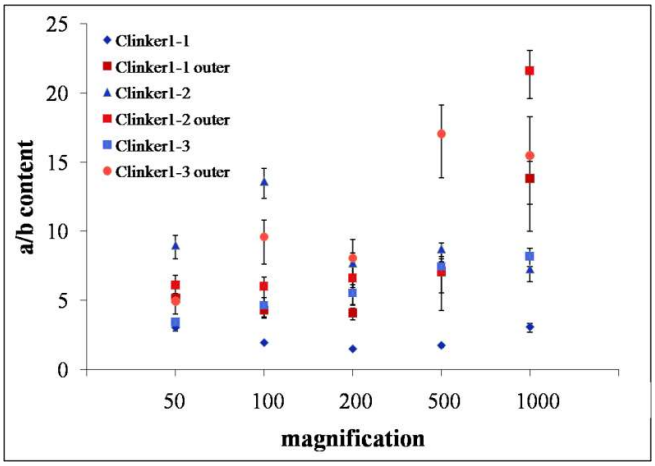

Figure 3.11. The alite/belite ratio of three nodules of clinker#1 in inner (blue) and outer (red) regions for various magnifications.

The quantified values of all clinker samples for only 50x magnification is shown in Figure 3.12. Overall, 6 regions including 3 inner and 3 outer parts were measured for their alite/belite values. The a/b values were distinguished by different colors on the graph. It is obvious that there was an error bar for the a/b values of each clinker. This error bar was the highest for clinker#1 and was the smallest for clinker#5, in which most of the nodules consistently showed a low a/b ratio in their microstructure.

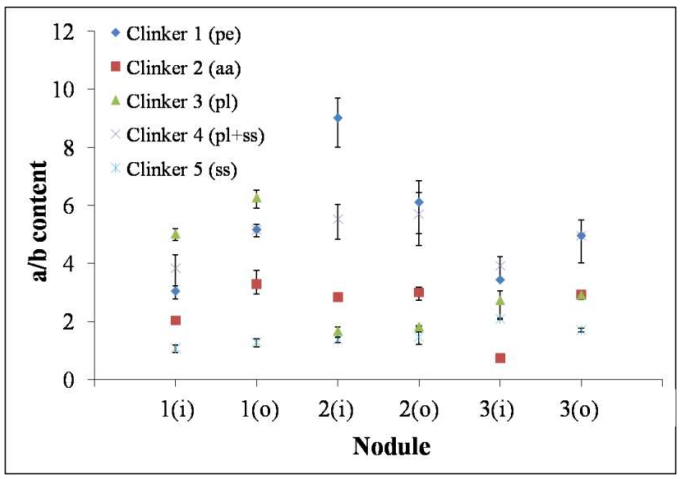

Figure 3.12. The alite/belite ratios of 5 clinker samples for their 3 nodules (inner and outer parts).

The values obtained using image analysis program gave a quantification on the areal or in other terms volumetric (vol%) data of the phases. In order to convert the values to weight percent (wt%), the atomic weight of alite (15.06) and belite (14.56) phases was used. Table 3.1 presents the average vol% and wt% of alite/belite ratios for the clinker samples obtained through microscopic images. It can be seen that the average alite/belite ratios of clinker#1 (clean) and clinker#4(waste plastics+sewage sludge) were the highest among all samples, while the values were the lowest for clinker#2 (dirty) and clinker#5 (sewage sludge). The clinker#3 (waste plastics) has an alite/belite weight ratio of 3.26, which is a moderate and acceptable value for OPCs.

Table 3.1. The average alite/belite ratios of five clinker samples. Both vol% and wt% are shown.

Clinker#	Alite/Belite (vol%)	Alite/Belite (wt%)
1	5.27	5.06
2	2.47	2.37
3	3.40	3.26
4	4.84	4.65
5	1.50	1.44

After calculating the amounts of the major alite and belite phases in the clinker samples, it is also important to quantify the matrix phase. Figure 3.13 shows the thresholding of the ferrite phase as the brightest (heaviest) phase in the microstructure using the image analysis software.

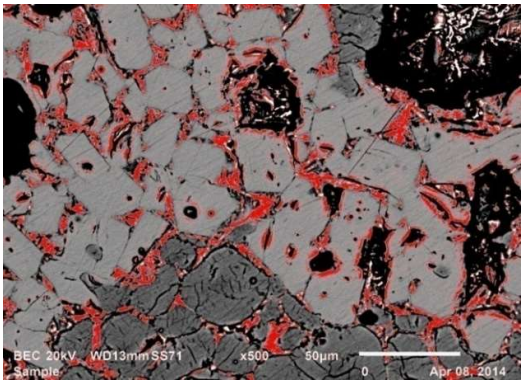

Figure 3.13. Thresholded ferrite phase in the microstructure of the clinker.

The ferrite values were calculated for 5 nodules of each clinker in two magnifications of 200x and 500x for the precision. Figure 3.14 presents the average ferrite vol% values of the clinker samples for two magnifications on the same graph.

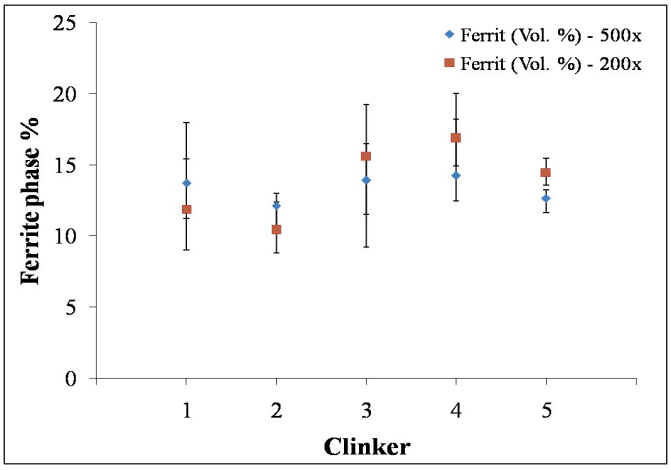

Figure 3.14. The ferrite phase values of 5 clinker samples calculated in two magnifications: 200x and 500x.

The wt% values of ferrite phase were calculated using its atomic weight (16.65) and is presented in Figure 3.15 for the 500x magnification images. Although the ferrite amounts are not same for different clinker samples, the variance is not very substantial and the average values are ranging around 14-16 wt%.

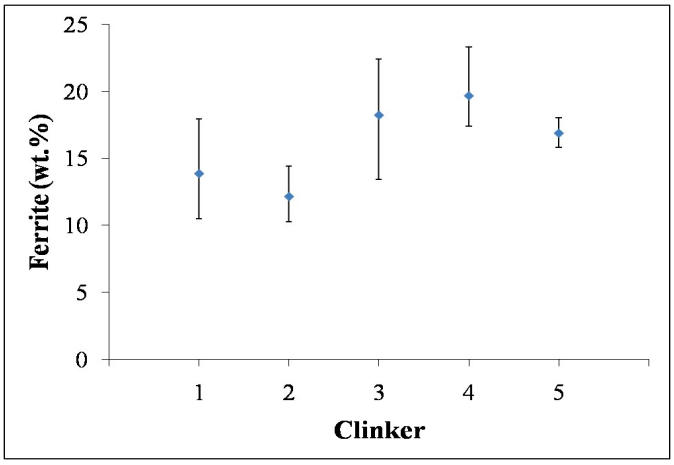

Figure 3.15. The ferrite phase values (wt%) of clinker samples for the mag. of 500x.

The last phase quantification was done for aluminate. The aluminate was the darkest (lightest in weight) phase among the main phases of clinker, but it had a contrast that was very close to the contrast of the belite phase. Due to this issue and for

preventing miscalculations, the quantification of the aluminate phase has been done slightly differently than for the other phases. The surface area of the aluminate crystals were measured by drawing geometric shapes around the entire matrix phase as shown in Figure 3.16. The total areal values were then used to calculate the aluminate values by subtracting the ferrite values of each clinker. It should also be mentioned that free lime values were not measured separately in this research, because it was assumed that its content is in the order of 1% in the composition. Due to free lime's close contrast to ferrite (average weight=16.58), it is unlikely to detect this minor phase with SEM. Therefore, if any, it was counted as a part of the matrix phase. Complementary calculations may be carried out through XRD analysis.

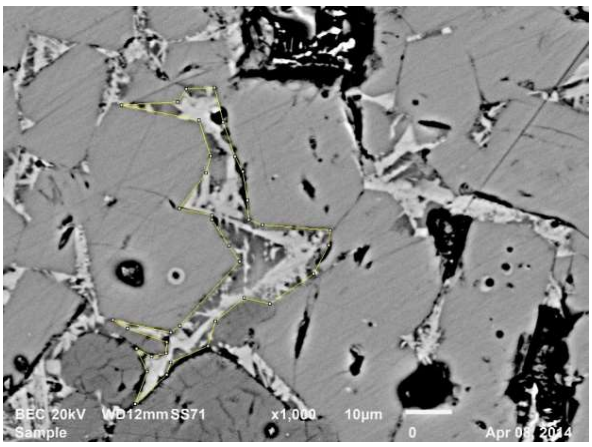

Figure 3.16. The SEM image presenting the quantification method for aluminate phase by drawing geometric shapes around the matrix phase.

The aluminate phase values (wt%) of the clinkers calculated using microscopic images are shown in Figure 3.17. It can be seen that there is a significant difference between the values of clinker samples, as clinker#1 and clinker#4 has the lowest aluminate amount among all phases.

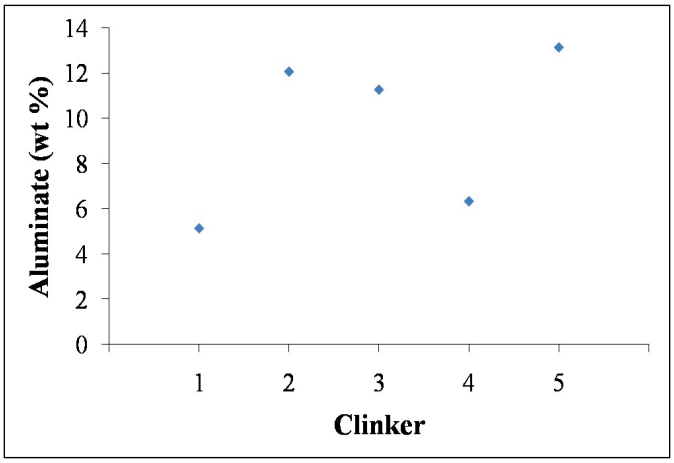

Figure 3.17. The aluminate phase values (wt%) for 5 clinker samples.

Table 3.2 presents the average wt% ferrite and aluminate phase amounts for all of the clinker samples prepared with different alternative fuels.

Table 3.2. The average ferrite and aluminate phase amounts of the clinker samples.

Clinker#	Ferrite (wt %)	Aluminate (wt %)
1	15.97	5.13
2	14.13	10.36
3	16.20	11.25
4	16.58	6.32
5	14.75	13.13

As we can see in the microstructural images, clinker is a porous material. The porosity content of the clinker nodules is an important property, as we discussed in chapter1. This property can give an idea of sintering grades in the cement burning kiln and following clinker cooling, which can directly affect the cement properties. Porosity content also could be an indication of the grindability of clinker. Therefore, the pore amount was also measured for all of the clinker samples using Image Analysis. Figure 3.18 shows the porosity percentage of each clinker which was calculated using 5 nodule images. The measurements were done on the images taken at both 50x and 100x magnifications for the precision. Although error bars are large, it can still be interpreted that the porosity amount is higher for clinker#3 and lower for clinker#4 with respect to

other samples. The difference in the 50x and 100x magnification values of clinker#5 could be an indication of the lower porosity at the core in comparison with the outer regions.

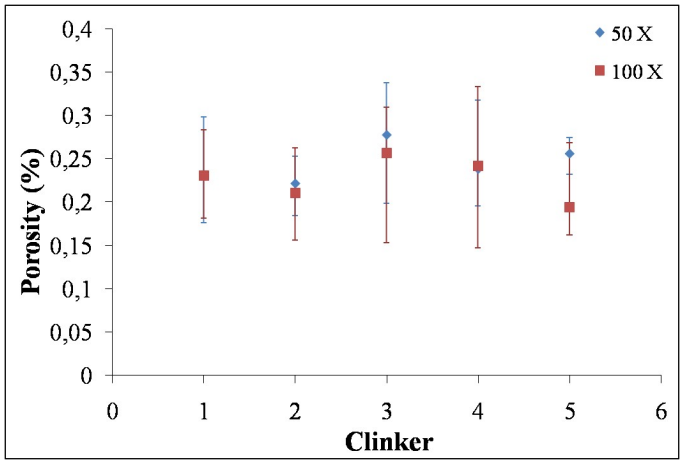

Figure 3.18. The porosity percentage for each of the clinker samples, measured from the SEM images at 2 magnifications of 50x and 100x.

3-2-2) EDS analysis

The chemical composition of the all clinker samples which have been produced using different alternative fuels was analyzed with Energy Dispersive X-ray Spectroscopy. The advantage of the EDS microanalysis is the capability of studying the chemical composition of the region of interest in the microstructure. It is possible to analyze a certain point or a region for acquisition of the elements (both qualitatively and quantitatively). Moreover, the element mapping (x-ray image) option provides scanning the entire surface of the sample for the existing elements. This method provides semi-quantitative information about the spatial distribution of individual elements.

The nodules which were observed with SEM were also analyzed by EDS. The investigation was done by both point analysis and element mapping. In Figure 3.19, an SEM BSE image of a nodule of clinker#1 is shown with the points which were analyzed with EDS. It was tried throughout the analysis to consider all the different phases to obtain the chemical composition of them.

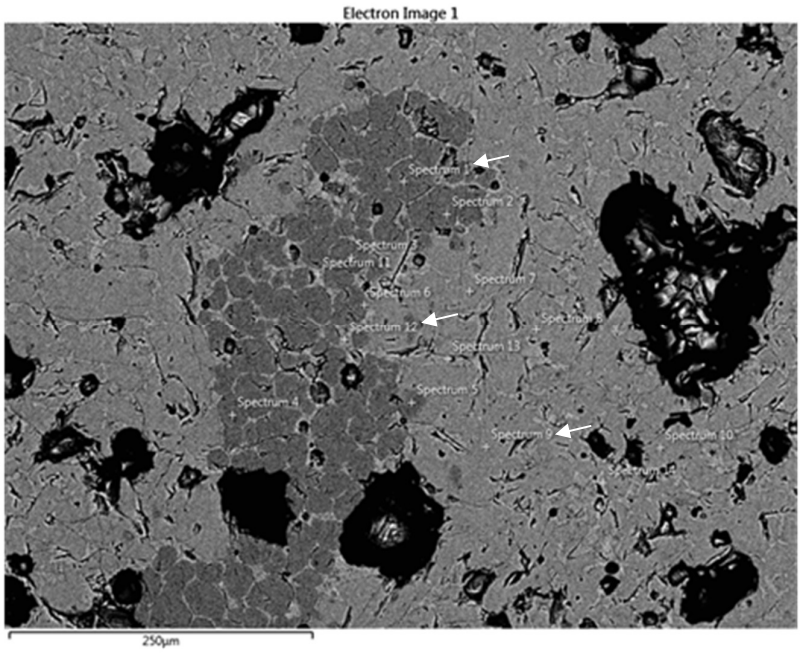

Figure 3.19. SEM BSE image of a nodule of clinker#1, showing the points analyzed with EDS.

In EDS, the x-rays produced due to the interaction of the electron beam with the atoms of the material are being detected. These x-rays are characteristic of elements and are used to construct a spectrum, in which, each peak represents an element. Studying this spectrum will provide the types of elements and their amount in the investigated volume (coarsely the interaction volume). With the EDS softwares, it is possible to acquire the chemical composition by weight %, atomic% and oxide%. Figure 3.20 presents the EDS spectrums of point1, point9 and point12 in Figure 3.19, which respectively represent belite (C_2S), alite (C_3S) and ferrite (C_4AF) phases. The peaks of the spectrums are labeled with the corresponding element. It can be seen that there is an obvious difference among the peak types and heights of each spectrum. For example, due to the higher amount of Ca in C_3S with respect to C_2S, its peak is larger.

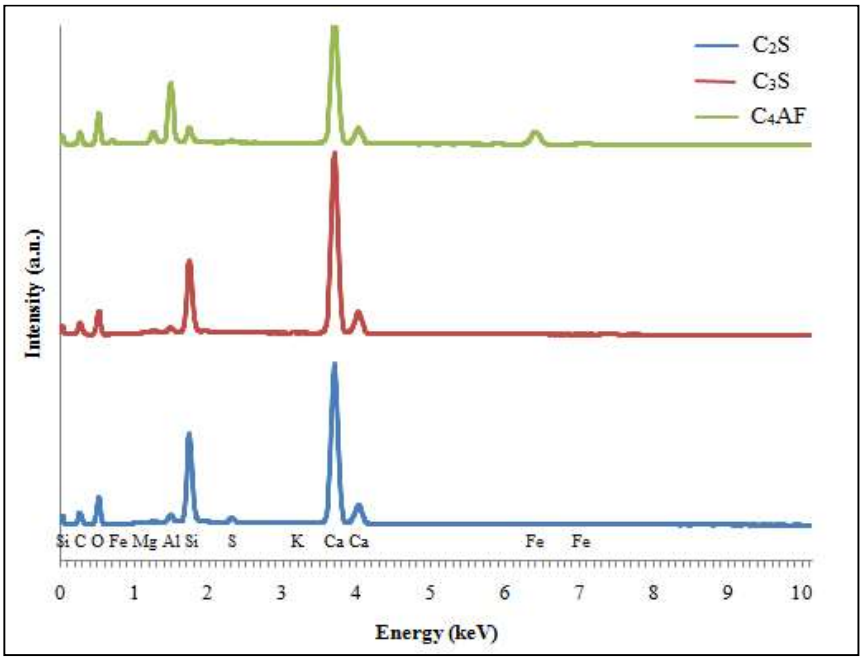

Figure 3.20. EDS spectrums of point1 (C_2S), point9 (C_3S) and point12 (C_4AF) at Figure 3.19.

The spectral data was obtained for all the different points on each region of nodules. The data has been included in tables for comparison. Table 3.3 contains a set of data as wt.% gained for the points marked on Figure 3.19. The blue-colored rows belong to belite particles, while the pink and green rows belong to alite and matrix phases, respectively.

Table 3.3. The EDS data related to points on Figure 3.19.

	Chemical Composition (Wt. %)												
Point	Ca	O	Si	Al	Fe	Mg	S	K	Mn	P	Na	Cl	Ti
S 1	48.0	34.5	14.3	1.2	0.8	0.3	1.0	0	0	0	0	0	0
S 2	48.6	33.9	13.9	1.3	0.9	0.3	0.8	0	0	0.1	0.2	0	0
S 3	48.6	34.1	14.3	1.2	0.9	0.3	0.7	0	0	0	0	0	0
S 4	48.2	34.2	14.3	1.2	0.8	0.4	0.7	0	0	0	0.2	0	0
S 5	48.8	34.1	15.4	0.7	0.6	0.2	0.2	0	0	0	0	0	0
S 6	48.5	34.2	14.3	1.2	0.8	0.3	0.6	0	0	0	0.2	0	0
S 7	54.4	32.4	11.8	0.5	0.4	0.5	0.1	0	0	0	0	0	0
S 8	54.1	32.5	11.6	0.6	0.6	0.5	0.1	0	0	0	0	0	0
S 9	53.9	32.5	11.6	0.7	0.6	0.5	0.2	0	0	0	0	0	0
S 10	53.0	33.1	12.3	0.6	0.4	0.4	0.2	0	0	0	0	0	0
S 11	39.8	32.1	2.7	10.9	11.6	2.2	0.3	0	0.4	0	0	0	0
S 12	38.4	32.6	3.0	11.2	11.7	2.4	0.3	0	0.4	0	0	0	0
S 13	37.6	31.5	2.4	11.7	12.2	2.1	1.2	1.1	0.3	0	0	0	0
S 14	41.5	32.1	3.3	11.1	10.0	1.7	0.2	0	0	0	0	0	0

The acquisition of EDS data was done for nodules of all clinker samples. The average concentration of each element in each phase for the nodules has been calculated and is shown in Table 3.4 for all 5 clinker samples. The data has been classified for each clinker consisting of the elements available in the main phases and color-coded likewise Table 3.3. The row named as "total" indicates the values obtained through scanning the whole area of the concerned nodule image at low magnifications.

Investigating the values provided in Table 3.4 is of utmost importance. It is possible to study the chemical composition of phases separately in each clinker and compare it to the values of other clinkers. It is especially significant to compare the minor elements like alkalis (K, Na), Mg, P and Cl. On the other hand, the chemical composition of the entire region of the clinker's nodule (mentioned as total) can be compared among all samples.

Table 3.4. The EDS data of the clinker samples shown as the average concentrations for each phase in each clinker.

		Chemical composition (Wt %)													
Clinker	**Phase**	**Ca**	**O**	**Si**	**Al**	**Fe**	**Mg**	**S**	**K**	**Mn**	**P**	**Na**	**Cl**	**Ti**	**Cr**
Clinker1 (Pe)	**C_3S**	53.1	33.5	11.6	0.61	0.51	0.5	0.15	0	0	0.01	0	0	0	0
	C_2S	48.7	34.9	13.9	1.2	0.91	0.33	0.54	0	0	0	0.1	0	0	0
	C_3A,C_4AF	38.6	32.8	2.46	12.1	11.2	2.04	0.4	0.05	0.2	0	0.03	0	0.07	0
	total	48.5	35.1	10	2.68	2.4	0.8	0.36	0	0.02	0	0.06	0	0	0
Clinker2 (AA)	**C_3S**	53.2	33.4	11.4	0.77	0.62	0.36	0.05	0.08	0.01	0.01	0	0.02	0	0.01
	C_2S	48.2	35.2	13.8	1.3	1.05	0.22	0.16	0.46	0.02	0.2	0.16	0.02	0	0.01
	C_3A,C_4AF	38.8	32.7	2.41	11.8	12.3	1.37	0.04	0.25	0.3	0	0.07	0.01	0.47	0.07
	total	46.5	35.1	9.3	2.15	2.2	0.92	0.7	0.6	0.02	0.1	0.15	0.02	0	0
Clinker3 (Pl)	**C_3S**	52.3	34.2	11.4	0.78	0.60	0.66	0.16	0	0	0	0	0	0	0
	C_2S	46.7	35.3	13.8	1.35	1	0.36	0.95	0.08	0	0	0.16	0	0	0.01
	C_3A,C_4AF	37.1	32.1	2.43	11.8	12.4	2.53	0.82	0.23	0.3	0	0.07	0.05	0.36	0
	total	45.7	36.0	9.43	3	2.93	0.96	1.1	0.6	0.03	0	0.23	0.07	0	0
Clinker4 (Pl+SS)	**C_3S**	53.6	33.2	11.3	0.73	0.76	0.64	0.14	0	0	0.04	0	0	0	0
	C_2S	47.6	34.7	13.9	1.15	1	0.31	0.91	0.10	0	0.16	0.25	0	0	0
	C_3A,C_4AF	37.5	31.7	2.2	11.2	13.3	2.07	0.30	0.06	0.40	0	0.08	0.04	0.65	0.03
	total	48.7	34.4	9.66	2.8	2.8	0.96	0.42	0	0.02	0.1	0.12	0	0	0
Clinker5 (SS)	**C_3S**	52.8	33.3	11.4	1.03	0.61	0.62	0.25	0	0	0.01	0	0	0	0
	C_2S	47.4	35.1	13.6	1.25	1.1	0.32	1.07	0.19	0	0.04	0.11	0	0	0.04
	C_3A,C_4AF	37.4	32.8	2.47	10.7	12.3	2.53	0.88	0.20	0.38	0	0.09	0.05	0.26	0.03
	total	46.0	35.4	10	1.93	1.93	0.93	0.86	0.43	0	0.07	0.17	0.03	0	0

In order to provide a better comparison condition, the elemental distributions of each entire clinker were graphed, as they are shown in Figure 3.21. The values of Ca, Si and O elements have been excluded from the element percentage in order to be able to compare the minor elements amount among overall composition of the clinkers. For example, by taking a look at the amounts of S and K, it is obvious that they are different for different clinker samples. These values are evidently lower in clinker#1 and clinker#4 in a comparison with clinker#2, #3 and #5. Also clinker#2 and clinker#5 contain a higher amount of Na.

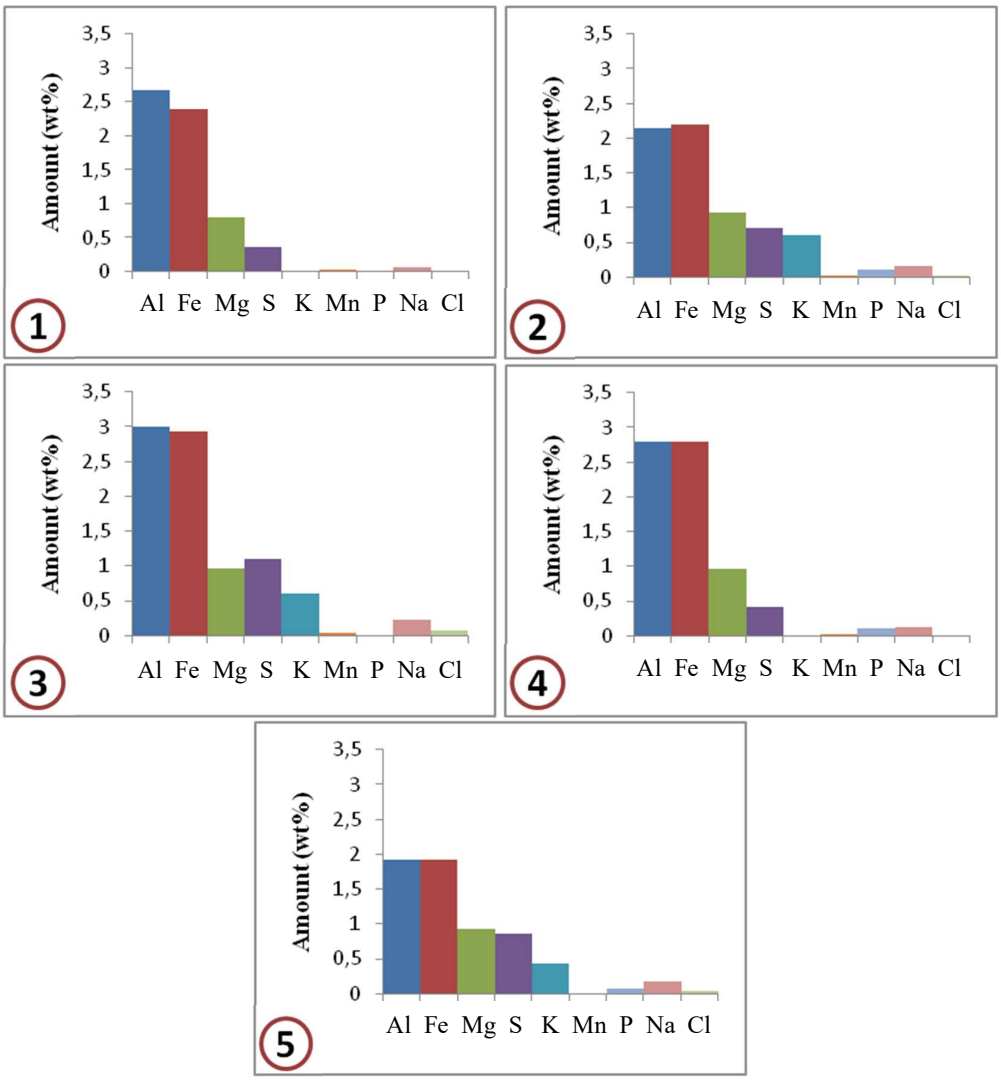

Figure 3.21. The overall elemental distribution in the entire clinkers obtained by EDS analysis. The values of Ca, Si and O are excluded in the graphs.

As indicated before, in addition to point analysis, element mapping was carried out on the microstructure of clinkers. Figure 3.22 shows the maps of eight elements present in the microstructure of clinker#3. The colored maps represent the distribution of each element separately. These maps were analyzed for all of the samples to understand the relation between elements in each phase. It can be seen in Figure 3.22 that Ca and Si are present in greater amounts in the main phases of alite and belite, whereas Al and Fe are highly present in the matrix phase. On the other hand, contrasting the S, K and Na maps shows that throughout the microstructure they appear together and mostly inside the pores. This matching is an indication that the Sulfur and alkalis are present as the potassium sulfate and sodium sulfate. The areas including only Na indicate the presence of it in the composition of main phases, which could be harmful for the clinker phases. In addition, Magnesium map shows an even distribution of Mg in the phases, with a small increment in the matrix phase with respect to silicate phases.

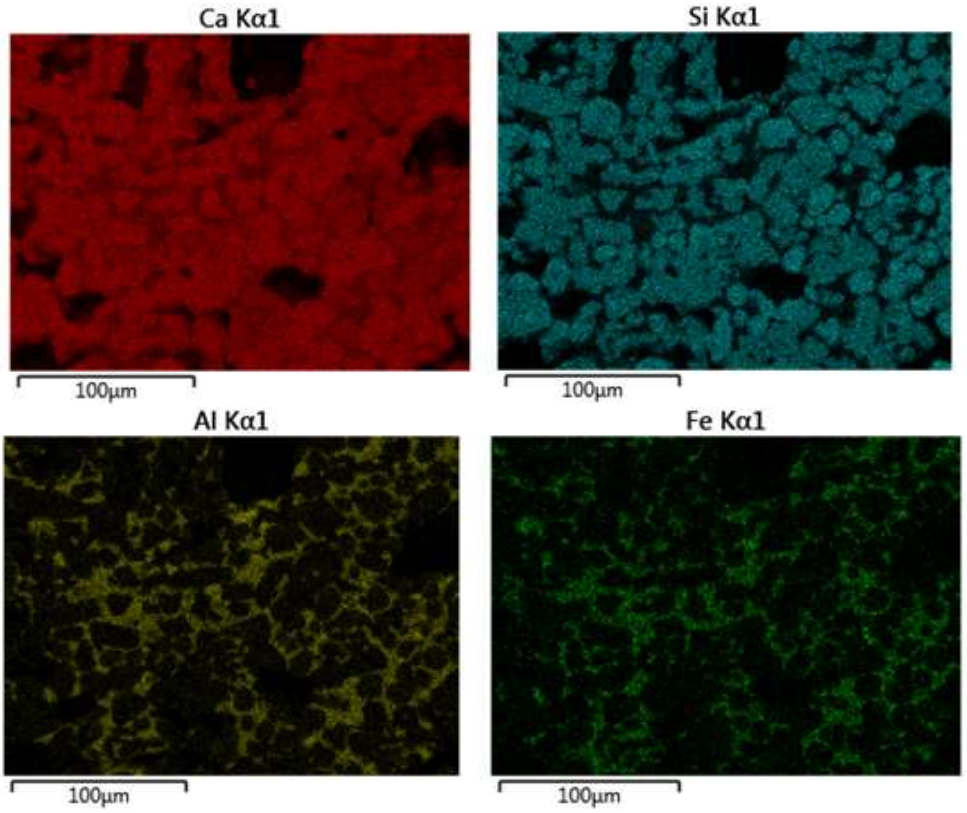

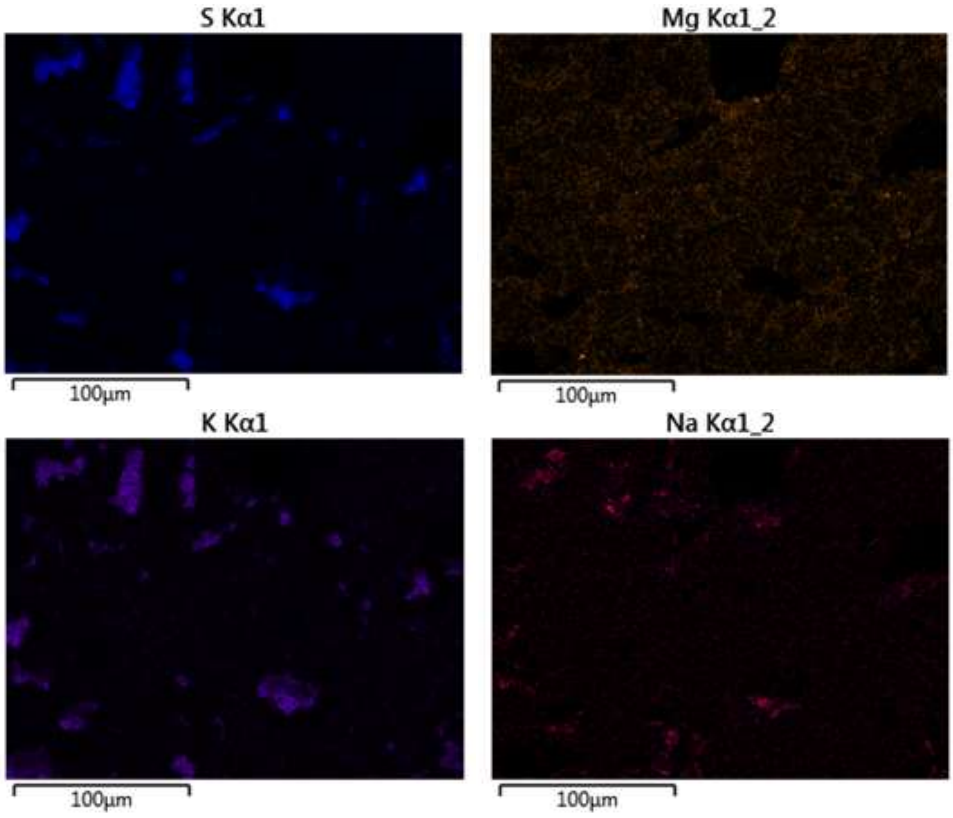

Figure 3.22. Elemental maps of the microstructure of clinker#3, representing the distribution of eight elements (Ca, Si, Al, Fe, S, Mg, K and Na) in the microstructure.

As indicated, the elemental maps of all the clinker samples were investigated as well. However, these investigations did not show any significant variance among the samples. In addition, no minor elements were detected to be present in significant amount and affect the major phases and their distribution.

One other potential of elemental color mapping is the ability of phase detection. Figure 3.23 presents the layered images obtained using the maps and BSE image for each clinker's microstructure. The distinction among the major phases is visible due to the various amounts of elements in each phase. This property can be utilized to differentiate among phases using color-coding.

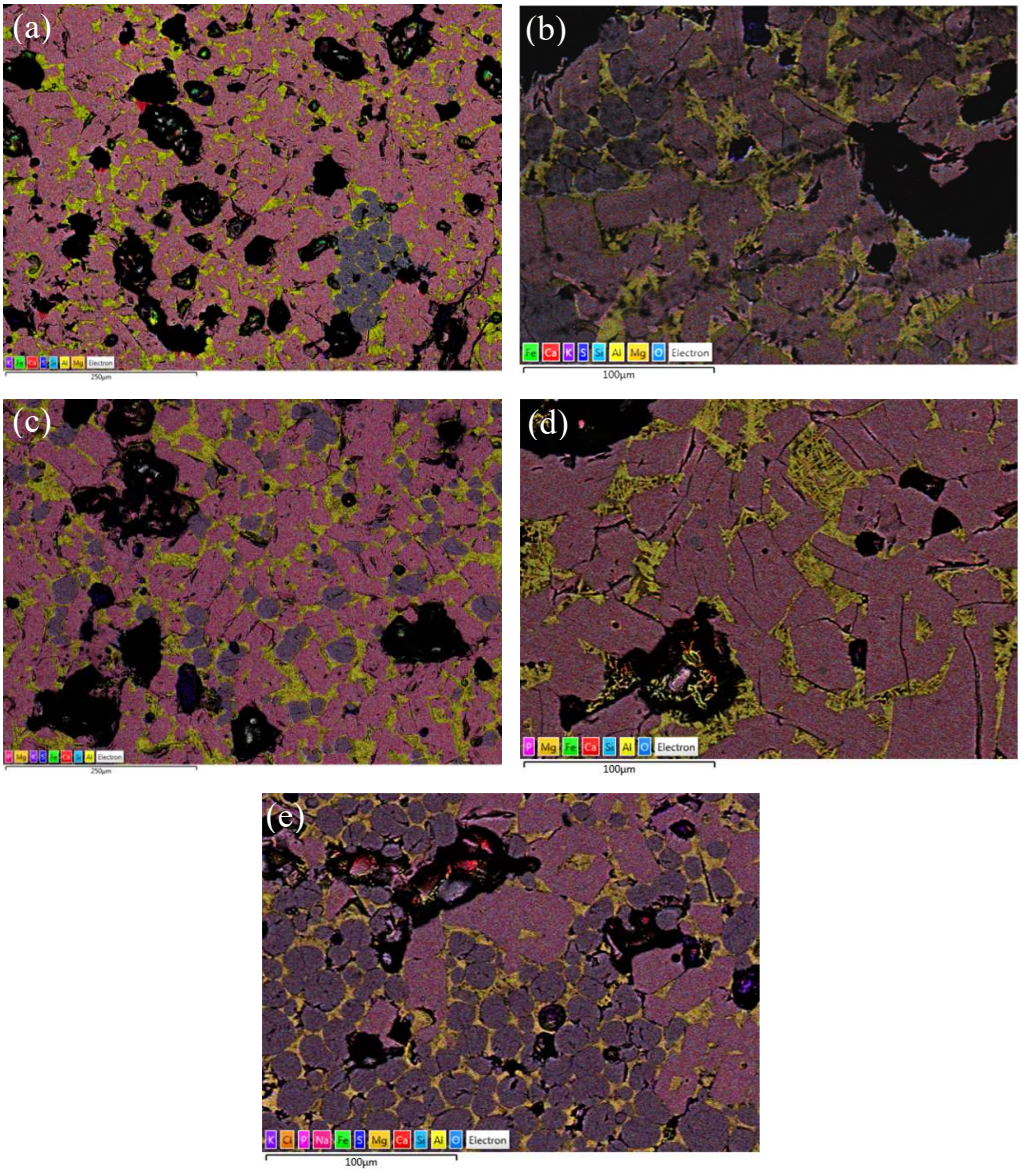

Figure 3.23. Layered images of clinker samples obtained with layering the color elemental maps of each sample.

3-2-3) XRF analysis

The chemical composition of the clinker samples was investigated also by X-Ray Fluorescence analysis. This analysis is an inseparable part of the cement manufacturing, as the data is used to calculate the phase distribution in clinkers with the Bogue calculations. Table 3.5 contains the XRF data obtained for 5 clinker samples manufactured using different alternative fuels.

Table 3.5. The chemical composition of clinkers obtained using XRF analysis.

Clinker#	CaO	SiO_2	Al_2O_3	Fe_2O_3	MgO	K_2O	Cl^-	Na_2O	TiO_2	SO_3	MnO
1	65.24	20.55	5.07	3.47	1.22	0.99	0.0016	0.01	0.29	1.46	0.00
2	65.34	20.44	5.10	3.50	1.21	1.00	0.0023	0.17	0.28	2.08	0.00
3	63.61	21.03	5.05	3.53	1.36	1.02	0.0001	0.01	0.40	1.92	0.00
4	64.94	20.81	5.05	3.64	1.35	0.82	0.0006	0.01	0.41	1.35	0.00
5	62.56	20.74	5.14	3.59	1.57	1.12	0.0001	0.01	0.38	2.27	0.00

The compositional data obtained with the XRF measurements was used to compute the main phase distributions with the Bogue method. Table 3.6 presents the values of the four main phases along with the free CaO amount and alite/belite ratios for each clinker.

Table 3.6. Phase distributions of five clinker samples, calculated with Bogue method.

Clinker#	C_3S	C_2S	C_3A	C_4AF	Free CaO	C_3S/ C_2S
1	59.27	14.19	7.55	10.56	1.72	4.17
2	57.85	14.96	7.59	10.66	1.87	3.86
3	52.13	20.97	7.41	10.73	0.62	2.48
4	60.46	14.07	7.23	11.06	0.67	4.29
5	48.07	23.21	7.56	10.91	0.68	2.07

3-2-4) XRD analysis

The phase distribution in the clinkers was also measured using X-ray Diffraction analysis. Rietveld analysis was utilized to calculate the phase amounts by investigating and fitting the peaks of each phase. As an example, XRD pattern of clinker#1 is shown in Figure 3.24, together with the Rietveld fit used to measure the alite/belite ratio.

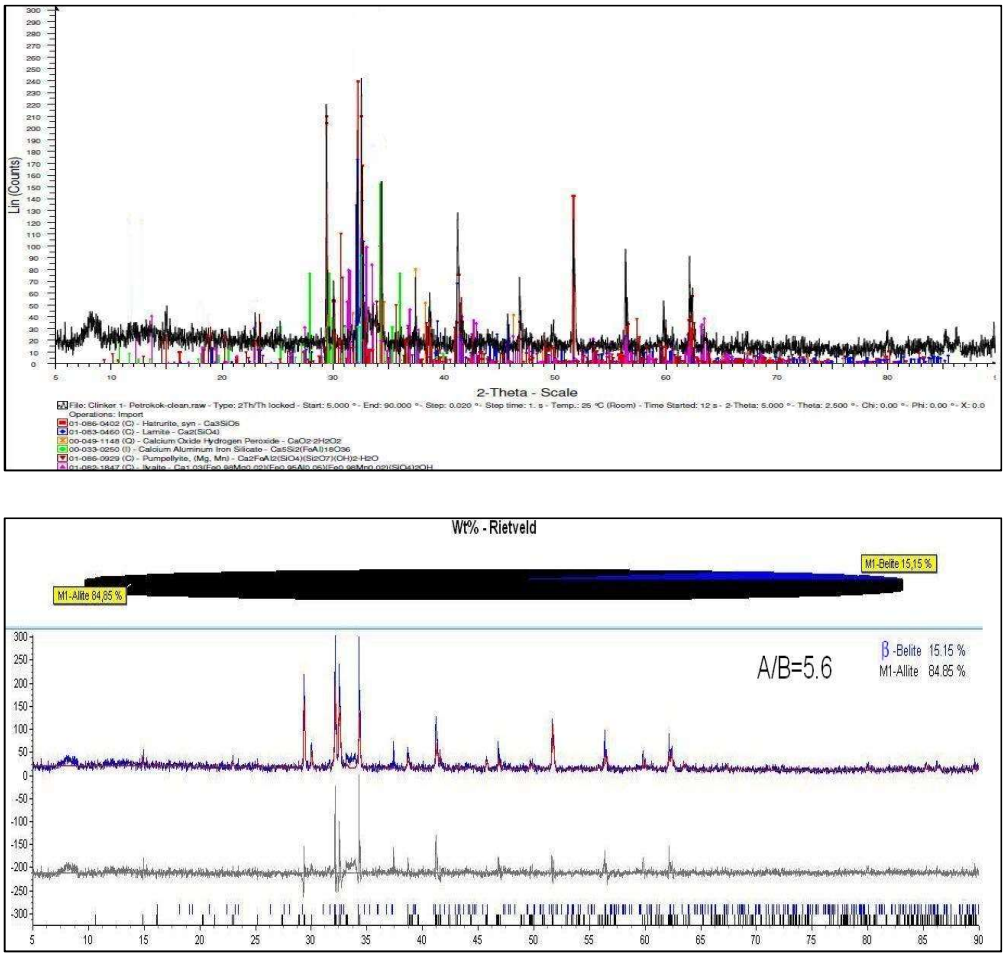

Figure 3.24. The XRD pattern of clinker#1 showing the phase detection using peaks, as it is taken from the software. The method used to perform the Rietveld analysis is also shown.

Figure 3.25 presents the XRD patterns of the five clinker samples. The main phases of clinkers including alite, belite, aluminate, ferrite, free lime and periclase are indicated on the image.

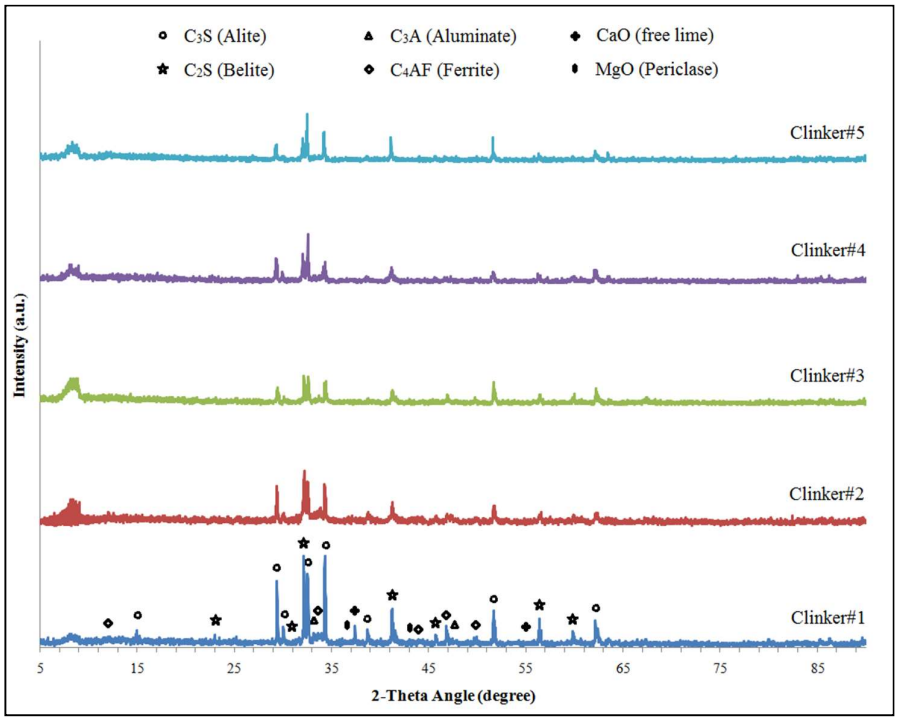

Figure 3.25. XRD patterns of five clinker samples. The peaks of clinker main phases have been indicated on the image.

The amounts of phases were measured for all of the clinkers. As indicated before, Rietveld method was used to calculate the alite and belite phase values. Aluminate and ferrite as the other main phases of clinker were measured by determining the area under their related peaks. Table 3.7 includes the wt% amounts of phases and alite/belite ratio obtained for the clinker samples.

Table 3.7. The phase distribution in clinker samples acquired using XRD analysis.

Clinker#	Alite	Belite	Aluminate	Ferrite	Alite/belite
1	70.17	12.53	5.3	12.0	5.6
2	41.24	34.36	10.6	13.8	1.2
3	54.15	21.65	9.1	15.1	2.5
4	64.49	15.01	7.4	13.1	4.3
5	49.33	32.77	12.4	15.5	1.5

In addition, the polymorphs of alite and belite phases were also investigated. Table 3.8 presents the alite and belite polymorphs in each clinker with their percentage value in each phase. Investigating the phase polymorphs is of utmost importance and is

the advantage of XRD method compared to SEM, since all polymorphs of each phase may appear similar under electron microscope. It can be seen in Table 3.8 that clinker#1 and #2 consist almost 100% of monoclinic polymorphs of alite (M_1) and belite (β_1). However, clinker#2 and #3 consist of 3 polymorphs of alite with monoclinic, triclinic and rhombohedral structures. Clinker#3 also contains 2 polymorphs of β_1 and β_2 for belite phase. Lastly, clinker#5 contains M_1 and T_1 alite polymorphs. All of these polymorphs are considered reactive in cement hydration, R_1 with a little higher reactivity.

Table 3.8. Alite and belite polymorphs in each clinker with their amount in the specific phase. M:monoclinic, T:triclinix, R:rhombohedral, β_1 andβ_2:monoclinic polymorphs of belite phase.

Clinker#	Alite polymorphs	Belite polymorphs
1	M_1(~100%)	β_1 (~100%)
2	M_1 (~100%)	β_1 (~100%)
3	M_1 (31%) T_1 (57%) R_1(12%)	β_1 (85%) β_2 (15%)
4	M_1 (55%) T_1 (24%) R_1(21%)	β_1 (~100%)
5	M_1 (93%) T_1 (7%)	β_1(~100%)

3-3) Hydrated cement paste analysis

In order to investigate the hydration reactions and analyze the hydrated cement properties, tests were conducted on the cement paste samples. The samples were prepared and a few characterization methods such as compression test, SEM and XRD were used to analyze them.

3-3-1) Compression tests

In order to investigate the mechanical properties and strength development in cement samples, hydration experiments were carried out. For these experiments, water to cement (w/c) ratios of 0.3 and 0.5 were used in preparing the samples. The data shown here were obtained using the standard cement compression testing machine.

3-3-1-1) Strength tests using w/c:0.3

Cement pastes were prepared with the cement powders provided from the AkçanSA company using the experimental methods explained in chapter3. Each cement powder was produced from the corresponding clinker which was made using a certain alternative fuel. The hydrated samples of w/c of 0.3 were tested for their compression strength on 1,2,3,7,14 and 28th day of their hydration. Figure 3.26 shows the strength development graphs for the 5 cement paste samples prepared with w/c:0.3.The extremely high values are attributed to the low water to cement ratio. Each color represents one of the samples; navy-blue:sample#1 (petrocoke), red:sample#2 (all alternatives), green:sample#3 (waste plastics), purple:sample#4 (waste plastics+sewage sludge) and blue:sample#5 (sewage sludge). The strength development graphs were rather similar to each other and the strengths were developing in the same orientation. The first day strength values were in the range of 50±5MPa for all of the samples, except for sample#2 which had ~23 MPa compressive strength. On the 2,3 and 7th day, the strength values of all samples spanned a range of ~15MPa. After 14 days of hydration, sample#2 again showed a lower strength value compared to the other samples. However, the 28th day compressive strength values were very close-ranged among all samples and it lied at 105±5 MPa.

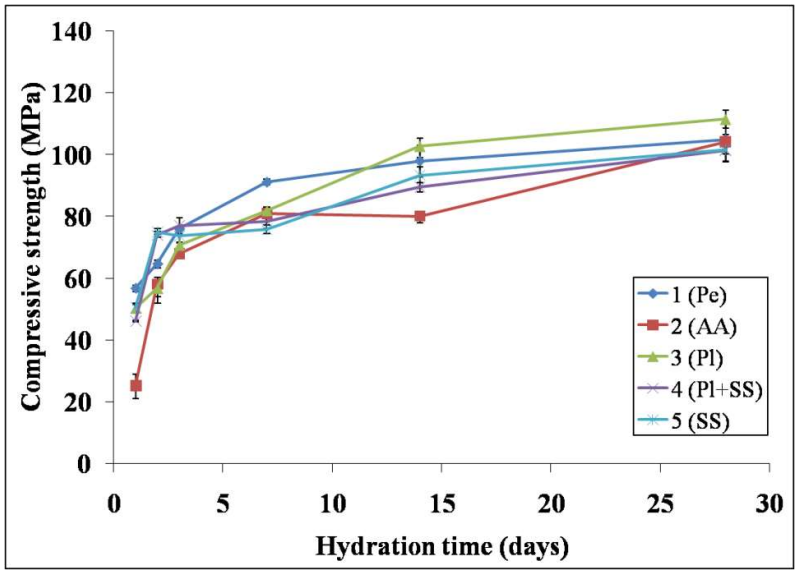

Figure 3.26. Compressive strength development graphs of 5 cement samples with w/c:0.3. Each color represents a different sample as indicated on the diagram.

For cement practitioners and manufacturers, the strength ratios of 2nd day/7th day and 7th day/28th day are also significant and of practical important. These data are important because they provide a simpler understanding of the rate of strength development among various samples. Moreover, the rate of strength increment of cement (obtained from 2/7 day and 7/28 day ratios) has a substantial importance in constructions. It shows the rate at which construction can be done. The normal 2/7 and 7/28 day strength ratios for the OPCs are usually around 0.6 and 0.8, respectively. Figure 3.27 presents the 2/7 and 7/28 day ratios of average compressive strength of our 5 cement paste samples. It can be seen that the 2/7 day ratios were higher than the standard values in all of the samples, especially in sample#4 and #5, in which the ratio was close to 1. This means that in these samples, there was a small increment of the strength in between the 2nd and 7th day of the hydration. In other words, strength reached to a relatively high value already on the 2nd day of hydration. On the other hand, the 7/28 day ratios seemed to be close to the standard values. They fluctuated around 0.8±0.05.

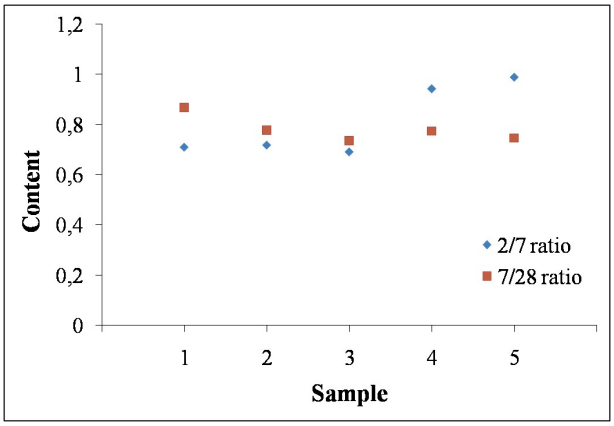

Figure 3.27. The 2/7 and 7/28 strength ratios of 5 cement samples prepared with w/c:0.3.

3-3-1-2) Strength tests using w/c:0.5

In order to understand the relation between the w/c ratio and strength development in cement pastes, compressive strength tests were also performed using w/c of 0.5. Since the w/c: 0.5 was the standard w/c for cement literature it also allowed direct comparison of the result obtained in this study with the existing OPC cement literature. The hydrated cement samples were prepared with w/c:0.5 and their compressive

strengths were measured on the 2, 7 and 28th day of hydration. Figure 3.28 presents the strength development graphs for the 5 cement samples which were manufactured using different alternative fuels. Again, each color represents the same sample as before, in the order described for Figure 3.26. It can apparently be seen that the overall strength values were ~50% lower when compared to the values of samples which were hydrated with a w/c:0.3. This fact shows the significant role of water amount in the cement pastes. It should be emphasized that the standard cement paste tests are performed with the w/c ratio of 0.45-0.5, mainly to provide the necessary workability for the paste.

In Figure 3.28, the compressive strength values on the 2nd day of hydration were in the range of 22±5 MPa. Sample#2 had the lowest and sample#1 and #4 had the highest values. It can be seen that sample#1,#3,#4 and #5 all maintain a close-range compressive strength values at 40±5 MPa after 7 day of hydration. On the other hand, sample#2 had a lower value of 28 MPa. The strength continued to increase in all samples. On the 28th day of the hydration, the overall range of compressive strengths reached 52±7 MPa among all of the cement samples. For the 28th day data, again sample#2 revealed the lowest and sample#4 and sample#1 had the highest compressive strength values. Overall, the strength value deviation among the 5 samples is higher compared with the one for a lower w/c ratio. This fact shows the importance of the water amount on the strength development in cement paste.

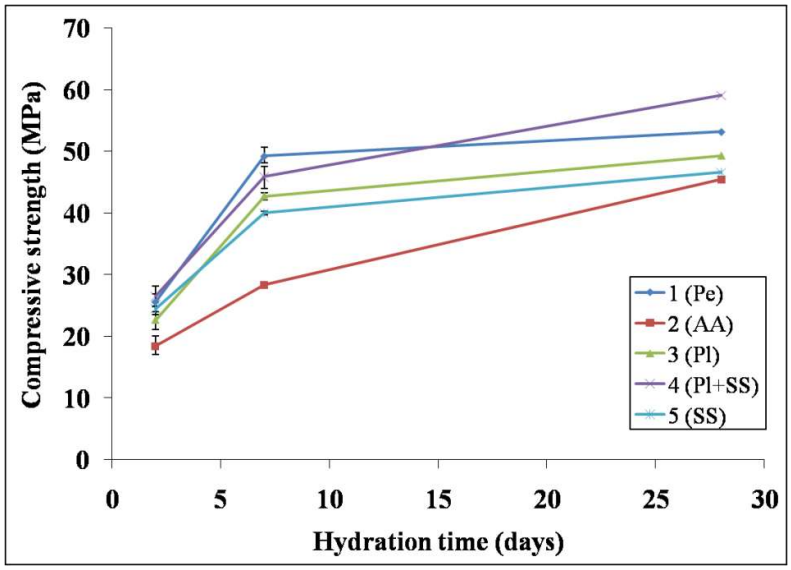

Figure 3.28. Compressive strength development graphs of 5 cement samples with w/c:0.5. Each color represents a different sample as indicated on the diagram.

The strength ratios of 2/7 and 7/28 days should also be investigated. The values obtained from the average strength values are shown in Figure 3.29 for the samples prepared with w/c:0.5. The 2/7 day values were close to the normal ones with a small deviation (0.6±0.06), however they were relatively lower compared to the samples prepared with w/c:0.3. This could mean that the higher amount of water to cementitious materials could decelerate the early hydration and the strength development was accelerated in the later days. By taking a look at the 7/28 days strength ratios, we can see that these values were only deviating for sample#1 and sample#2, which are respectively higher and lower than the customary, expected values. The strength of sample#1 did not develop as expected after the 28th day of the hydration. For sample#2, the low 7/28 day value was due to the low value of 7th day strength.

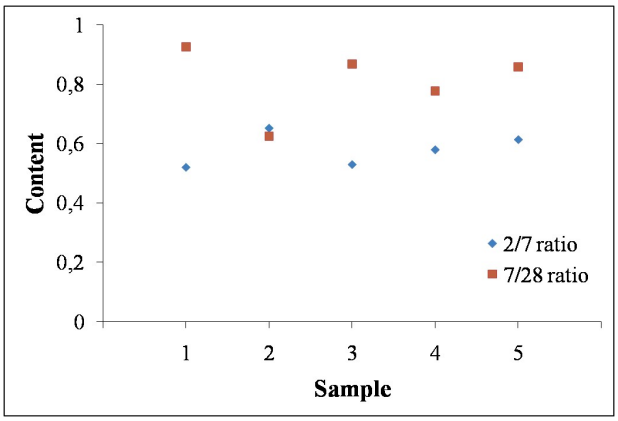

Figure 3.29. The 2/7 and 7/28 strength ratios of 5 cement samples prepared with w/c:0.5.

3-3-2) SEM analysis

The scanning electron microscopy was used to investigate the microstructural evolution of hydrated cement samples. The microscopy samples were prepared from the hardened cement pastes which were broken at the compression tests. Studying the fracture surface in the SEM allows the examination of microstructure of these regions. This method is very useful for the qualitative investigations, however, due to the favor of cracks to propagate in the weaker regions of cement, fracture surfaces are not representative of the cement as a whole [146].

For the microscopic observations, cement samples which were produced with water to cement ratio of 0.3 were utilized. The pieces of the fractured cement were

taken and prepared in two different shapes with the methods explained in the second chapter. Figure 3.30 presents the images of two different specimens of one sample, one fracture surface and another one polished surface, taken with SEM. The distinction in the morphology of two specimens was obvious and each of them can be used to obtain different information.

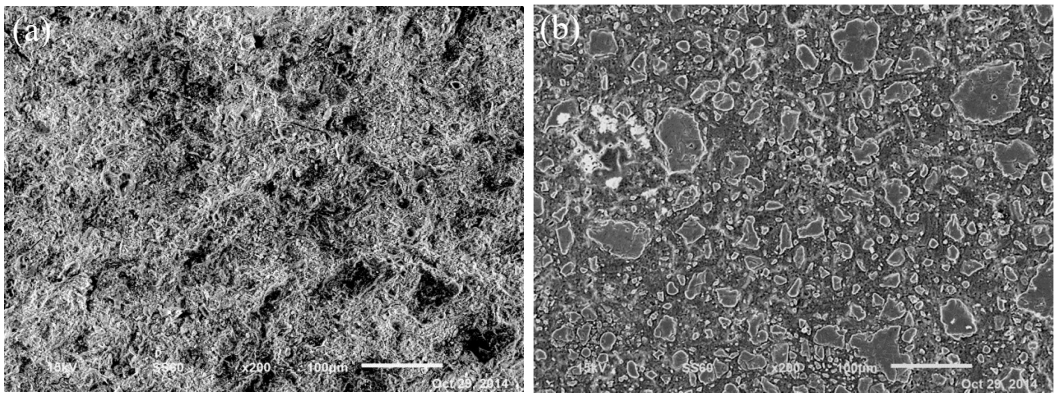

Figure 3.30. SEM SE images of hydrated cement sample#5: a) fracture and b) polished surface.

During the microscopic observations, both SE and BSE modes were utilized to investigate the microstructure. As it was mentioned before, BSE mode is the best to obtain the compositional contrast. Therefore, in order to study the phases with different average atomic weight, using backscattered electrons in imaging, will allow us to differentiate between phases. On the other hand, the secondary electrons are less energetic compared to the backscattered ones and so, the depth they are produced from on the surface is smaller. This fact results in obtaining a better spatial resolution and thus, SE mode is better for studying the topology in a comparison with BSE mode. Figure 3.31 shows the SEM images of fractured (31-a & 31-b) and polished (31-c &31-d) cement samples at both SE and BSE modes taken from the same region. The distinction between the two modes can be observed readily. It can be inferred that SE modes is more suitable to study the fracture surfaces because of the higher resolution of the morphological features. Nevertheless, polished surfaces which were aimed to investigate the phase distribution and quantifying the phases, are best to be observed with BSE mode. It is worth mentioning that at the polished surfaces, the topographical features were already removed by polishing the surfaces and this increased the contrast.

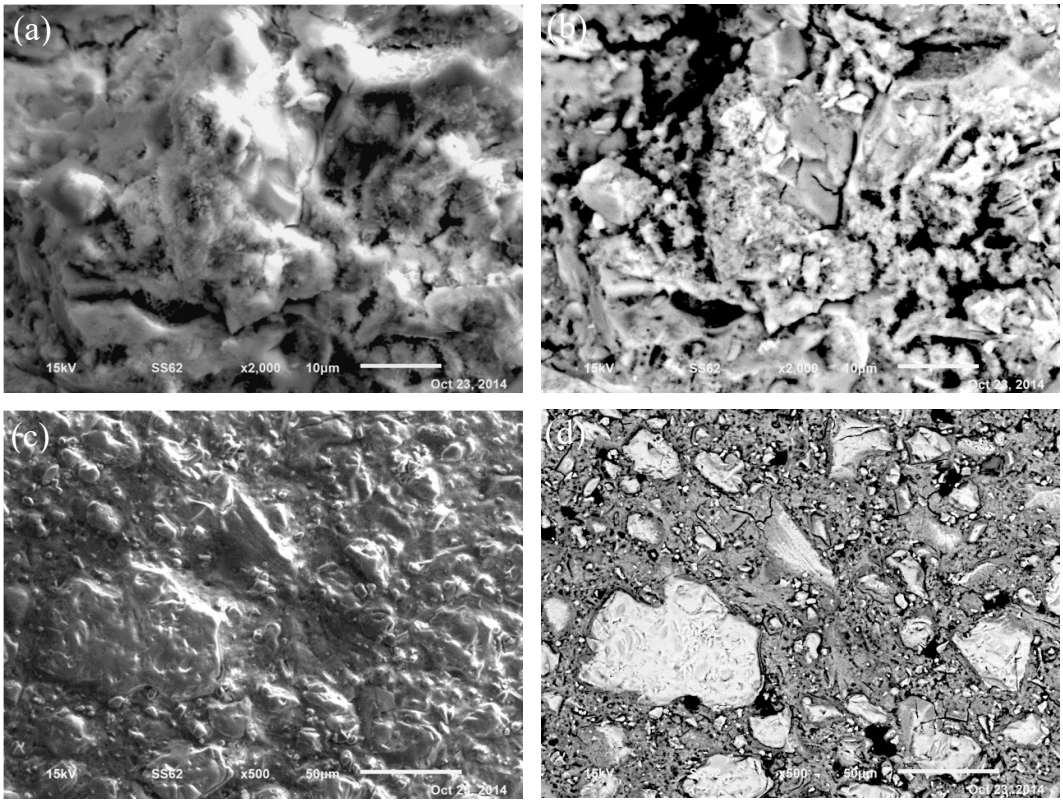

Figure 3.31. SEM images of hydrated cement samples taken using different imaging modes, fracture surface as imaged using a)SE and b)BSE electrons, and polished surface as imaged using c)SE and d)BSE electrons.

As it was discussed in the first chapter, when cement is mixed with water, new phases are produced through the hydration reactions. However, not all the hydration reactions take place at the same pace. Some parts of cement continue to react inside the material maybe for years. Therefore it is quite common to observe the unhydrated regions besides the hydrates in the structure of the cement paste. These phases can be seen in Figure 3.32 which shows the SEM BSE image of polished sample#3 at the 7^{th} day of hydration. The unhydrated phases had a brighter grey contrast compared to the hydrated phases and were therefore easily distinguished in the microstructure of the paste. The C-S-H gel is shown as the outer product and inner product. The inner product is the result of continuing hydration of the unhydrated silicates, which occurs like a ring around the anhydrous cement particles. It was not easy to differentiate between the different hydrated phases in the polished surface images.

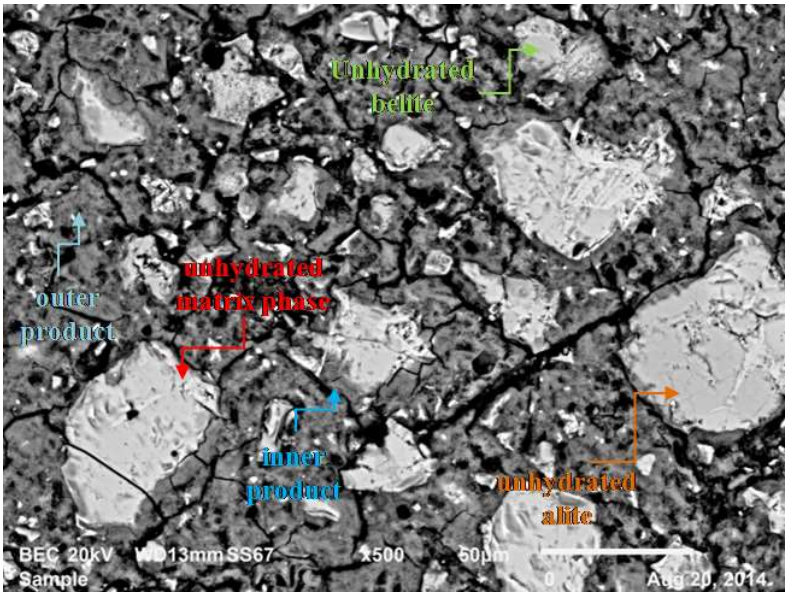

Figure 3.32. SEM BSE image of the polished surface of sample#3 at the 7th day of hydration. The phases are distinguished on the image.

Figure 3.33 shows the SEM SE images of fracture surface of hydrated cement sample#4 at the 2nd day (Figure 3.33-a) and sample#3 at the 7th day of hydration (Figure 3.33-b&Figure 3.33-c). The hydrated phases can be identified as they are remarked on the images as ettringite and C-S-H (Figure 3.33-a), monosulfate (Figure 3.33-b) and CH (Figure 3.33-c).

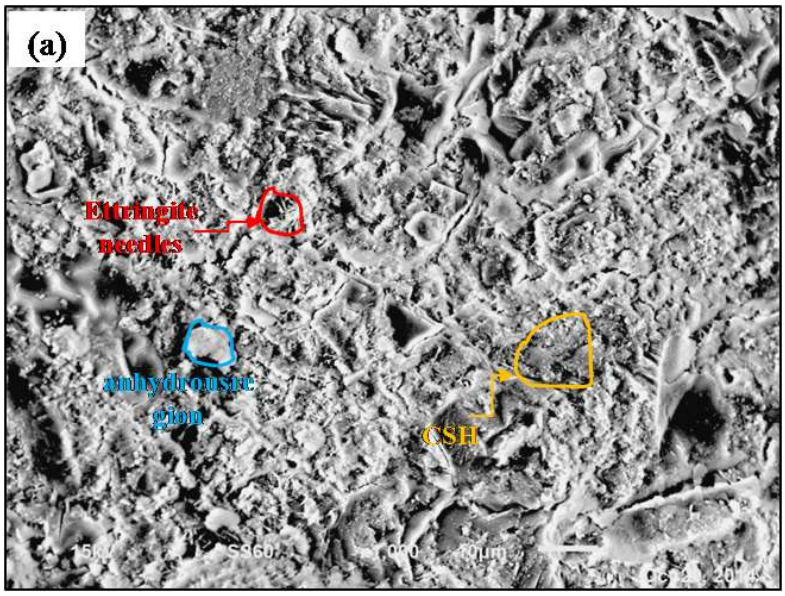

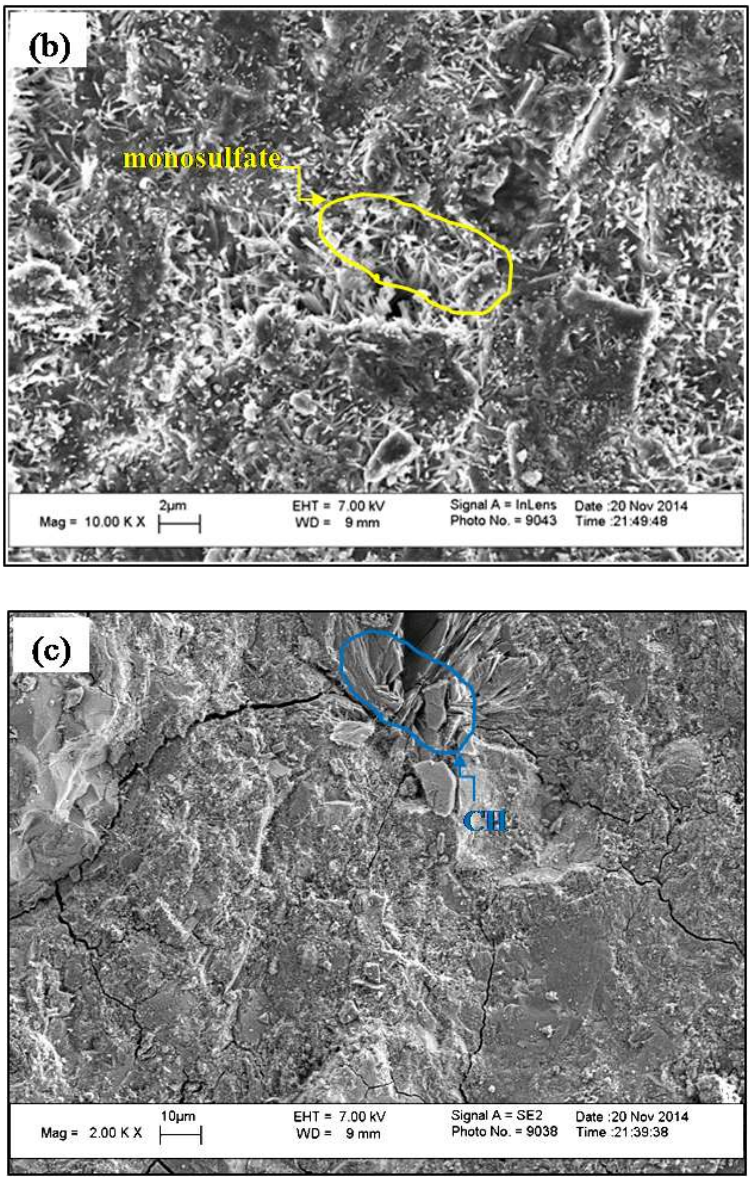

Figure 3.33. SEM SE images of the fracture surface of hydrated cement a)sample#4 at the 2nd day and b&c)sample#3 at the 7th day of hydration. The phases are marked on the images.

In order to investigate the microstructure of the hydrated cement samples, SEM observations were done at different magnifications and the images were taken. In Figure 3.34, the SEM images of sample#1 at the 28th day of hydration are shown in 4 different magnifications (50,200,500 and 2000x).The advantage of these observations was the capability of investigating all of the phases in different scales.

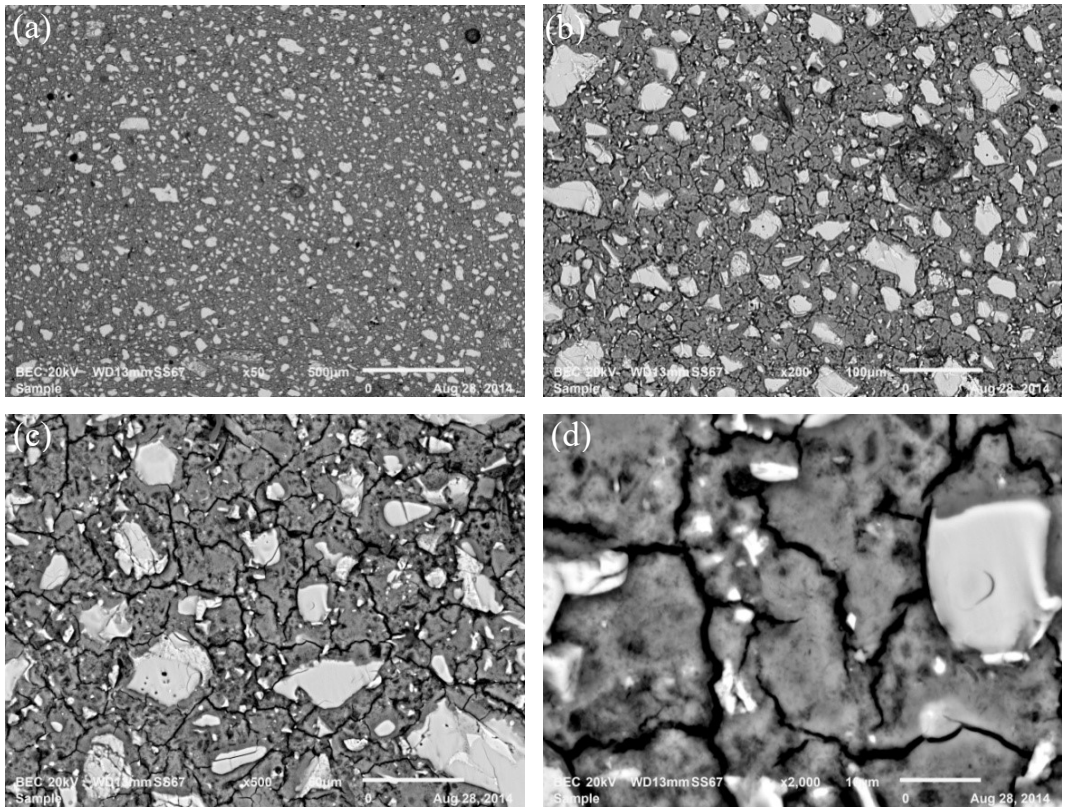

Figure 3.34.SEM BSE images of sample#1 at the 28th day of hydration in 4 different magnifications.

The SEM observations of the cement samples were carried out in the different hydration days like 1,2,3,7,14 and 28th days. In Figure 3.35, Figure 3.36 and Figure 3.37 present the polished surfaces of the hydrated specimens respectively at the 2,7 and 28th day of hydration for all 5 cements prepared with different alternative fuels. It can be seen in Figure 3.35 that the microstructure of the 2nd day samples were similar to each other with regard to the hydration products and they did not differ much. The most visible feature of these microstructures is the unhydrated (anhydrous) cement regions. These regions seem to be similar in size and number, which means the hydration progresses with a close rate among samples. The cracks in sample#2 and sample#4 were the result of drying stage during sample preparation and could not be taken into account as a specific characteristic of these samples.

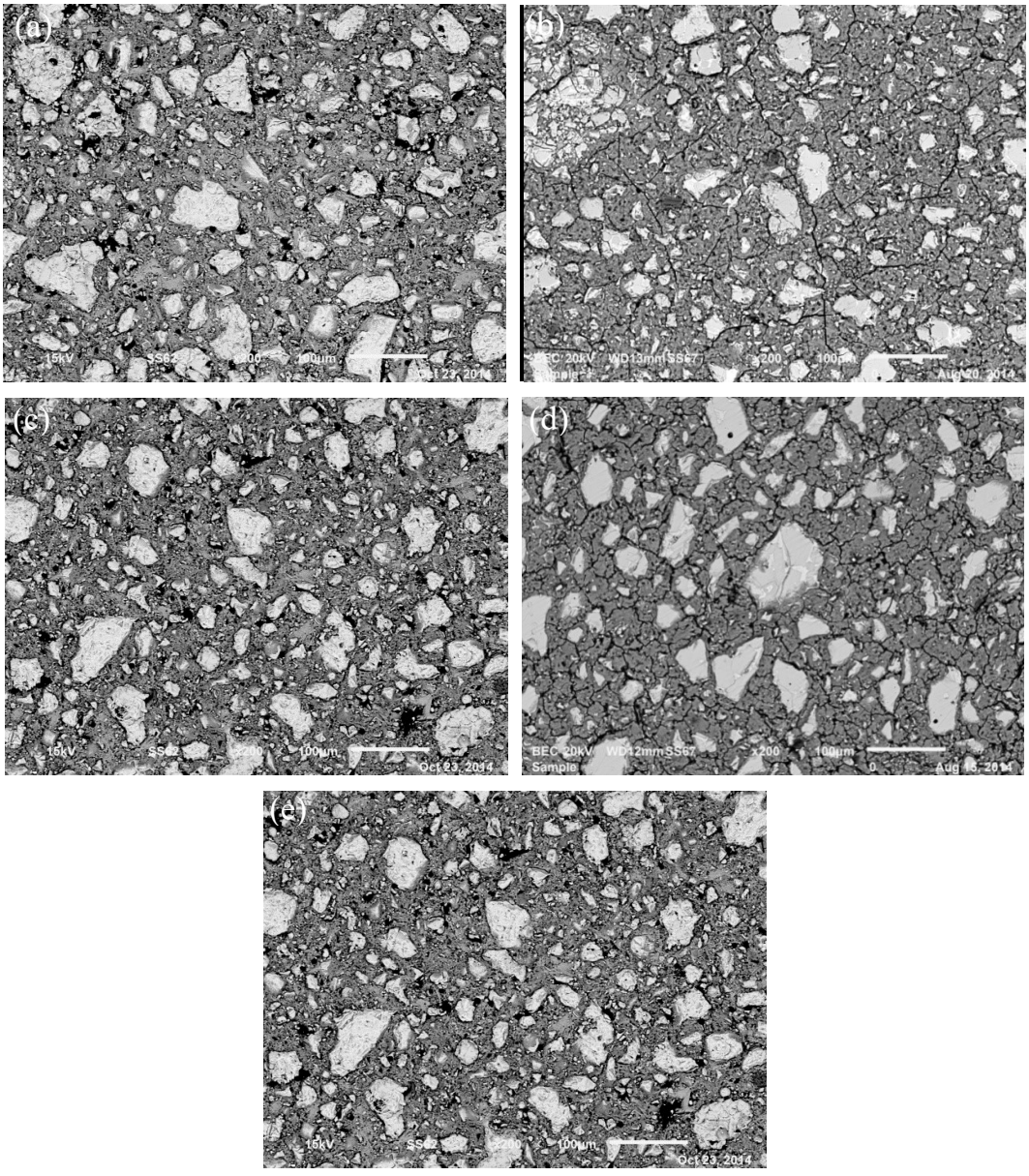

Figure 3.35. SEM images of polished cement specimens at their 2nd day of hydration, a)cement#1, b)cement#2, c)cement#3, d)cement#4 and e)cement#5.

The SEM images of the samples at their 7th day of hydration can be seen in Figure 3.36. Again, it can be seen that like the 2nd day samples, the difference in the anhydrous regions is small among five samples. The content and size of the unhydrated regions was decreased compared to the 2nd day samples. The clinker minerals could also be differentiated in the anhydrous particles. However, it is unlikely to measure these phase amounts through these microscopic images.

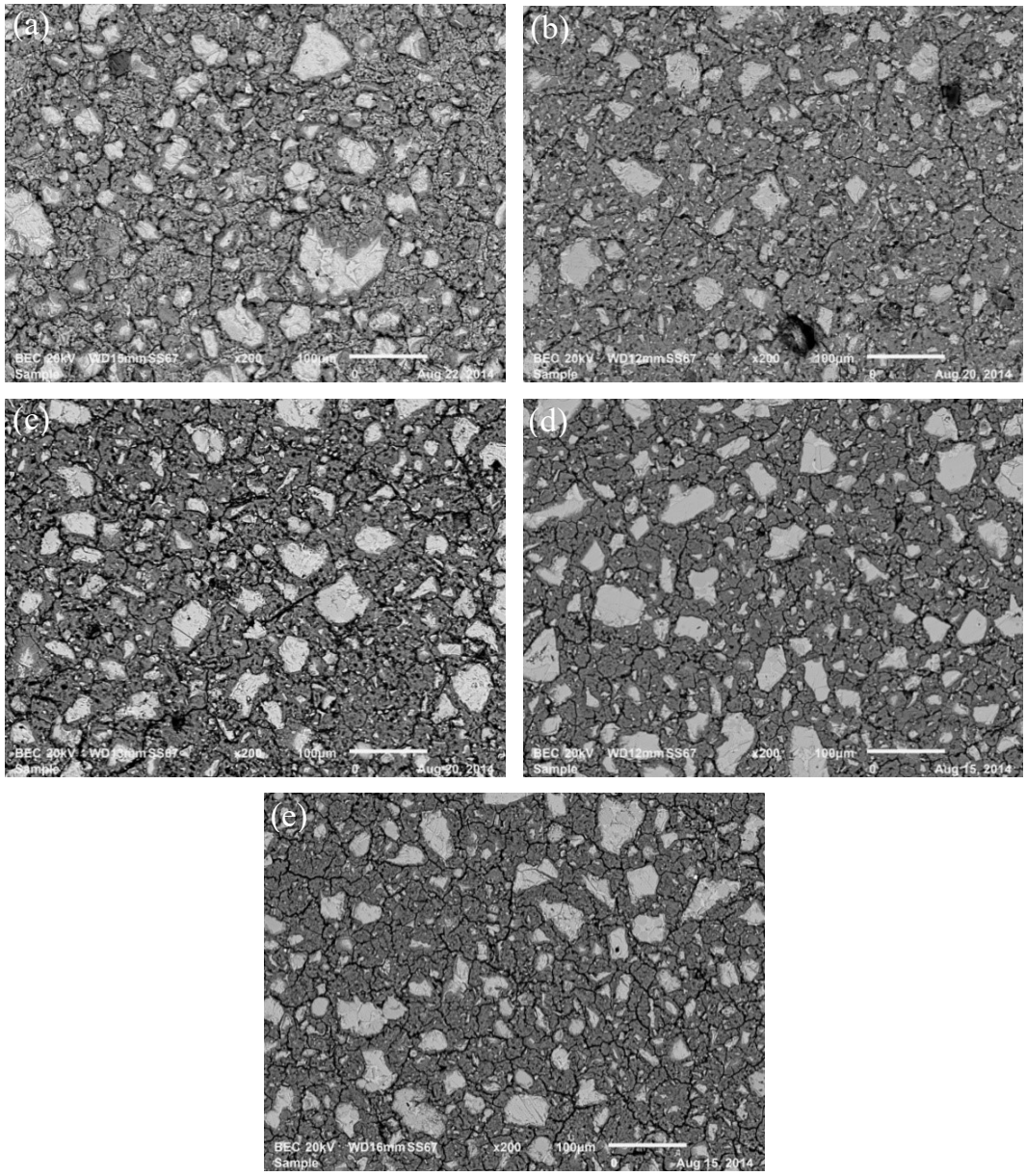

Figure 3.36. SEM images of polished cement specimens at their 7th day of hydration, a)cement#1, b)cement#2, c)cement#3, d)cement#4 and e)cement#5.

The microstructure of the hydrated cement samples at 28th day of hydration can be seen in Figure 3.37. The anhydrous phase contents again seemed to be similar among 5 samples. It can be said that the smaller unhydrated parts were being hydrated faster than the bigger ones. It means that the small particles are being consumed in the early days. However, after the formation of C-S-H layer around the particles, it becomes more difficult for the big particles to continue hydration. Therefore, the smaller particles cause a higher reactivity for cement grains. Sample#1 and sample#5 have a lower

content of anhydrous regions in the microstructure. Overall, the hydration did not seem to advance much with respect to the 7th day samples.

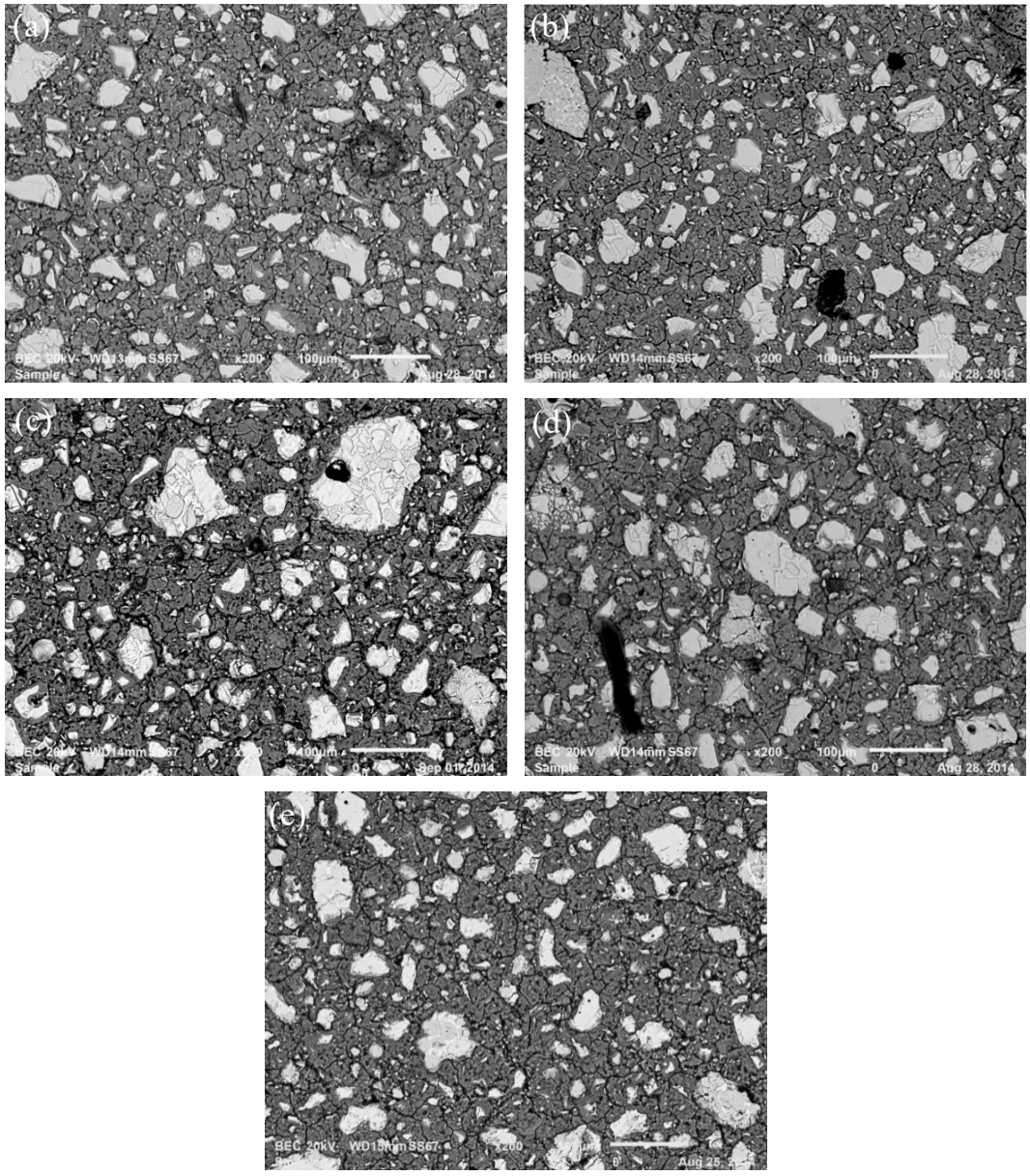

Figure 3.37. SEM images of polished cement specimens at their 28th day of hydration, a)cement#1, b)cement#2, c)cement#3, d)cement#4 and e)cement#5.

The microstructural evolution of the hydration was shown in the figures. But, it is also needed to quantify the speed of the hydration process. For this reason, the image analysis software was used to measure the unhydrated regions through the grey color contrast in the microscopic images. The measured values were used to estimate the overall silicate phases (alite and belite). Anhydrous silicate phases determine the

progress of the hydration process, as discussed in chapter1.Figure 3.38 shows the graphs of the silicates consumption during the 28 days of the hydration. These graphs tell us the reason of the high compressive strength values of the hydrated samples at the early stage of hydration. The steep slope of the graph between 0-2 days indicate that about ~70% of the hydration was completed at the 2nd day. Afterwards, the speed of the hydration decreases and as a result, the strength increment also decelerates. The ratio of amounts of anhydrous cement particles in the total silicates amount for 7 to 28 days of hydration were close to 1.

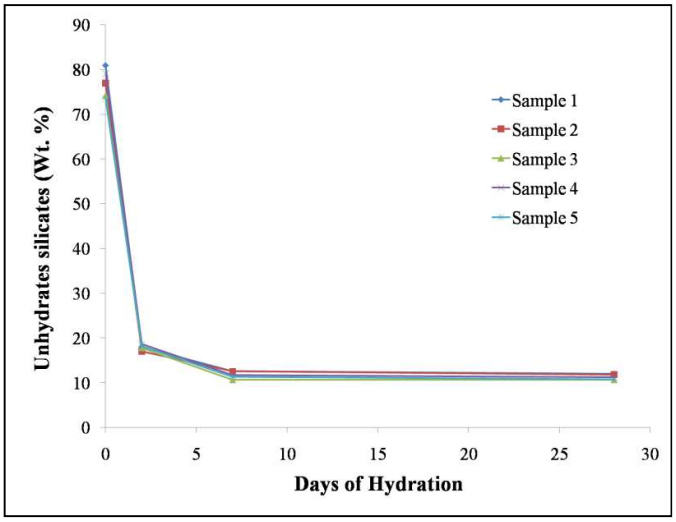

Figure 3.38. Consumption of the silicates during the hydration process of the 5 cement sample, measured using image analysis.

3-3-3) XRD analysis

The x-ray diffraction analysis was also utilized to investigate the hydration process of the cement samples. Using XRD, it is possible to determine the phases during the hydration along with their quantities. Therefore, the rate of evolution or consumption of each phase could be measured separately, which was not feasible with SEM because of the low contrast among hydrated phases. However, there are a few drawbacks related to XRD measurements of the cement phases, like the low crystallinity of some phases (particularly C-H-S), which makes their identification difficult. Also, the high amount of different phases results in crowded XRD patterns with lots of overlapping peaks and arduous quantification.

The XRD measurements were implemented on the hydrated cement samples right after the compression tests without stopping the hydration. The reason was to prevent the probable modification of the phases by their reaction with the organic solvents used for the drying procedures. After pulverization of the fractured samples, they were used in XRD analysis. In the following pages, the XRD patterns for each sample at different hydration days along with the graphs showing the values of main phases will be presented separately.

Figure 3.39 shows the XRD patterns of sample#1 at the 0 (clinker), 2,7 and 28th day of the hydration. The main phases of unhydrated (alite, belite, aluminate, ferrite) and hydrated cement (CH, ettringite and monosulfate) are shown on the patterns. The peak positions related to the crystalline C-S-H (Tobermorite) are also indicated on the patterns. However, due to the heavy peak overlap in the range of 25-40°, it is mostly likely that these peaks may be mixed with peaks of alite or belite minerals in the anhydrous part of cement.

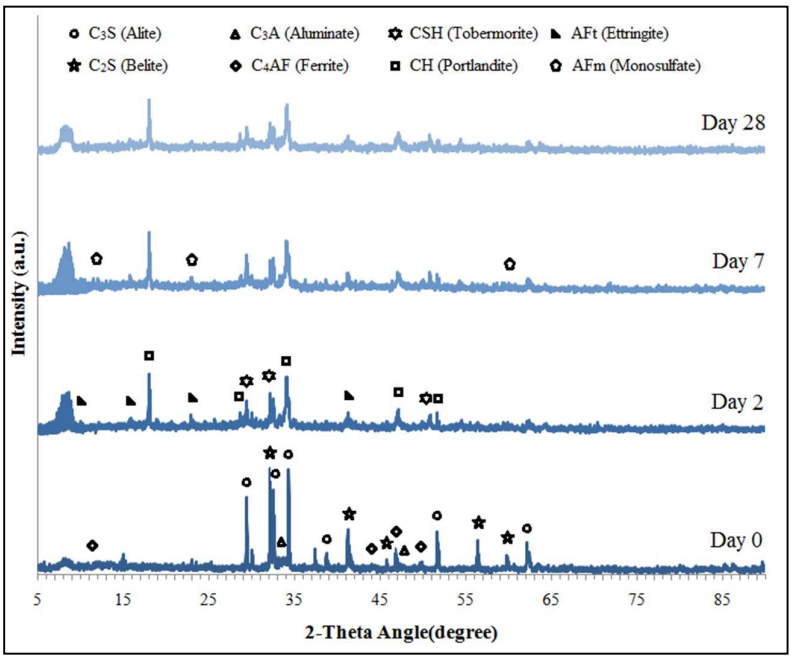

Figure 3.39. XRD patterns of cement#1 during the hydration process at the age of 0, 2, 7 and 28 days. The unhydrated (day 0) and hydrated (day7 and day 28) phases are shown.

The phases were quantified using Rietveld analysis method and their values were used to plot graphs of phase alterations during the hydration process. Figure 3.40 shows

the results in separate graphs for alite/belite ratio, aluminate and ferrite, and ettringite and monosulfate values. The a/b ratio was decreasing from 5.6 for the unhydrated sample to 0.9 at the 28th day, which indicated the higher speed of alite hydration with respect to belite in the initial days of hydration. Aluminate and ferrite phases were hydrating and so their values were also decreasing with the progress of hydration. Ettringite was produced as the hydration process began and its amount became ~2 wt% at the 2nd day. Continuation of the hydration resulted in the conversion of ettringite to monosulfate and it can be seen in the graphs as a decrement in ettringite value along with an increment in monosulfate value.

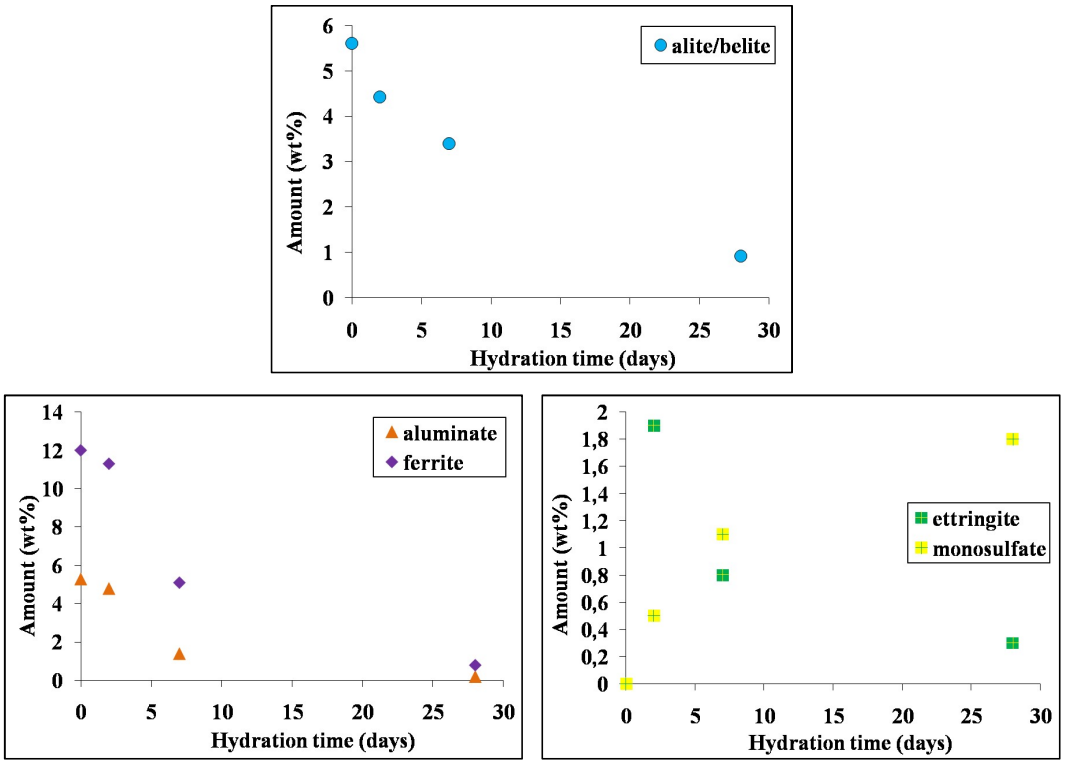

Figure 3.40.The graphs of a/b, aluminate, ferrite, ettringite and monosulfate alterations during the hydration process of cement#1 from 0th day till 28th day of hydration.

In addition to the major phases, some minor phases were also detected in the XRD measurements of cement#1. These phases include $Ca(SO_4)(H_2O)_2$, $Ca_5(SiO_4)_2(OH)_2$, $Ca_2Mn_2Si_4O_{11}(OH)_4{\cdot}2H_2O$, and $K_{1.74}Ca_{2.72}Mg_{0.80}(Al_{8.22}Si_{27.78}O_{72})(H_2O)_{31.56}$.

Figure 3.41 shows the XRD patterns of sample#2 at different hydration days of 0, 2, 7 and 28. The peaks of main phases are marked on the patterns. Formation of CH as a crystalline phase is obvious on the patterns. Its amounts increased at the 7th day and

decreased at the 28th day of hydration. This decrement could be an indication of CH's reaction with AFt phases in order to form new phases.

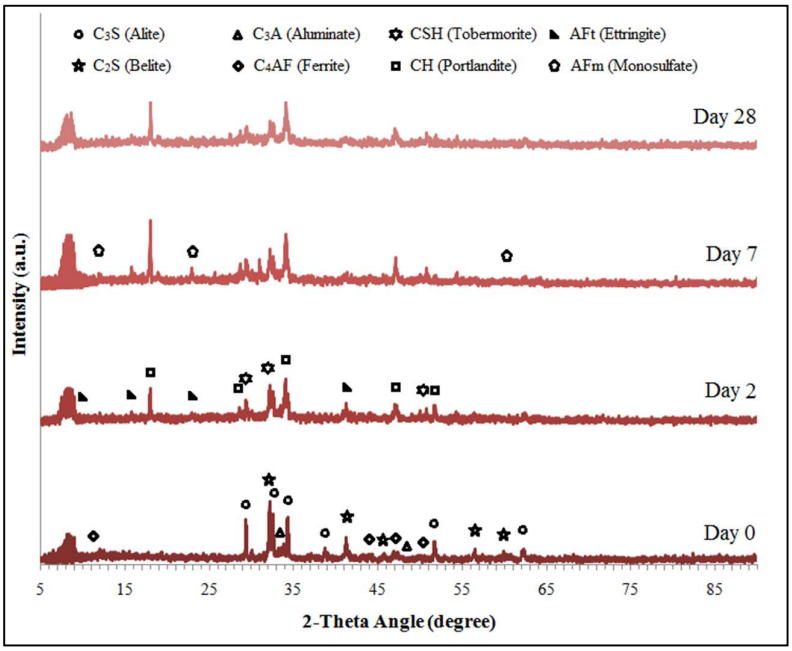

Figure 3.41. XRD patterns of cement#2 during the hydration process at the age of 0, 2, 7 and 28 days. The unhydrated (day 0) and hydrated (day7 and day 28) phases are shown.

The changes in the content of main phases are shown in Figure 3.41 for the first 28 days of the hydration. The slow decrement rate of a/b ratio is obvious in the graph. This can mean either no reaction of alite or the reaction of both alite and belite phases with a similar speed. Since the compression strength was increasing and it was dependent on the hydration of alite and belite, it could be concluded that both of the phases were reacting in the first days of hydration. The hydration rate was also observed to be high in the microscopic image analyses. This can be an indication of a reactive belite phase, probably due to the minor elements doped in the structure of belite crystals.

Figure 3.42 also shows that the matrix phases (aluminate and ferrite) of cement#2 were reacting rather slowly until the 7th day of hydration, compared to cement#1. Even so, there is a huge amount of ettringite formed on the 2nd day of hydration (>6 wt%). On the 7th day, there is still around 5 wt% ettringite present in the paste. Monosulfate

formation starts as soon as some ettringite convert to a low-sulfate phase in the 2nd day. There is around 4 wt% monosulfate at the 28th day of hydration.

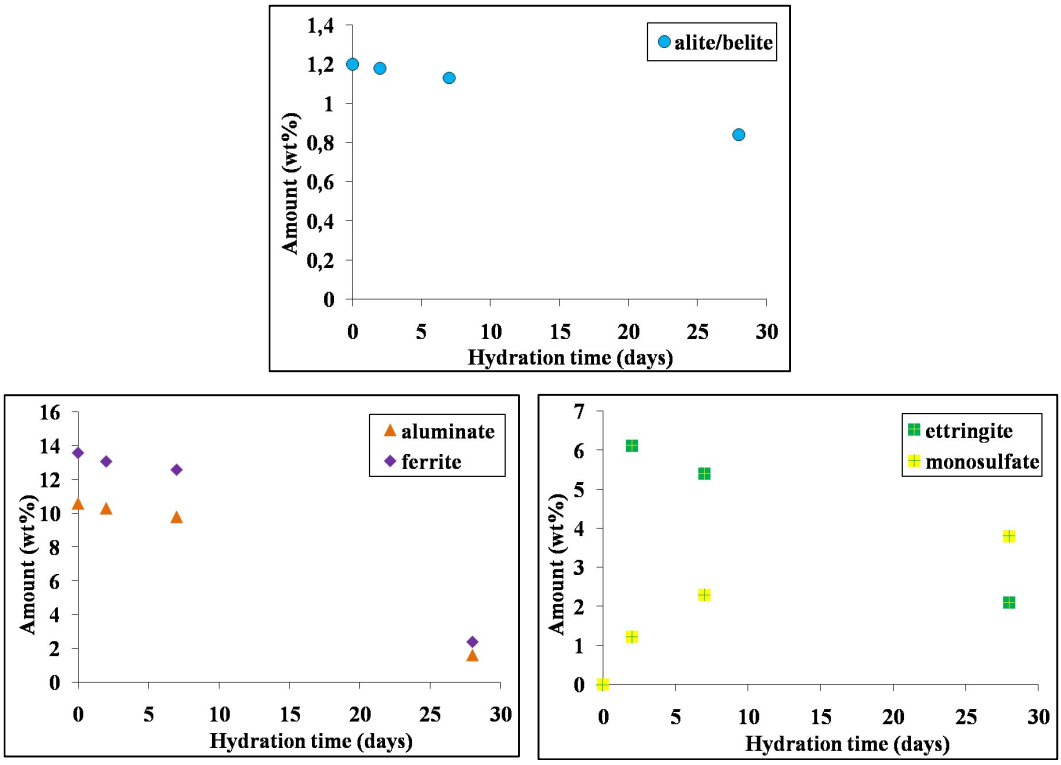

Figure 3.42.The graphs of a/b, aluminate, ferrite, ettringite and monosulfate alterations during the hydration process of cement#2 from 0th day till 28th day of hydration.

A number of the minor phases detected during the XRD measurements included$Ca_6Al_2(SO_4)_3(OH)_{12} \cdot 26H_2O$, $K_3Na(SO_4)_2$, $(Mg.6Fe.2Al_2)Ca(Si1.5Al_5)O_6$, $Ca_3(Mg_4Al)Si_5Al_3O_22F_2$, $(Na_3.88Ca0.12)(Al_3.12Si8.88)O_24Cl$ and $NaCa_2(Mg,Fe)_4Ti(Si_6Al_2)O_32(OH)_2$.

Figure 3.43 presents the XRD patterns of cement#3 during its hydration process. Again, the main phases are indicated on the patterns. The CH peaks appeared at the 2nd day of hydration. The peak heights have decreased at the 7th day and increased again at the pattern of 28th day of hydration.

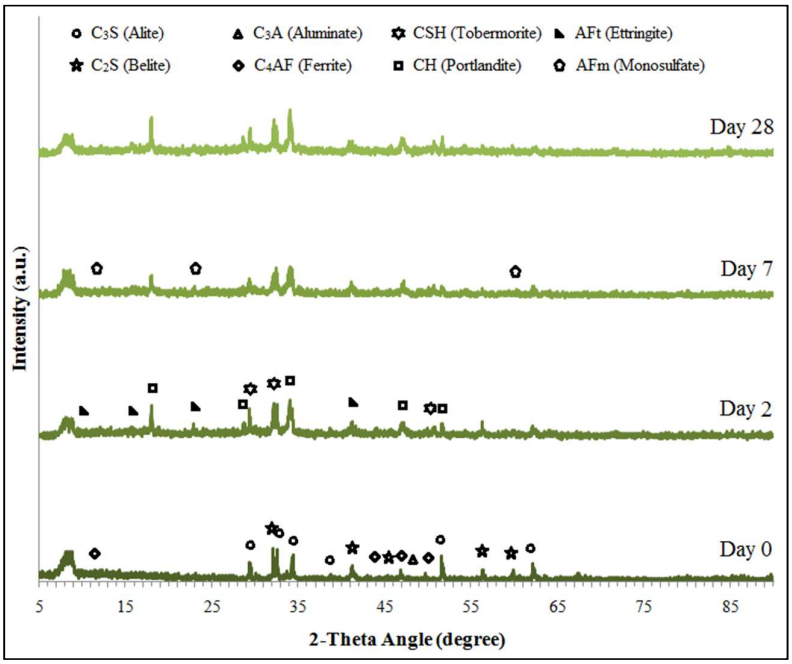

Figure 3.43. XRD patterns of cement#3 during the hydration process at the age of 0, 2, 7 and 28 days. The unhydrated (day 0) and hydrated (day7 and day 28) phases are shown.

The quantified phase values of cement#3 can be seen in Figure 3.44. The alite/belite value did not change at the 2nd day of hydration and it decreased after the 7nd day. It means alite and belite were being consumed with a similar rate until the 2nd day. The pace at which the aluminate and ferrite phases were being consumed seems as expected in the OPC hydration reactions. The ettringite has formed about 4% at the 2nd day, but its decrement rate is low. At the 28th day of hydration, there is still 1.5% ettringite in the composition.

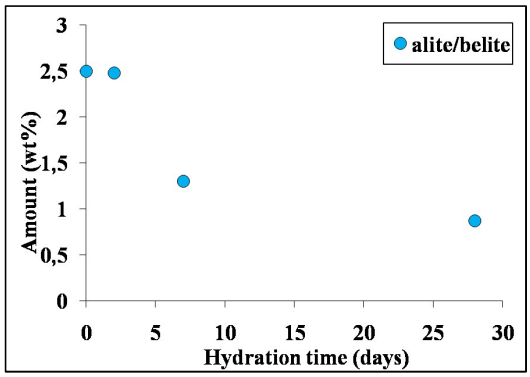

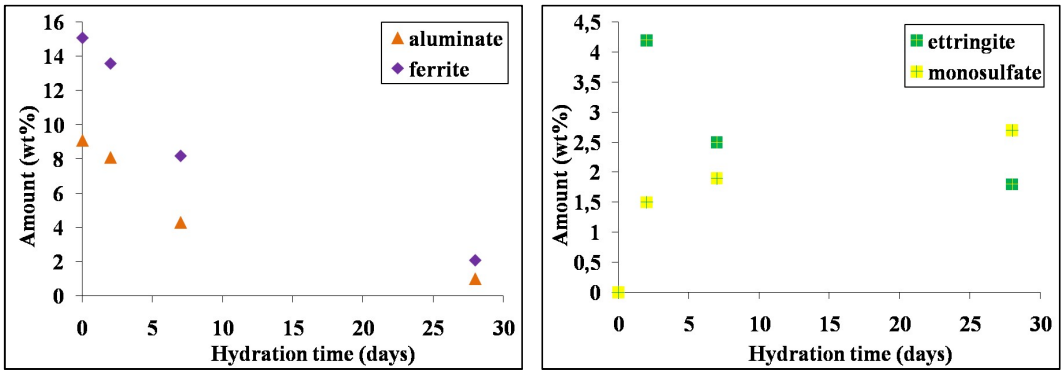

Figure 3.44. The graphs of a/b, aluminate, ferrite, ettringite and monosulfate alterations during the hydration process of cement#3 from 0th day till 28th day of hydration.

In addition, some other minor phases like $CaO(A_2O_3)_6$, $Ca(A,Fe)_{12}O_{19}$, $Ca_6Al_2(SO_4)_3(OH)_{12}\cdot 26H_2O$, $Ca_5(SiO_4)_2(OH)_2$, $NaCa_2(Mg,Fe)_4Al_3Si_6O_{22}$, $KO.29Ca_5.8Al_{18}.7Si_4.15O_{32}$were detected in the XRD measurements of cement#3. It was not very straightforward to calculate the amounts of these phases due to the complicated XRD patterns of hydrated cement.

The XRD patterns of cement#4 during the hydration days of 0, 2, 7 and 28 can be seen in Figure 3.45. The phases are also shown on the image.

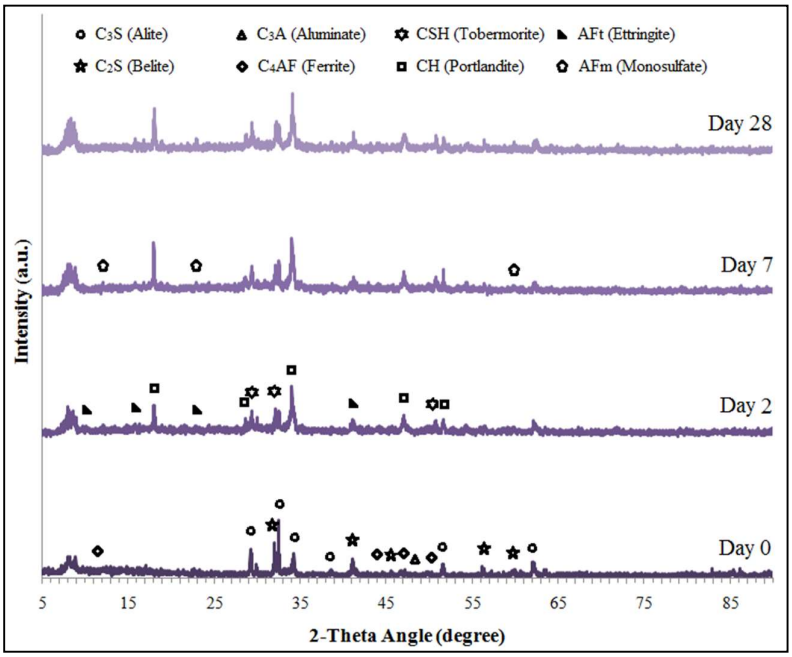

Figure 3.45. XRD patterns of cement#4 during the hydration process at the age of 0, 2, 7 and 28 days. The unhydrated and hydrated (day7 and day 28) phases are shown.

The quantifications were done for cemen#4's phases as well. The graphs of Figure 3.46 show the related phase value alterations. The anhydrous phase values changed similar to cement#1, meaning an ordinary hydration reactions pace. The formation and consumption of ettringite and monosulfate also seem as expected in OPC hydration.

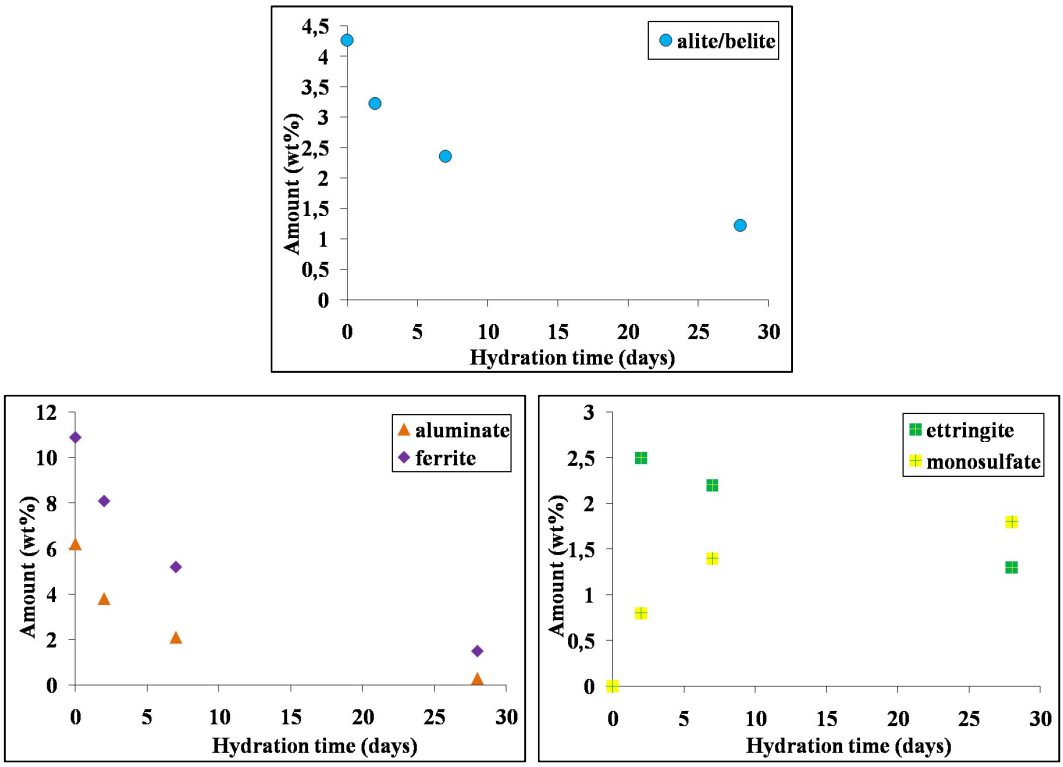

Figure 3.46. The graphs of a/b, aluminate, ferrite, ettringite and monosulfate alterations during the hydration process of cement#4 from 0th day till 28th day of hydration.

Also in cement#4, some minor phases were detected during the hydration process like $CaSO_4 \cdot 0.5H_2O$, $Ca_4Al_2(SO_4)(OH)_{12} \cdot 6H_2O$, $CaAl_2(Al_2Si_2)O_{10}(OH)_2$, $Ca_9H_2Si_6O_{18}(OH)_8 \cdot 6H_2O$, $Ca_6Al_2(SO_4)_3(OH)_{12} \cdot 26H_2O$, $CaAl_6(SO_4)_4(OH)_{12}$.

The phase distibution of hydrated cement#5 was also carried out using XRD. Figure 3.47 shows the XRD patterns during the 0, 2, 7 and 28th day of hydration.

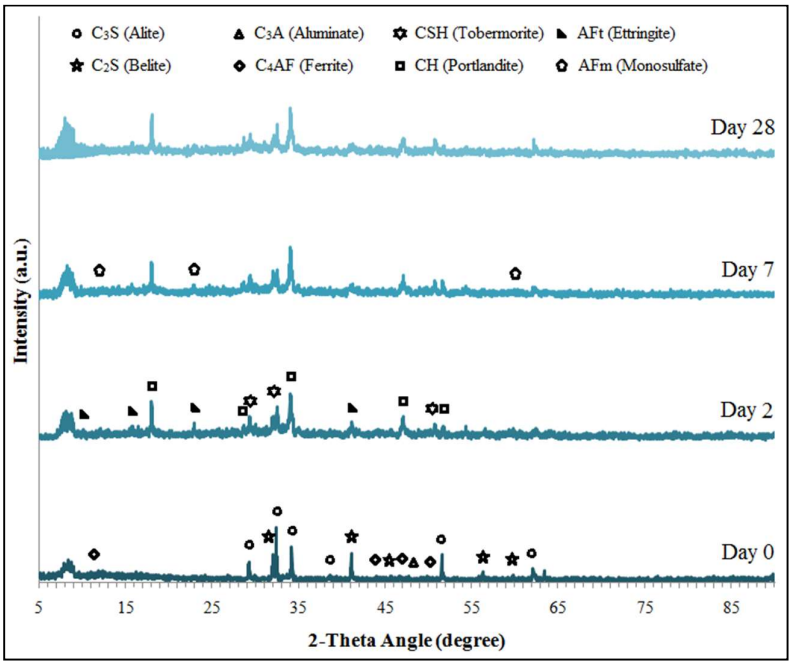

Figure 3.47. XRD patterns of cement#5 during the hydration process at the age of 0, 2, 7 and 28 days. The unhydrated (day 0) and hydrated (day7 and day 28) phases are shown.

Figure 3.48 presents the phase modifications during the hydration of cement#5. It was observed that the alite/belite ratio decreases slowly. This fact could be related to the already small amount of alite phase in this sample, meaning that there was not much alite to be consumed fast. The phase amounts of aluminate and ferrite reduced similar to other samples. The amount of formed ettringite on the 2nd day of hydration is high (~7 wt%) for this sample. It is converted to monosulfate with a high pace, although there is still ~2 wt% ettringite in the composition at 28th day of hydration.

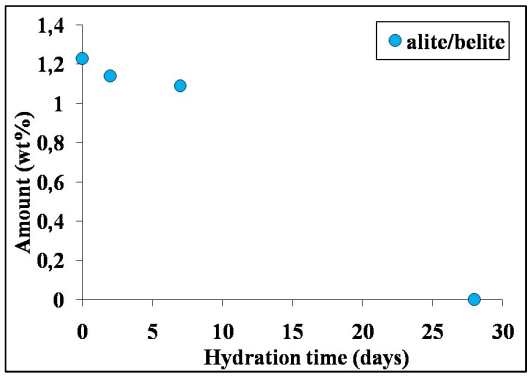

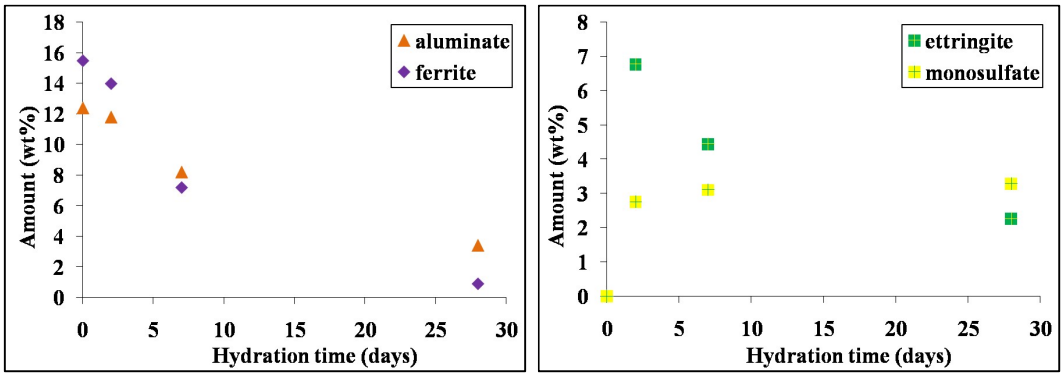

Figure 3.48. The graphs of a/b, aluminate, ferrite, ettringite and monosulfate alterations during the hydration process of cement#5 from 0th day till 28th day of hydration.

A few of the minor phases observed in the XRD measurements of hydrate cement#5 included$Ca_4Si_3O_{10}\cdot 2H_2O$, $Ca_6Al_2(SO_4)_3(OH)_{12}\cdot 26H2O$, $Ca_6(SiO_4)(Si_2O_7)(OH)_2$, $Ca_3(HSiO_4)_2(H_2O)_2$, $Ca_6(Al(OH)_6)_2(SO4)_3(H_2O)_{25.7}$, $Ca_{2.25}(Si_3O_{7.5}(OH)_{1.5})(H_2O)$.

The aluminate and ferrite phases hydration controls the setting of cement, whereas hydration of alite and belite phases provides the strength by forming strength-giving phases like C-S-H and CH. Therefore, it was concluded that for determining the characteristics of cement pastes it is more useful to analyze alite and belite values.

3-4) Control cement samples

As the last part of the project, two new cement samples were provided by the AkçanSA company. Theses samples were produced at two separate days using a mix of waste plastics and sewage sludge as fuels. These samples were the control samples for sample#4 and therefore are called 4N1 (sample#4-New-1) and 4N2 (sample#4-New-2). The samples were characterized for their microstructure, compressive strength and phase distribution.

3-4-1) SEM analysis of cement powders

The microstructure of the new cement powders was investigated using scanning electron microscopy. Using cement powders instead of clinker for microscopic observation is very problematic, since most of the microstructure of the clinker nodules is lost[3].This fact can be seen in the SEM images of sample 4N1 and 4N2 in Figure 3.49. The figure includes both BSE (left) and SE (right) images. Bright particles of

cement in the image were impregnated in the epoxy resin dark matrix. It was shown that each cement grain contains alite, belite and other phases. However, it was almost impossible to quantify the phase values, as the phases were even difficult to be distinguished. Nevertheless, these samples could be used to estimate the particle size and distribution in the pulverized cement powders. The samples were observed to have particle sizes in the range of <10 μm-50 μm with a higher distribution in 10-30 μm.

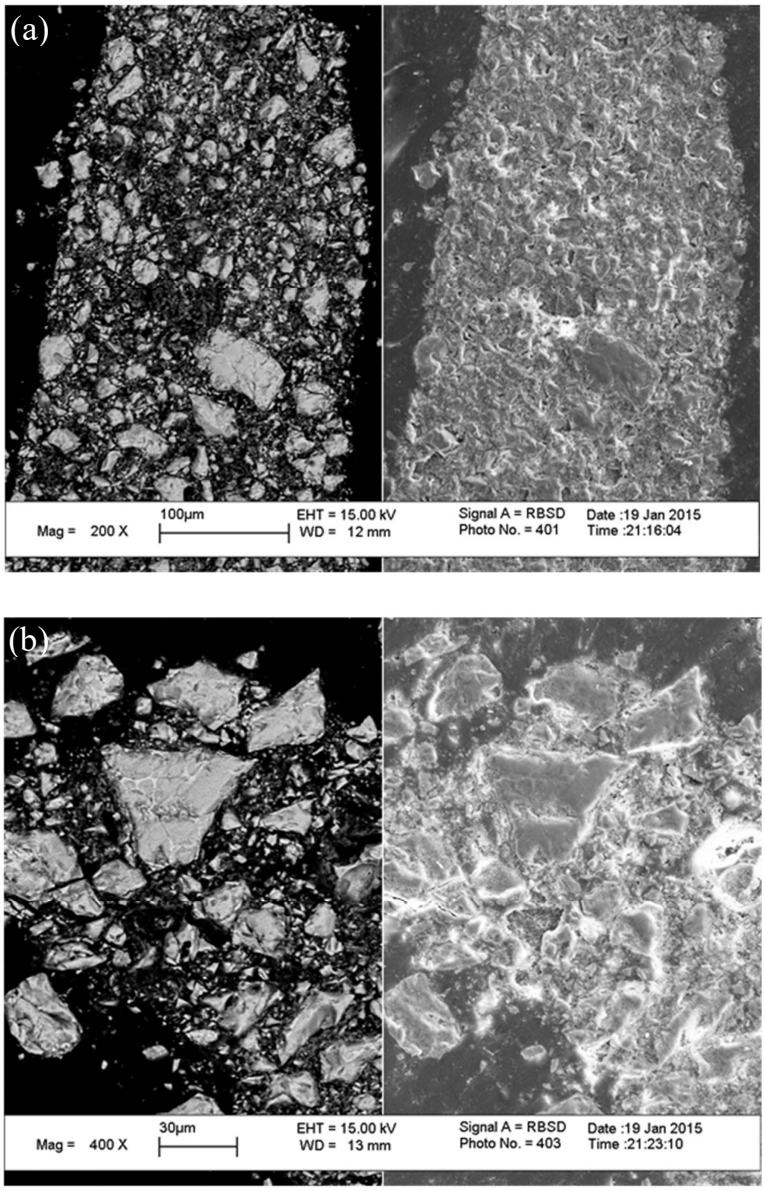

Figure 3.49. SEM (BSE:left,SE:right) images of the powder cement samples a)4N1 and b)4N2, prepared using epoxy resin as the matrix.

3-4-2) XRD analysis of cement powders

The phase distribution of the cement samples 4N1 and 4N2 was investigated using XRD analysis. Figure 3.50 presents the XRD patterns of these two samples.

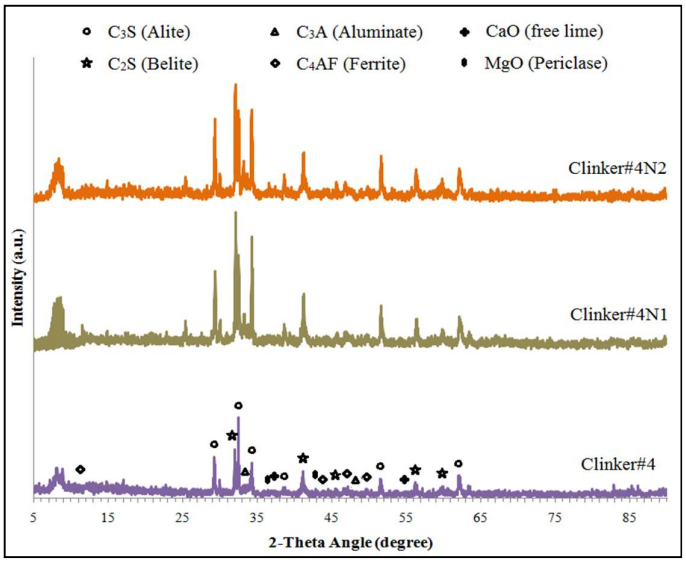

Figure 3.50. XRD patterns of clinker#4 along with the two new cement powder samples (4N1 and 4N2)

The phase amounts were calculated using Rietveld analysis method and are shown in Table 3.9. The values of sample#4 are also presented in the table for a comparison. It can be seen that the phase contents of sample 4N1 and sample 4N2 were very close to each other and to the values of sample#4. This consistency in the phase amounts in three different samples produced in three different days could be considered as a reassurance for the validity of the methodology used in our studies and the effect of using each kind of alternative fuel on the properties of clinker and cement.

Table 3.9. Phase amounts of unhydrated cement samples 4N1 and 4N2 obtained from XRD analysis. The values of clinker#4 are also shown for the comparison.

sample#	alite	belite	alite/belite	aluminate	ferrite
4N1	63.98	15.49	4.13	7.52	13.01
4N2	64.16	15.55	4.14	7.31	12.92
4	64.49	15.01	4.3	7.4	13.1

3-4-3) Compression tests of hydrated samples

The two cement powders were used to make hydrated cement paste samples using 0.3 as the water to cement ratio. Their compressive strengths were measured in various days of hydration. The results are shown in Figure 3.51 for sample 4N1, sample 4N2 and sample#4 for the comparison. The strength graphs are developing almost identical for the new samples. Comparing them to the curve of sample#4, we can see that although there was a difference, the strength development behavior was similar. Moreover, the 28th day strength is almost the same for all the 3 samples prepared with the same mix of fuels.

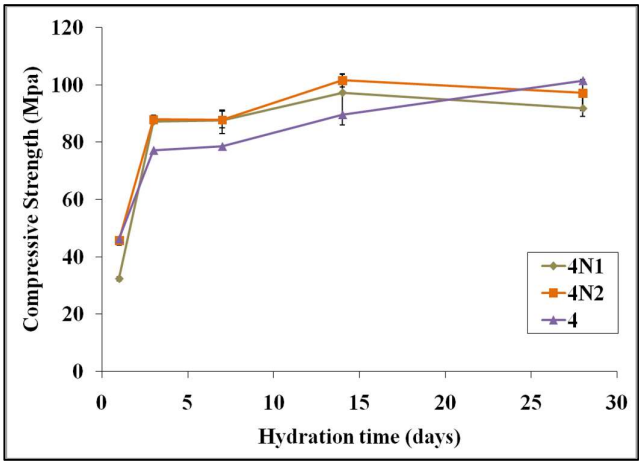

Figure 3.51. The compressive strength development of samples 4, 4N1 and 4N2 prepared with w/c:0.3.

3-4-4) XRD analysis of hydrated samples

The phase identification of hydrated specimens of 4N1 and 4N2 was carried out using XRD. The XRD patterns of hydrated cement#4N1 and cement#4N2 for the 0, 3, 7 and 28th day of hydration can be seen respectively in Figure 3.52 and Figure 3.53. The peaks of main phases are illustrated on the figures.

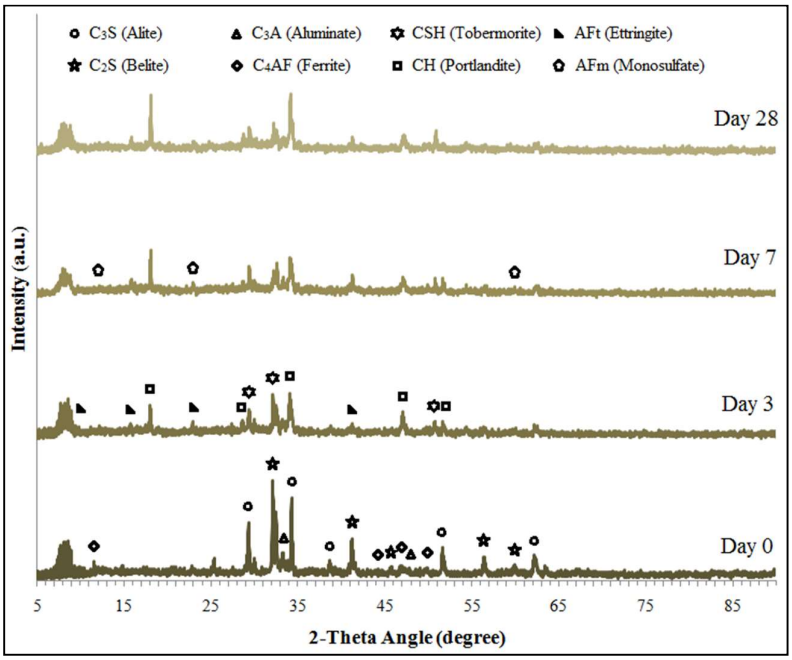

Figure 3.52. XRD patterns of cement#4N1 during the hydration process at the age of 0, 3, 7 and 28 days. The unhydrated (day 0) and hydrated (day7 and day 28) phases are shown.

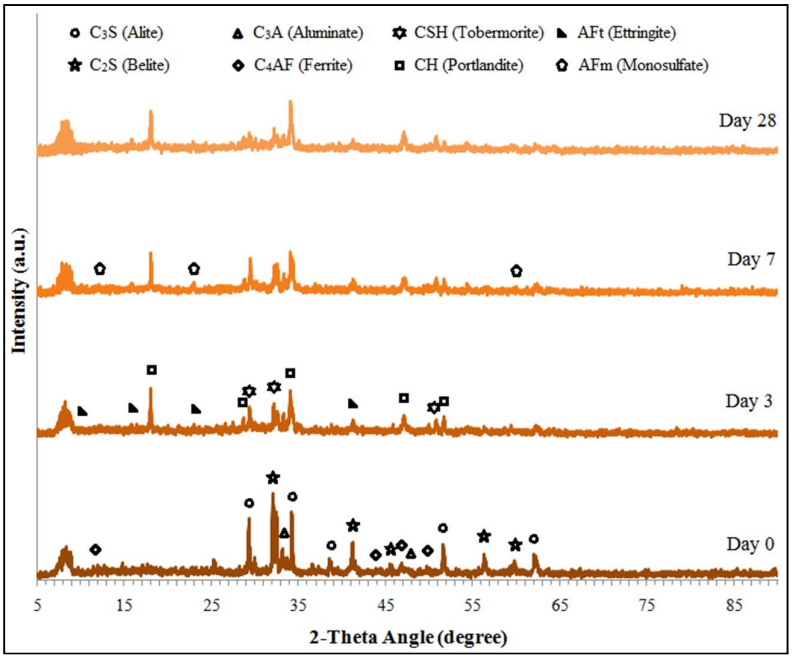

Figure 3.53. XRD patterns of cement#4N2 during the hydration process at the age of 0, 3, 7 and 28 days. The unhydrated (day 0) and hydrated (day7 and day 28) phases are shown.

The phase quantifications have also been performed for the two new samples. Figure 3.54 shows the phase alterations during the hydration process for sample#4N1, sample#4N2 and sample#4 for a better comparison. The similarity of phase value modifications is obvious among the three samples prepared using the same alternative fuel of waste plastics and sewages sludge mix.

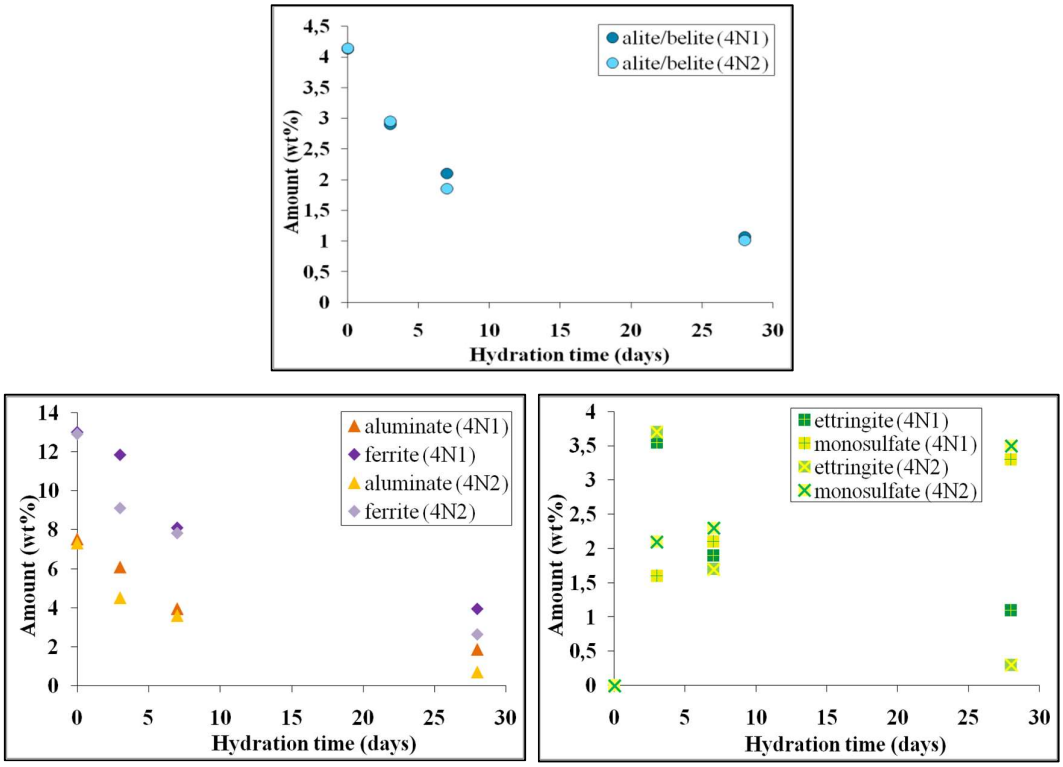

Figure 3.54. The graphs of a/b, aluminate, ferrite, ettringite and monosulfate alterations during the hydration processes of cement#4N1, cement#4N2 and cement#4 from 0th day till 28th day of hydration.

Chapter4: DISCUSSIONS

In this chapter, the data acquired during the project will be discussed. It was the intention to look at all the results through the big picture and make connections between them.

4-1) Clinker analysis

As it was described in chapter3, the phase distribution of clinker samples was investigated using SEM (BSE) and XRD methods. Moreover, the phase amounts were also calculated with Bogue formulas using the data acquired from XRF analysis. Table4.1 presents the alite and belite phase amounts, and alite/belite ratios obtained using all the three approaches. The distribution of aluminate and ferrite phases for these methods is given in Table 4.2. This table also contains the free lime (CaO) content of the clinkers estimated in Bogue method. All of the values are shown in wt%. Comparing the results of XRD and SEM for each sample, we can see that the deviation among them were in most cases within the acceptable ranges and the results are in good agreement. This fact could be an indication of the accuracy in the measurements of the two methods.

On the other hand, the calculated values of Bogue method should also be considered and compared with SEM and XRD results. The Bogue method is the common method to estimate the phase distribution, using the chemical analysis data, in cement manufacturing. However, it is believed that the Bogue calculations are with potential intrinsic biases, as it was discussed in chapter1. The estimated values usually have deviations from the realistic values. Standard deviation (1σ) values of about 9.6% for alite and belite, and 2.2% and 1.4% for aluminate and ferrite have been determined[130]. Comparing the values in Table 4.1, we can see that there are some deviations between the alite and belite measured values (SEM and XRD) and calculated values (Bogue). However, the deviation is lower for the alite/belite values. These values are within a close range, except for clinker#2, in which alite/belite value has been calculated to 60% and 200% higher than SEM and XRD results, respectively.

Table 4.1. Alite, belite and alite/belite distribution (wt%) in clinker samples obtained using SEM, XRD and Bogue calculations.

Clinker #	Fuel	SEM ali.	XRD ali.	Bog. ali.	SEM bel.	XRD bel.	Bog. bel.	SEM a/b	XRD a/b	Bog. a/b
1	petrocoke	65.8	70.4	59.3	13.0	12.5	14.2	5.1	5.6	4.2
2	petrocoke all a. fuels	53.1	41.3	57.8	22.4	34.4	14.9	2.3	1.2	3.8
3	petrocoke waste plastics	55.5	55.6	52.1	17.0	12.2	20.9	3.2	2.5	2.5
4	petrocoke waste plastics sewage sludge	63.4	67.3	60.5	13.6	15.5	14.1	4.6	4.3	4.3
5	petrocoke sewage sludge	42.5	40.6	48.1	29.5	32.5	23.2	1.4	1.5	2.1

A comparison between aluminate amounts of SEM and XRD methods, in Table 4.2, shows that the values are very close. The highest deviation is for clinker#3 in which aluminate value is 20% higher for SEM method. The ferrite values are also similar for two methods, although the SEM results are overall higher than XRD results. The most deviated value is for clinker#1. The ferrite value is 30% higher for XRD method. The deviation of Bogue-calculated values is much higher for aluminate and ferrite values compared to alite and belite values. The free lime content of clinker#1 and clinker#2 has been estimated to be higher than the other samples, as indicated in Table 4.2.

Table 4.2.Aluminate and ferrite distribution (wt%) in clinker samples obtained using SEM, XRD and Bogue calculations. The amount of free CaO in samples is also given.

Clinker #	Fuel	SEM alu.	XRD alu.	Bog. alu.	SEM fer.	XRD fer.	Bog. fer.	free CaO
1	petrocoke	5.1	5.2	7.5	15.9	12.0	10.6	1.7
2	petrocoke all a. fuels	10.3	10.6	7.6	14.1	13.8	10.7	1.9
3	petrocoke waste plastics	11.2	9.0	7.4	16.2	15.1	10.7	0.6
4	petrocoke waste plastics sewage sludge	6.3	7.4	7.2	16.5	13.0	11.1	0.7
5	petrocoke sewage sludge	13.1	12.3	7.6	14.7	15.4	10.9	0.7

As it was discussed in the previous chapters, all of the mentioned methods have advantages and disadvantages. While Bogue formulas are more practicable, they are biased by errors. SEM and XRD methods result in more precise phase amount measurements, while they may suffer from sampling errors and are also more time-consuming. There is still need to study about the phase distribution measurements of cement to be able to find the most-accurate and most-practical method.

In order to provide a better comparison among the results of different methods for all of the samples, graphs have been sketched. Figure 4.1-a, 4.1-b and 4.1-c, respectively illustrate the alite/belite, aluminate and ferrite values of 5 clinker samples and 2 control cement powder samples. All of the methods indicate that there are differences among the phase ratios of the clinkers produced using different alternative fuels.

Figure 4.1-a shows the alite/belite ratios for all samples. The results are in good accordance for three methods, except for clinker#2 that has a high difference for Bogue calculations compared to two other analysis methods. Clinker#1 which was produced using only petrocoke as the fuel in the clean kiln (after the restoration) shows the highest a/b values. After that, clinker#4 (fuel: mix of waste plastics and sewage sludge) and clinker#3 (fuel: waste plastics) respectively possess the highest a/b values. Therefore, it is obvious that the alite/belite ratios were decreasing with the usage of alternative fuels in the burning process in kiln. This decline continued as the cement clinkers were produced in dirty kilns continuously being contaminated during use (before the restoration).Clinker#2, and clinker#5 (fuel: sewage sludge) showed very low a/b values. It can also be seen that the control samples, which were also produced using the mix of waste plastics and sewage sludge, had an alite/belite ratio that was close to the one from clinker#4. The values were in the range of 3-4 and it could be concluded that the effect of fuels on alite and belite phase formation during clinkerization was unambiguous.

Figure 4.1-b depicts the aluminate phase values for all samples using three methods. The values obtained with Bogue method are very close to each other. However, SEM and XRD measured values show that aluminate phase has a lower content in clinker#1 and clinker#4 compared to other samples. The control samples shows aluminate values very close to clinker#4.

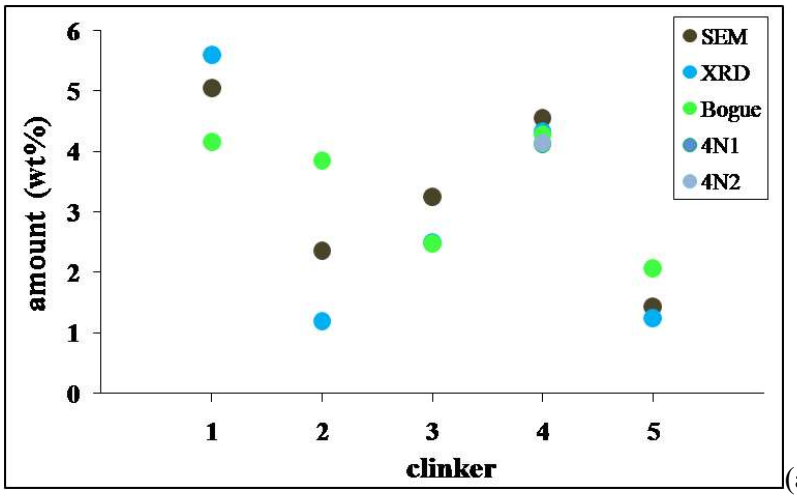

(a)

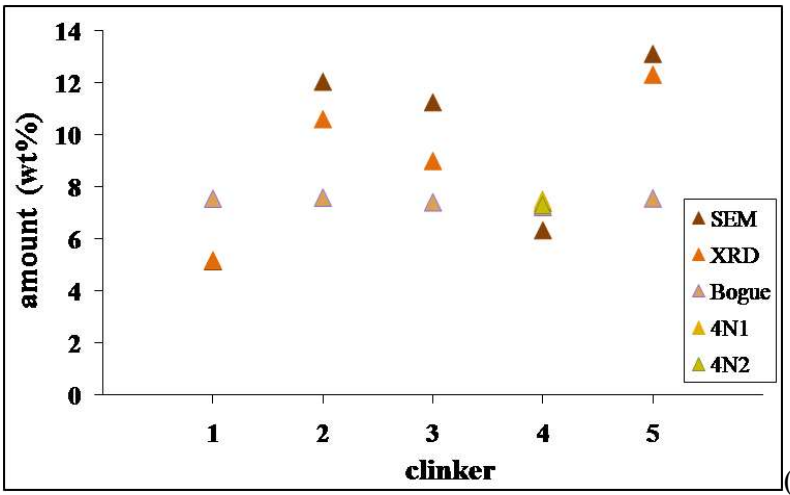

(b)

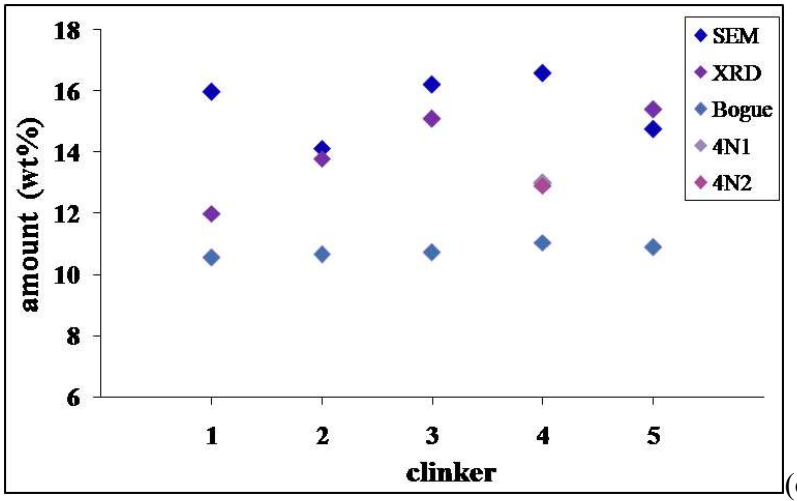

(c)

Figure 4.1. Alite/belite (a), aluminate (b) and ferrite (c) values obtained using SEM, XRD and Bogue method for five clinker samples and two control cement samples.

Figure 4.1-c shows the ferrite phase values for clinker and cement powder samples. It can be seen that Bogue-calculated values are nearly the same for all the samples. SEM and XRD-measured values have more deviation among each other for ferrite values than the previous phases. According to SEM results, clinker#2 and clinker#5 have the lowest and clinker#4 has the highest ferrite phase amounts.

Due to the overall similarities in SEM and XRD phase analysis results, in the following evaluations of clinker samples' behavior, only SEM results will be considered.

An investigation on the probable effect of each phase on the formation of other phases is also important. Figure 4.2 (a-c) shows the comparison between alite and belite phase values with the ferrite and aluminate phase values. A comparison of the alite/belite ratios and aluminate phase amounts shows that an increase of the a/b ratio (in an accordance with increasing the alite and decreasing the belite)was associated with decrease of the aluminate amounts. This is opposing the fact that higher liquid phase would help easier formation of alite phase during clinkering. However, it is possible that ferrite phase could compensate the aluminate shortage for clinker#1 and clinker#4, as they have a high ferrite phase amount. A possible explanation regarding this issue is that aluminate as a phase that formed at lower temperatures is capable of Ca ion capturing in contrast to alite which formed as a high-temperature phase. In other words, CaO was consumed by the liquid phase before mixing with belite (C_2S) to form alite (C_3S). Since there was not enough CaO, lower amount of alite was formed in clinker#2 and clinker#5. But, how is it possible that aluminate (C_3A) phase would capture higher amounts of Ca ions. This issue could be related to the kiln conditions. A poor heat distribution due to the type of used fuel may result in deviations in burning conditions [17]. It is possible that the kiln feed would stay a longer time in solid state reaction zone (900˚ - 1300˚C) and a shorter time in clinkering zone (1300˚C – 1450˚C). This issue could result in formation of higher amounts of liquid phase and lower alite formation. If this is the case, it can be concluded that using sewage sludge as the alternative fuel does not provide a sound heat distribution in the kiln (clinker#5). However, if it is used along with waste plastics as the other alternative fuel (clinker#4), the heat distribution would be fine enough to produce clinkers as good as ones produced without alternative fuels (clinker#1). It is worth mentioning that the burnability factor is controlled constantly

during the clinker sintering to be kept at ~115 with the lowest deviation. This factor results in temperatures ~1390±40 °C. Different amounts of each fuel is used because of different calorific values (Chapter1) to provide this amount of heat in the kiln.

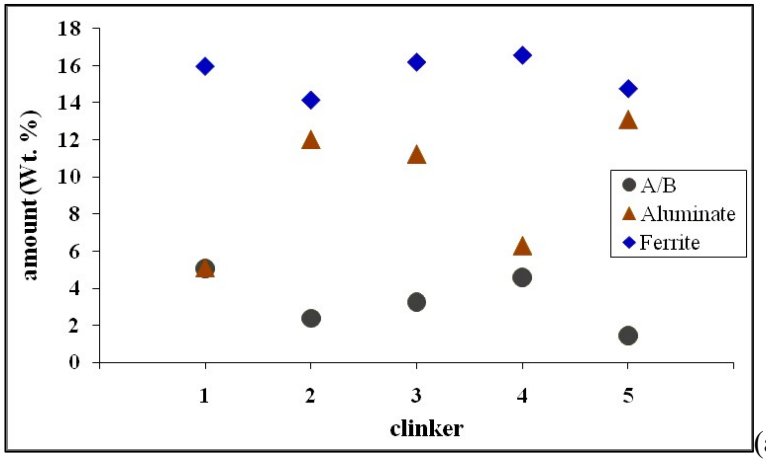

(a)

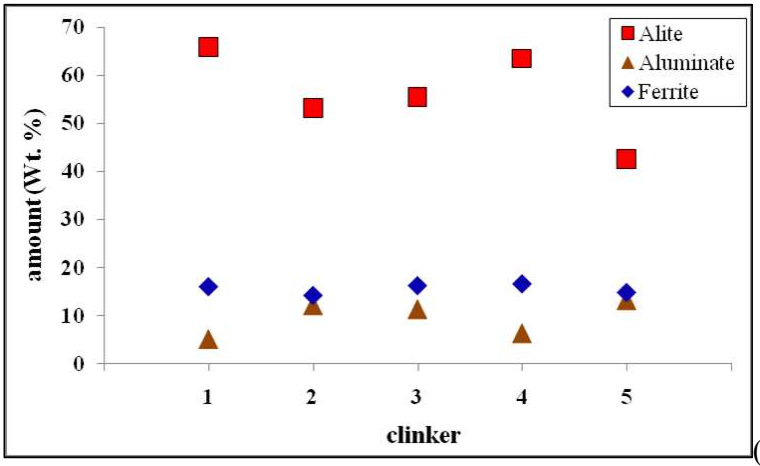

(b)

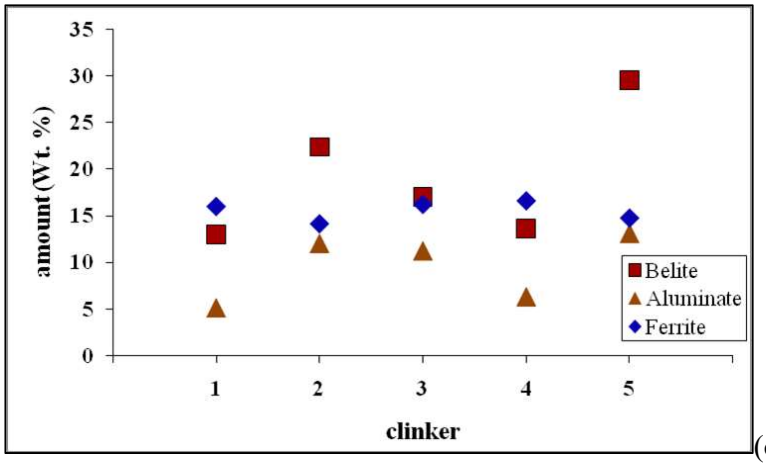

(c)

Figure 4.2. Alite/belite, alite and belite amounts in comparison with aluminate and ferrite phase amounts. Each color represents a phase, as it is indicated on the graphs.

For illuminating the other possible reasons of the variances in the phase distribution of clinkers prepared with different alternative fuels, it is of utmost importance to analyze the chemical composition. As it was discussed in the first chapter, minor elements like sulfur, magnesium and alkali metals are able to influence the phase formation during the clinkerization. Therefore, EDS analyses were carried out through the microstructure of the clinkers, as a whole and on each phase separately. This way, it is possible to measure each element amount in each phase and realize its effect on the formation of that phase. Figure 4.3, Figure 4.4 and Figure 4.5 compare respectively a/b, aluminate and ferrite phase values in each clinker with the elemental amounts of sulfur, magnesium and alkali metals (Potassium plus Sodium) on the all microstructural region and each phase separately. Taking a look at all of the graphs shown in these figures, it can be realized that there is not a sound correlation between the element amounts and phase distribution of our clinker samples. In other words, it is unlikely to readily investigate the effect of all the elements all together. Some elements may promote alite formation, while others may prohibit it. The evaluation becomes more difficult when all these elements are available in clinker composition to some extent. For example, Figure 4.3-a shows that high S amount has caused belite formation (decrement of a/b ratio) in clinker#2, while clinker#3 with a higher S amount has a lower belite phase amount. This Figure also shows that S amount in alite is extremely low and most of it has entered belite and liquid phase (where it reduces the viscosity), if not present as alkali sulfates. It is also worth mentioning that chemical analysis of clinker samples was also carried out by XRF method, as described in chapter3. By taking a look at the results in Table 3.5, we could see that clinker#2 (dirty kiln sample) and clinker#5(sewage sludge fuel) had a higher sulfur amount (>2 wt%) with respect to other samples. This is in accordance with EDS data and also the fact that increasing sulfur amount decreases alite formation.

Mg amounts are almost the same for all of the samples. It is mostly present in the matrix phase. The most sensible relation was that increasing the alkali metal amounts resulted in decreasing the alite/belite ratio. So, it means that alkalis inhibited the conversion of belite to alite, which is in accordance with the existing literature [22].

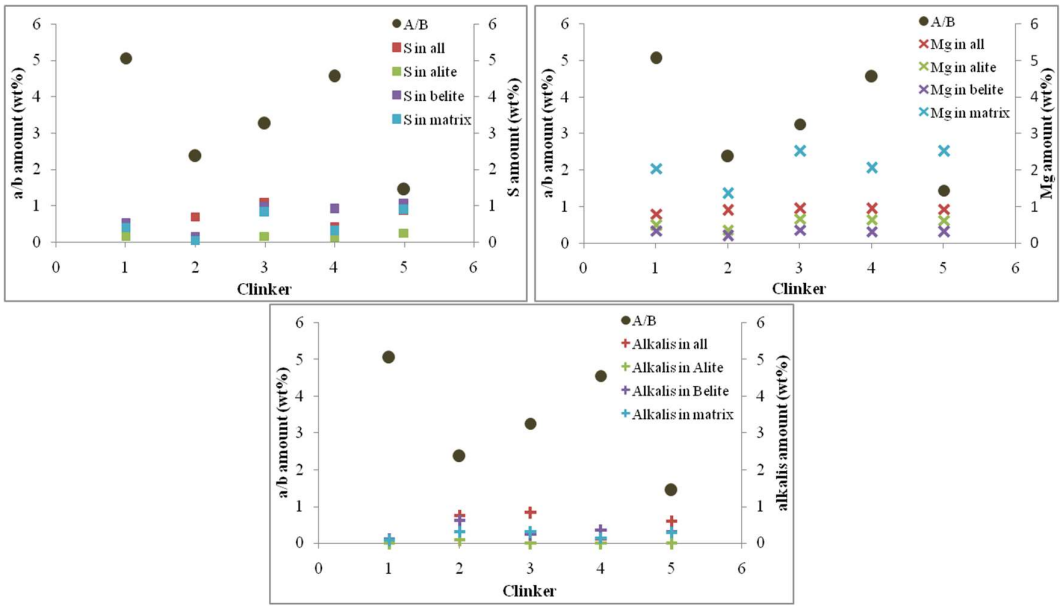

Figure 4.3. Graphs showing a comparison between a/b phase ratios with S, Mg and alkalis amounts in the all nodule region and in each phase separately.

Figure 4.4 shows the relation between elements and aluminate phase amounts. It can be seen that there is a relative correlation between the sulfur and aluminate values. In the samples with a higher S amounts (clinker#2, clinker#3 and clinker#5), aluminate amounts are higher than the other samples. According to Taylor, high amounts of aluminate and sulfur (as inclusion in cement particles) together can be hazardous to cement paste in long times. The excess S amount may react with aluminate minerals of anhydrous cement particles in presence of water and result in formation of secondary ettringite (delayed ettringite). The formation of secondary ettringite damages cement and concrete due to the expansion and enlarging the cracks[147].

The Mg and alkali metals contents do not seem to have affected the aluminate phase formation.

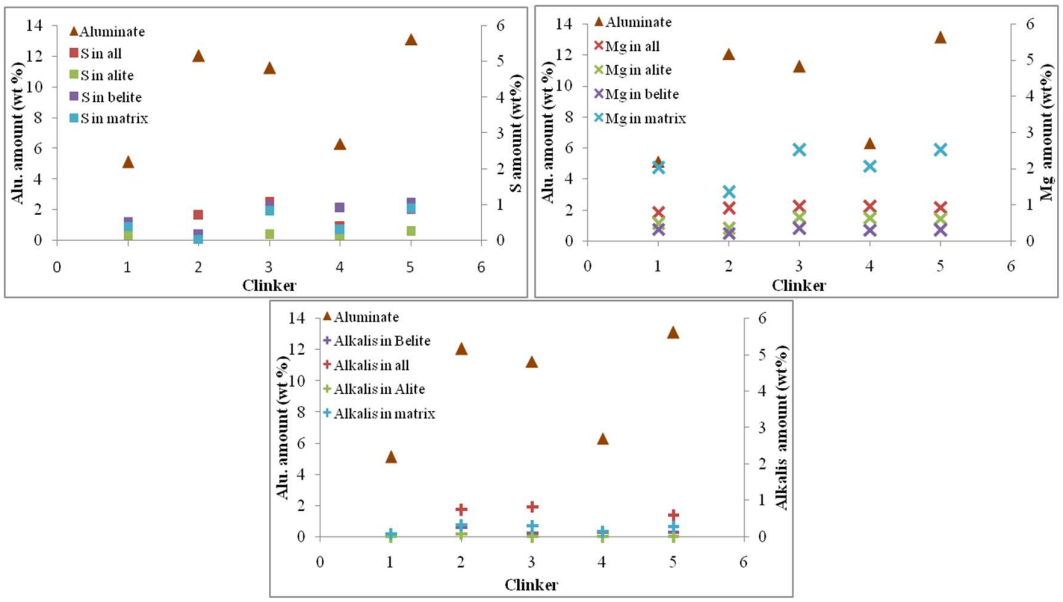

Figure 4.4. Graphs showing a comparison between aluminate phase ratios with S, Mg and alkalis amounts in the all nodule region and in each phase separately.

The comparison of ferrite phase and elemental distribution is presented in Figure 4.5 to provide the complementary information. However, Mg, S and alkalis have not influenced the formation of ferrite phase to the extent that could be distinguished among different samples.

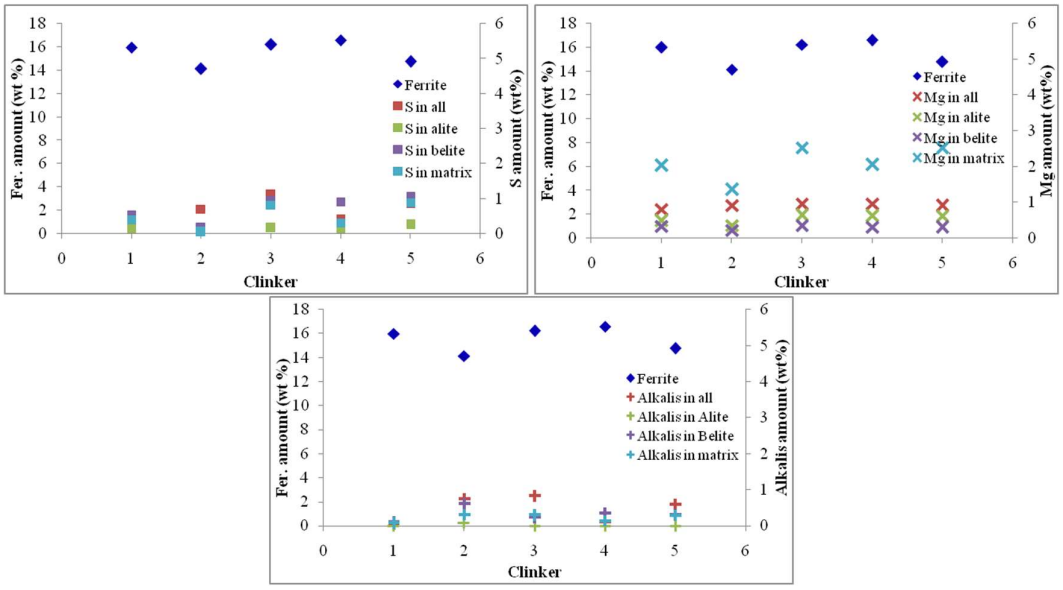

Figure 4.5. Graphs showing a comparison between ferrite phase values with S, Mg and alkalis amounts in the all nodule region and in each phase separately.

Moreover, in this study it was shown that the amounts of the elements like phosphorous and chlorine are lower than the dangerous limits. Phosphorous (P_2O_5) is typically present in clinker composition up to amounts of 0.2 wt%. EDS results showed that clinker#2 and clinker#4 possess the highest P values of 1 wt% (equal to 2 wt% of P_2O_5). XRF results did not show any phosphorous in the composition. According to Bhatty [22],P_2O_5 values of up to 1 wt% do not harm clinker. Chlorine, which is a trace element (~90 ppm) in clinker composition, was detected to very low amounts (<0.002 wt%) in our samples by XRF (even in the samples prepared with waste plastics). This means that Cl^- was not an influencing parameter in the phase distribution of clinker, or moreover behavior of cement and concrete.

Overall, it can be concluded that different phase distributions could also be influenced by minor elements from different alternative fuels. Some elements like sulfur and phosphorous could enter the structure of cement by using alternative fuels and alter the phase formation to some extent. For example, excessive sulfur in the sample prepared using sewage sludge decreased alite formation. On the other hand, EDS and XRF chemical analysis results showed that hazardous elements like zinc, lead and vanadium are not present in the hazardous values [22] in the samples produced with alternative fuels.

As a conclusion to this section, clinker samples produced using different alternative fuels showed different phase distributions. These variations may be a result of different heat distributions in the kiln due to the burning alternative fuels. In addition, some minor elements like sulfur were detected to influence the phase formations. However, it is still needed to study these effects more thoroughly.

4-2) Hydrated cement analysis

After characterizing the phase and chemical distribution of clinker samples, cement pastes of the 5 clinker samples(plus the new 2 cement powders) were prepared. Compressive strength of the pastes prepared with water to cement ratio of 0.3 and 0.5 were measured. Figure 4.6 shows the strength development values obtained for both of the w/c ratios in the same graph. The same color-code has been used for each sample for the two strength data. It can be seen that the strength amounts of samples prepared with w/c of 0.3 are nearly 100% higher than the values for w/c of 0.5. The reason was

discussed more precisely in the previous chapters. The higher content of capillary pores in a cement paste prepared with higher water content results in decreasing the strength.

The cement samples produced with different alternative fuels are developing the compressive strength within a similar manner. However, there are also some variations among them. These variations differ for two w/c samples. The strength development of the samples prepared with w/c:0.5 is close to the standard OPC strength development, in which the 2nd day and 28th day hydrated samples should respectively have a minimum of 20 MPa and 42.5 MPa compressive strength [148].

Cement#2 which was produced with all alternative fuels in the dirty kiln presents a lower compressive strength values in both w/c ratios. Cement#1, the clean kiln sample produced with only petrocoke) on the other hand, overall has higher strength values comparing to other samples in both w/c ratios. The other samples behave differently, i.e. have variable strength values for two w/c ratios. These results show that using alternative fuels affect the strength development of hydrated cement samples, for which the amount of the used water also matters.

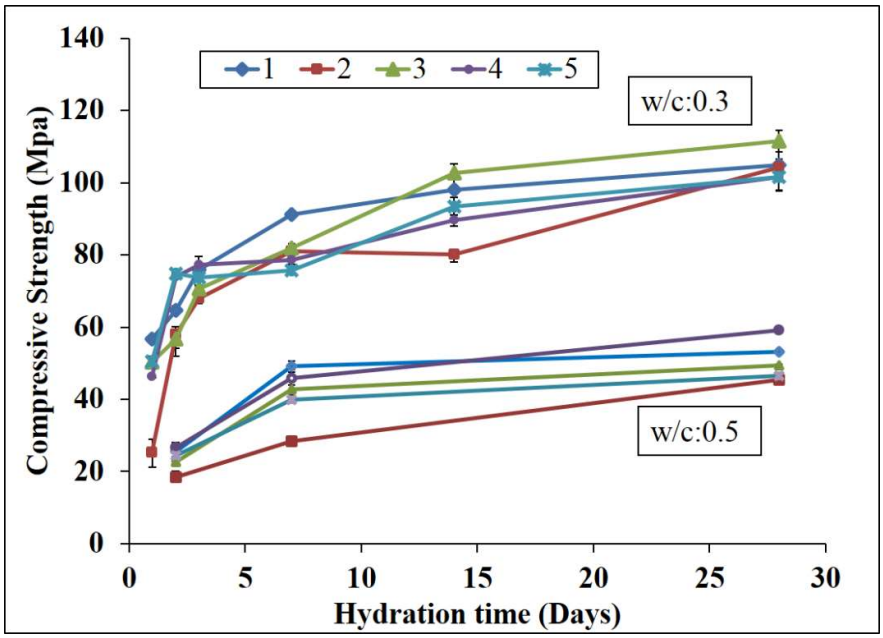

Figure 4.6. Strength development graphs of cement samples produced with different alternative fuels, prepared with w/c of 0.3 and 0.5.

As it was discussed in chapter1, hydration of the clinker phases and mainly alite and belite results in formation of hydrated phases. The compressive strength of cement

is due to the formation of these hydrates, especially C-S-H gel. Clinker phases play different roles during the hydration and strength development. For example, alite provides the early strength and belite provides the late strength of cement paste. Aluminate and ferrite phases are mostly responsible of the setting and contribute little to strength. Therefore, it is necessary to correlate the compressive strength values of cement pastes with the phase distribution of each related clinker. The strength development graphs for w/c of 0.3 and 0.5 are shown along with the main phase values in Figure 4.7-a and Figure 4.7-b, respectively. The clinkers and cements are color-coded for the sake of a better comparison. As discussed for the previous figure, cement#1 has an overall high strength values. This sample also has a high alite/belite ratio. The high alite amount results for higher reactivity and formation of strength-giving phases. Cement#2 has an overall low compressive strength values throughout the 28 days of hydration. Particularly, the 1st day sample of w/c:0.3 has a strength value as low as half the other samples (100% lower). Low alite content results in a slower strength gain and a lower strength in early days. When belite starts to react, its hydration products start to contribute to strength development of cement paste. It can be seen that the strength of cement#2 for w/c:0.3 increased after 2nd day, however the samples of w/c:0.5 were not able to develop strength with the same rate. So, it can be said that in excess of water, belite does not react early. Cement#3 with a moderate alite/belite amount, also shows a moderate behavior in hydration reactions, particularly for w/c:0.5. For w/c:0.3, cement#3 has a relatively lower early strength, however its strength increases at later ages. Cement#4 with a high alite/belite content, shows high compressive strength values, especially for w/c:0.5. The high early strengths are obvious for both w/c ratios. Cement#5, which has low alite/belite content, behaves very similar to cement#2. For w/c:0.5, the strength develops with a slower rate, which could also be an indication of lower reactivity of belite with higher water contents.

The overall high reactivity and therefore high compressive strength of all samples could also be attributed to the small grain sizes of cement powders. It was seen in Figure 3.49 that our cement powders' particles are relatively small in size. Smaller particles with higher surface area result in higher reactivity, especially within the first day, in which grains of smaller 10 μm provide the strength [6]. Small grain size of powders could be due to their better grindability, which could be because of the relatively high sulfur amounts in clinkers.

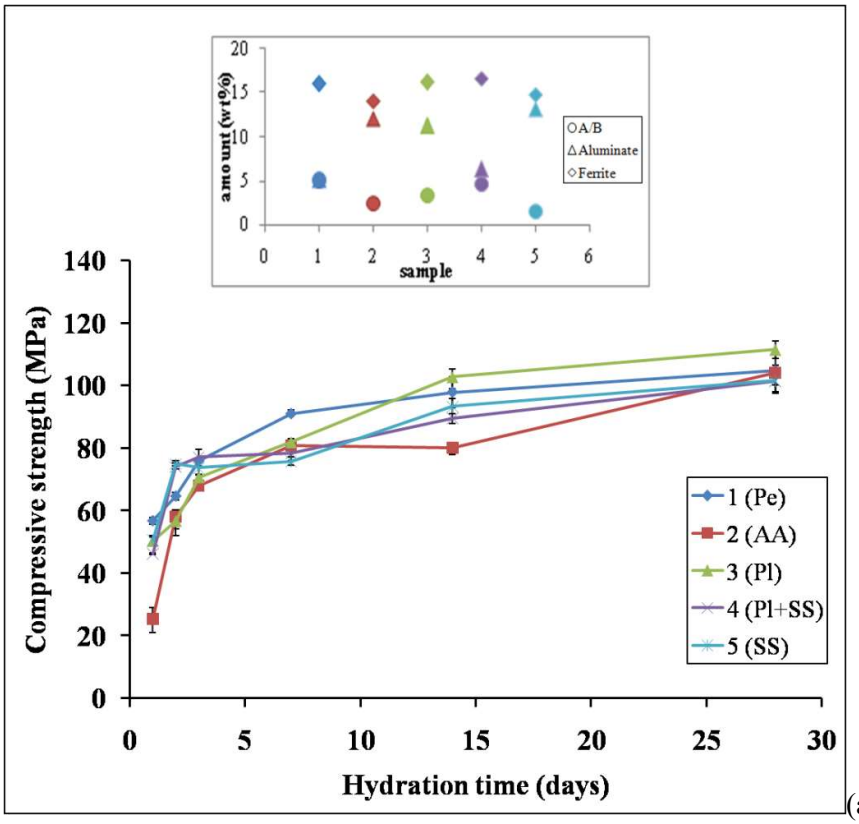

(a)

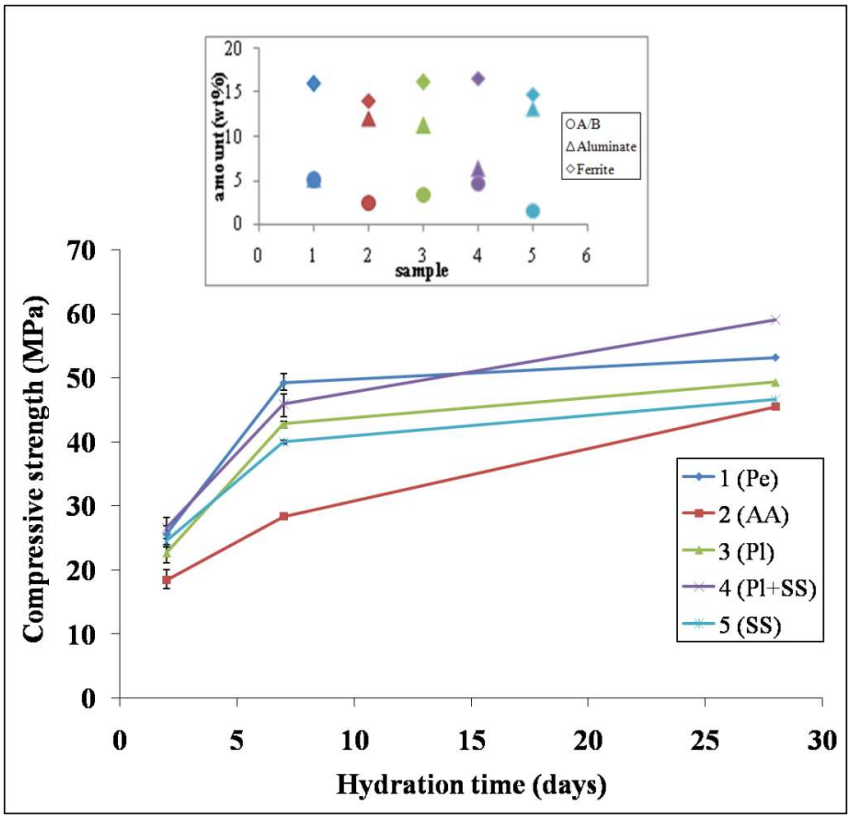

(b)

Figure 4.7. Strength development graph of cement pastes prepared with a) w/c:0.3 and b) w/c:0.5, along with the phase distribution in clinkers. Each sample is color-coded.

The SEM and XRD analyses were used to investigate the hydration products of the cement paste samples prepared with water/cement ratio of 0.3. Figure 4.8 presents the progress of hydration reactions in sample#4, as it was monitored with SEM images. The clinker phases (Figure 4.8-a) reacted with water to form the hydrated cement phases at the 2nd day of hydration (Figure 4.8-b). It can be seen that approximately half of the phases were consumed, yet some regions were still unreacted and remained anhydrous (the bright islands). The hydration reactions continued slightly in the cement paste, particularly around the anhydrous regions. Figure 4.8-c shows the image of cement paste at the 28th day of hydration. The unhydrated regions reduced in size and formed new hydrated phases. For instance, alite and belite crystals transformed to CH crystals and C-S-H gel. The hydration process was observed for all of the samples with the same method.

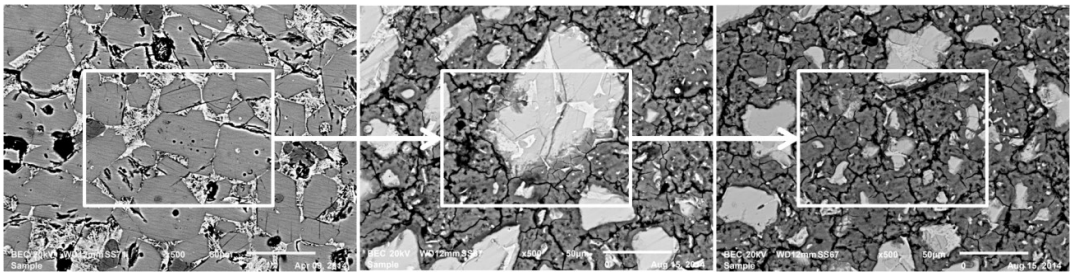

Figure 4.8. SEM images of sample#4, a)anhydrous clinker, b)hydrated paste at the 2nd day and c)hydrated paste at the 28th day.

Microscopical images were used to determine the progression of hydration process by measuring the unhydrated (anhydrous) cement regions in the paste. Figure 3.38 showed the unhydrated silicates amounts for all five samples, estimated by the unhydrated regions amounts. The high rate of hydration reactions could be seen in the figure. About 70% of the hydration was completed at the 2nd day. Then, the speed of the hydration decreased due to the formation of C-S-H layers around the cement particles. As a result, the strength increment also decelerated. The ratio of amounts of anhydrous cement particles in the total silicates amount for 7 to 28 days of hydration were close to 1.

The change in the alite/belite amount of all samples during 28 days of hydration process is shown in Figure 4.9. Reaction of alite with water, results in the formation of hydration products. Therefore, hydration results in decreasing the alite amounts in the

early days. When belite starts to react, usually after 7th day of hydration, it is also consumed to form hydration products. The changes in alite and belite contents, causes alterations in alite/belite values, as it can be seen in Figure 4.9.The a/b value decreases with a normal rate for samples with a high a/b. However, cement#2 and cement#5 do not show high change amounts in their a/b during hydration process. Could this be an indication of reactive belite which could hydrate in early days of hydration? Could using alternative fuels assist in formation of such phases in cement? It seems Yes!

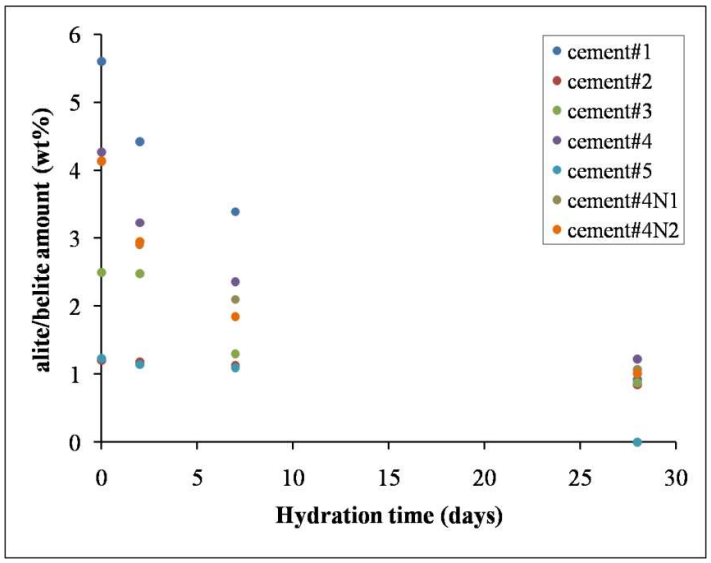

Figure 4.9. Changes in alite/belite values of cement samples produced with different alternative fuels and prepared with w/c:0.3, during 28 days of hydration.

Chapter5: CONCLUSIONS

This study aimed to investigate the effect of alternative fuels on the phase distribution and strength development of cement. Five samples were produced by using different alternative fuels in cement kiln. The anhydrous clinker and hydrated cement samples were analyzed separately with a few characterization methods like SEM, EDS, XRD, XRF and compression test.

- The SEM and XRD results of clinker samples showed that the distribution of main phases of alite (C_3S), belite (C_2S), aluminate (C_3A) and ferrite (C_4AF)are affected by the usage of different alternative fuels. Alite/belite weight ratios of the samples were calculated to be in the wide range of 1.5-5.2 within the samples. Aluminate values also vary from 5 to 13 wt%, whereas the ferrite values of the clinkers are much closer to each other.

- A comparison of Bogue-calculated and measured phase values using XRD and SEM analysis methods showed that aluminate and ferrite values have a higher deviation rather than alite and belite phase values among these methods.

- A comparison between the alite/belite ratios and aluminate phase values showed that the increment of the alite/belite ratio (or simply increasing the alite values) corresponds to the decrement of the aluminate values. It can be concluded that this issue is due to Ca ion capturing capability of aluminate as a low-temperaturephase in contrast with alite as a high-temperature phase. The formation of higher liquid phase could be due to the poor heat distribution through the usage of alternative fuels in kilns. This is more sensible for the sample produced using sewage sludge as the alternative fuel.

- Chemical composition of the clinker samples was analyzed using XRF and EDS analysis methods. The results showed that the amount of hazardous minor elements like Cl, Zn, Pb, etc. are within the safe range mentioned in the literature. The sulfur contents of sample produced in dirty kiln and sample produced with using sewage sludge were higher than 2 wt%. These values correspond to lower alite and higher aluminate phase values. The alkali metals (K and Na) inhibited the formation of alite.

- The hydrated cement tests were performed for various curing times within the first 28 days for two water to cement ratios by mass of 0.3 and 0.5. The compressive

strengths of samples prepared with w/c:0.3 are about 100% higher than the values for w/c:0.5. This means that although the water is necessary for hydration reactions and the production of strength giving phases in the cement, excessive amounts decrease the strength due to formation of higher amounts of capillary porosity.

- The strength test results showed that the strength development behavior of all samples is more or less similar in the samples prepared with w/c of 0.3. Increasing the w/c ratio to 0.5, opens up the difference among hydrated samples' strengths to up to 30% at 28th day of hydration, while the lowest value is for the dirty kiln sample (#2) and highest for the sample produced with the mix of waste plasticsand sewage sludge (#4). Overall, using the alternative fuels does not incredibly influence the strength amounts of hydrated cement samples.

- The 2 days strength/7 days strength values are respectively higher for the samples prepared with w/c:0.3 compared with w.c:0.5. This shows that higher water content in the cement paste decreases the early strength more intensely. The 7 days strength/28 daysstrength values are overall close to standard (~0.8), although sample#1 (clean) posses the highest and sample#2 (dirty) posses the lowest values.

- A comparison between the strength and phase distribution of the samples produced with different alternative fuels showed that increasing the alite/belite ratios did not necessarily increase the strength values, particularly in the early days. Considering the low contribution of matrix phases in the strength evolution, it is assumed that it could be because of reactive belite crystals, which start to react in the early days of hydration.

- The high reactivity of silicate phases in the hydrated cement was also observed in microscopic images. The microstructural investigations showed that the unhydrated silicates in cement paste decreased to ~18% in the second day of hydration for w/c:0.3.

- Formation of reactive belite-rich clinkers is estimated to be one of the consequences of alternative fuel usage in cement kilns. However, a thorough research is suggested as a future work in this field.

- Burnability, heat distribution and flame temperature of alternative fuels are concluded as important factors in clinker phase formation during kiln processes. Therefore, this issue is also suggested to be studied as another future work.

References

1. Hewlett, P., *Lea's Chemistry of Cement and Concrete*. Butterworth-Heinemann, Elsevier Science, 2003.
2. Buckley, J., *A History of Cement.* Portland Cement Association, Available from: http://www.rumford.com/articlemortar.html, 2001, cited: 2015.
3. Winter, N.B., *Understanding Cement,* United Kingdom: WHD Microanalysis Consultant, 2009.
4. *United States and world cement production in 2010 and 2014.* Statistica, the statistics portal, Available from: http://www.statista.com/ statistics/219343/cement-production-worldwide/, cited: 2015.
5. Bye, G.C., *Portland Cement*. 2nd ed., London E14 4JD: Thomas Telford Publishing, 1999.
6. Taylor, H.F.W., *Cement chemistry*. 2nd ed., London: Thomas Telford, 1997.
7. *ASTM C150 / C150M-12, Standard Specification for Portland Cement, ASTM International.* DOI: 10.1520/C0150_C0150M-12, 2012.
8. *EN 197-1 EUROPEAN STANDARD : Composition, specifications and conformity criteria for common cements,* 2000.
9. Jeff Thomas, H.J., *The science of concrete.* Northwestern University Center of Cement based Materials, Available from: http://iti.northwestern.edu/ cement/index.html, cited: 2015.
10. Tokheim, L.A., *The impact of staged combustion on the operation of a precalciner cement kiln.* Doctoral thesis at Norwegian University of Science and Technology, Porsgrunn, 1999.
11. Kosmatka, S.H., B. Kerkhoff and W.C. Panarese, *Design and Control of Concrete Mixtures, 14th Ed.* Skokie, IL.: Portland Cement Association, 2002.
12. Roy, D.M., *Portland cement: Constitution and Processing, Part 1: Cement manufacture (Instructional modules in cement science.* Journal of Materials Education, 1985: p. 73-89.
13. CEMBUREAU, *Environmental Benefits of Using Alternative Fuels in Cement Production.* Brussels, The European Cement Association: 25, 1999.
14. Available from: *http://gulfcement.ae/* cited: 2015.
15. *Reference Document on Best Available Techniques in the Cement and Lime Manufacturing Industries.* Integrated Pollution Prevention and Control (IPPC) Bureau, European Commission, Technologies for Sustainable Development, Available from: http://www.jrc.es/pub/english.cgi/d733211, 2000, cited: 2015.
16. Bogue, R.H., *The Chemistry of Portland Cement*, New York: Reinhold Publishing Co., 1947.

17. Chinyama, M.P.M., *Alternative Fuels in Cement Manufacturing*, in *Alternative Fuels*, M. Manzanera, Editor. 2011, In Tech.

18. Available from: *http://ncfuae.com/products/* cited: 2015.

19. Hills, L.M., *The influence of clinker microstructure on grindability : Results of an extensiveliterature review.* Proceedings of the 17th International Conference on Cement Microscopy 1995: p. 344-352.

20. Hills, L.M., *Clinker Microstructure and Grindability: Updated Literature Review, SN2967.* Portland Cement Association, Skokie, Illinois, USA, 2007.

21. Mindess, S., J. F. Young and D. Darwin,, *Concrete (2nd Edition)*. 2002, Upper Saddle River, NJ, USA: Pearson Education Inc. .

22. Bhatty, J.I., *Role of minor elements in cement manufacture and use*. 1995, Portland Cement association, Research and development bulletin.

23. Moore, D., *Cement kilns,* Available from: http://www.cementkilns.co.uk, 2010, cited:2015.

24. Winter, N.B., *Understanding cement, Cement Chemistry Information and Training for the Cement and Concrete Industries.* WHD Microanalysis Consultants Ltd, Available from: http://www.understanding-cement.com, cited: 2005.

25. Stutzman, P.E., *Scanning electron microscopy imaging of hydraulic cement microstructure.* Cement & Concrete Composites, 2004. **26** (8): p. 957-966.

26. Campbell, D.H., *Microscopical examination and interpretation of Portland cement and clinker, 2nd ed.* 1999, Skokie: Portland Cement Assoc.

27. DeHayes, S.M. and D. Stark, *Petrography of Cementitious Materials*. 1994: ASTM.

28. Stutzman, P.E., *Microscopy of Clinker and Hydraulic Cements.* Reviews in Mineralogy and Geochemistry, 2012. **74**(1): p. 101-146.

29. Johansen, V., *Manufacturing processes and clinker performance: Characterization and performance prediction of cement and concrete.* Proceedings of the Second Engineering Foundation Conference 1983: p. 1-10.

30. Gebauer, J., M. Kristmann, *The influence of the composition of industrial clinker on cement and concrete properties.* World Cem Technol, 1979 (46-51).

31. Gavel, V., L. Opoczky, L. Sas, *Relationship between technological parameters, structure and grindability of clinkers.* Epitoanyag, 2000. **52**(2): p. 34-38.

32. Kilhara, Y., S. L. Centurione, M. Cunha and A. Flavio, *An approach to the prediction of portland clinker grindability and strength by microscopy.* 9th International Congress on the Chemistry of Cement, 1992. **6**(182-188).

33. Altun, A., *Microscopic criteria for quality control of clinker.* Cimento ve Beton Dunyasi, 1998. **2**(16): p. 22-32.

34. *Impact of Burning and Cooling Conditions on clinker quality.* European Cement Research Academy (ECRA) newsletter, 2010. **3**.

35. Alemayehu, F., O. Sahu, *Minimization of variation in clinker quality.* Advances in Materials, 2013. **2**(2): p. 23-28.

36. Bentz, D.P., et al., *Cellular automaton simulations of cement hydration and microstructure development.* Modelling and Simulation in Materials Science and Engineering, 1994. **2**(4): p. 783.

37. Bullard, J.W., et al., *Mechanisms of cement hydration.* Cement and Concrete Research, 2011. **41**(12): p. 1208-1223.

38. Scrivener, K.L. and A. Nonat, *Hydration of cementitious materials, present and future.* Cement and concrete research, 2011. **41**(7): p. 651-665.

39. Thomas, J.J., et al., *Modeling and simulation of cement hydration kinetics and microstructure development.* Cement and Concrete Research, 2011. **41**(12): p. 1257-1278.

40. Bennison, P., *The Design of Reinforced Cement-based Protective Coatings, available from:* http://www.cortecvci.com/Publications/Papers/MCIProducts/Aston_U/Aston.html, 2001, cited:2015.

41. Brewer, J., *Cocrete, scientific principles.* Website of Materials Science and Technology Teacher's Workshop at Department of Materials Science and Engineering, University of Illinois Urbana-Champaign, 2015.

42. Kosmatka, S. H., B. Kerkhoff and W. C. Panarese, *Design and Control of Concrete Mixtures*. 14th ed. 2003, USA: Portland Cement Association.

43. Tennis, P.D. and H.M. Jennings, *A model for two types of calcium silicate hydrate in the microstructure of Portland cement pastes.* Cement and Concrete Research, 2000. **30**(6): p. 855-863.

44. Jawed, I., J. Skalny, and J. Young, *Hydration of Portland cement.* Structure and Performance of Cements. Essex: Applied Science Publishers, 1983: p. 284-285.

45. Bentz, D.P., *Three-Dimensional Computer Simulation of Portland Cement Hydration and Microstructure Development.* Journal of the American Ceramic Society, 1997. **80**(1): p. 3-21.

46. *Cement, Front desk architects,* Available from: http://frontdesk.co.in/cement.html#.VaTLDPlUyro, 2011, cited: 2015.

47. Scrivener, K.L., *Ph.D. Thesis, University of London.* 1984.

48. Trigo, A.P.M. and J.B.L. Liborio, *Doping technique in the interfacial transition zone between paste and lateritic aggregate for the production of structural concretes.* Materials Research, 2014. **17**(1): p. 16-22.

49. *Concrete strength gain rate, factors affecting, Available from:* http://www.aboutcivil.org/concrete-strength-gain-rate.html, 2014, cited: 2015.

50. Kovler, K. and N. Roussel, *Properties of fresh and hardened concrete.* Cement and Concrete Research, 2011. **41**(7): p. 775-792.

51. Abd Elaty, M.A.A., *Compressive Strenght Prediction of Portland Cement Concrete with Age using a new Model.* HBRC Journal, 2014. **10**: p. 145-155.

52. Giddings, D., C.N. Eastwick, S.J. Pickering and K. Simmons, *Computational fluid dynamics applied to a cement precalciner.* Proc. Instn. Mech. Engrs. , 2000. **214A.**

53. European Commission (EC), *Integarted Pollution Prevention and Control. Reference Document on Best Available Techniques in the Cement and Lime Manufacturing Industries.* 2001.

54. *The Cement Sustainability Initiative: Progress report.* World Business Council for Sustainable Development, 2002.

55. Ali, MB, R. Saidur and MS Hossain, *A review on emission analysis in cement industries.* Renewable and Sustainable Energy Reviews, 2011. **15**: p. 2252-61.

56. Kim, Y. and E. Worrel, *CO2 emission trends in the cement industry: an international comparison.* MitigationandAdaptationStrategiesforGlobalChange, 2002. **7**: p. 115-133.

57. Taylor, M., C. Tam and D. Gielen, *Energy efficiency and CO2 emissions from the global cement industry.* Energy technology policy division. International Energy Agency, 2006.

58. Habert, G., C, Billard, P. Rossi, C. Chen and N. Roussel, *Cement production technology improvement compared to factor 4 objectives.* Cement and Concrete Research, 2010. **40**: p. 820-826.

59. Aranda Usón, A., et al., *Uses of alternative fuels and raw materials in the cement industry as sustainable waste management options.* Renewable and Sustainable Energy Reviews, 2013. **23**(0): p. 242-260.

60. Madlool, N.A., et al., *A critical review on energy use and savings in the cement industries.* Renewable and Sustainable Energy Reviews, 2011. **15**(4): p. 2042-2060.

61. Nielsen, P.B., *SO2 and NOx Emissions From Modern Cement Kilns With a View to Future Regulations.* Zement-Kalk-Gips, Bauverlag GMBH/Maclean Hunter, 1991. **9**: p. 449-456.

62. CEMBUREAU, *Alternative Fuels in Cement Manufacturing: Technical and Environmental Review.* Brussels, The European Cement Association: 24, 1997.

63. Mokrzycki, E. and A. Uliasz- Bocheńczyk, *Alternative fuels for the cement industry.* Applied Energy, 2003. **74**(1–2): p. 95-100.

64. Hochdahl, O, *Fuels and heat economy.* Process Technology of Cement Manufacturing, VDZ Congress, Berlin: Bauverlag GMBH, 1985: p. 286-312.

65. Willitsch, F., et al., *Alternative fuels in the cement industry*. 2010, PMT-Zyklontechnik GMBH Krems, Austria.

66. Shi, C., A.F. Jiménez, and A. Palomo, *New cements for the 21st century: the pursuit of an alternative to Portland cement.* Cement and Concrete Research, 2011. **41**(7): p. 750-763.

67. *Trends in Beneficial Use of Alternative Fuels and Raw Materials*. 2008, ICF International: U.S. Environmental Protection Agency Office of Policy, Economics, and Innovation Sector Strategies Division.

68. *Supporting the use of alternative fuels in the cement industry*. 2008, ALF-CEMIND.

69. Albino, V., et al., *alternative energy sources in cement manufacturing*. 2011, Network for Business Sustainability.

70. Rahman, A., et al., *Recent development on the uses of alternative fuels in cement manufacturing process.* Fuel, 2015. **145**: p. 84-99.

71. Worrell, E.G., Christina. *Energy Efficiency Improvement Opportunities for Cement Making*. January 2004 [cited 2015 June].

72. Gabbard, W.D., and D. Gossman, *Hazardous waste fuels and the cement kilns: The Incineration Alternative.* ASTM Standardization News, 1990.

73. Roy, G.R., *Petcoke combustion characteristics.* World Cement, 2002.

74. Co., F.L.S., *Dry process kiln systems, technical brochure.* 2000.

75. International Energy Agency (IEA), *The use of petroleum coke in coalfired plant.* Coal Research., 2001.

76. Bryers, R.W., *Utilisation of petroleum coke and petroleum coke/coal blends as a means of steam raising.* Fuel Processing Technology., 1995. **44**: p. 121-141.

77. Commandre, J.M., and S. Salvador, *Lack of correlation between the properties of petroleum coke and its behaviour during combustion.* Fuel Processing Technology. **86**: p. 795 – 808.

78. *Petroleum coke,* Available from:http://www.laxmimineral.com/, cited 2015.

79. *Petroleum Coke: The Coal Hiding in the Tar Sands",.* OilChange International priceofoil.org, 2013.

80. Werther, J. and T. Ogada, *Sewage sludge combustion.* Progress in Energy and Combustion Science, 1999. **25**(1): p. 55-116.

81. Available from: http:/newenergyandfuel/com/2014/11/20/fertilizer-for-energy-crops-from-sewage-sludge/., cited 2015

82. Kroiss H., H. Rechberger and L. Egle., *Phosphorus in Water Quality and Waste Management.* 2011.

83. Lin, K.-L., D.F. Lin, and H.L. Luo, *Influence of phosphate of the waste sludge on the hydration characteristics of eco-cement.* Journal of Hazardous Materials, 2009. **168**(2–3): p. 1105-1110.

84. Lin, Y., et al., *Utilization of municipal sewage sludge as additives for the production of eco-cement.* Journal of Hazardous Materials, 2012. **213–214**(0): p. 457-465.

85. Husillos Rodríguez, N., et al., *The effect of using thermally dried sewage sludge as an alternative fuel on Portland cement clinker production.* Journal of Cleaner Production, 2013. **52**(0): p. 94-102.

86. Yen, C.-L., D.-H. Tseng, and T.-T. Lin, *Characterization of eco-cement paste produced from waste sludges.* Chemosphere, 2011. **84**(2): p. 220-226.

87. Lin, K.L., K.Y. Chiang, and C.Y. Lin, *Hydration characteristics of waste sludge ash that is reused in eco-cement clinkers.* Cement and Concrete Research, 2005. **35**(6): p. 1074-1081.

88. Lin, K.-L. and C.-Y. Lin, *Hydration characteristics of waste sludge ash utilized as raw cement material.* Cement and Concrete Research, 2005. **35**(10): p. 1999-2007.

89. Shirasaka, T., S. Hanehara, and H. Uchikawa, *Influence of six minor and trace elements in raw material on the composition and structure of clinker.* World Cement, 1996. **27**(3).

90. Shirasaka, T., D. Sawaki, and H. Uchikawa, *Influence of Phosphorus on Clinker Constituent Phase and Hydration of Cement.* Japan Cement Association Proceedings Of Cement & Concrete, 1996. **50**: p. 8-13.

91. Kwon W.-T., et al., *Effect Of P2O5 And Chloride on Clinkering Reaction.* Online Journal of Materials, 2005. **1**.

92. Monzo, J., et al., *Reuse of sewage sludge ashes (SSA) in cement mixtures: the effect of SSA on the workability of cement mortars.* Waste Management, 2003. **23**(4): p. 373-381.

93. Cyr, M., M. Coutand, and P. Clastres, *Technological and environmental behavior of sewage sludge ash (SSA) in cement-based materials.* Cement and Concrete Research, 2007. **37**(8): p. 1278-1289.

94. Tay J.H. and K.Y. Show, *Utilization of municipal wastewater sludge as building and construction materials.* Resour. Conserv. Recycl, 1992. **6**: p. 191–204.

95. United States Environmental Protection Agency (EPA), *Municipal Solid Waste Generation, Recycling, and Disposal in the United States: Facts and Figures for 2006.*

96. United States Environmental Protection Agency (EPA), *Municipal Solid Waste Generation, Recycling, and Disposal in the United States: Facts and Figures for 2011.*

97. Caliendo, H., *Plastic waste into fuel: a new form of recycling?* Plastics Today, Available from: http://www.plasticstoday.com/articles/Plastic-waste-into-fuel-a-new-form-of-recycling-0424201202**,** cited: 2012.

98. Harrisson, A.M., *Clinker Microscopy.* Available from: http://www.arthurharrisson.com/clinker%20microscopy.html, cited: 2011.

99. Trezza, M.A. and A.N. Scian, *Burning wastes as an industrial resource: Their effect on Portland cement clinker.* Cement and Concrete Research, 2000. **30**(1): p. 137-144.

100. Trezza, M.A. and A.N. Scian, *Waste fuels: their effect on Portland cement clinker.* Cement and Concrete Research, 2005. **35**(3): p. 438-444.

101. Trovaag, K., *Hazardous Waste Incineration in a Cement Kiln*, in *Hazardous Waste Disposal*, J. Lehman, Editor. 1983, Springer US. p. 201-214.

102. Yousuf, M., et al., *The interfacial chemistry of solidification/stabilization of metals in cement and pozzolanic material systems.* Waste Management, 1995. **15**(2): p. 137-148.

103. Díez, J.M., J. Madrid, and A. Macías, *Characterization of cement-stabilized Cd wastes.* Cement and Concrete Research, 1997. **27**(3): p. 337-343.

104. Madrid, J., J. M. Diez, S. Goiii and A. Marcias, *Durability of Cement Matrices Used for Stabilization of Hazardous Wastes.* Special Publication. **170**.

105. Odler, I. and O. Schmidt, *Structure and Properties of Portland Cement Clinker Doped with Zinc Oxide.* Journal of the American Ceramic Society, 1980. **63**(1-2): p. 13-16.

106. Tashiro, C., et al., *Hardening property of cement mortar adding heavy metal compound and solubility of heavy metal from hardened mortar.* Cement and Concrete Research, 1977. **7**(3): p. 283-290.

107. Newman, J. and B.S. Choo, *Advanced Concrete Technology 3: Processes*. 2003: Elsevier Science.

108. Taylor, H.F.W., *Distribution of sulfate between phases in Portland cement clinkers.* Cement and Concrete Research, 1999. **29**(8): p. 1173-1179.

109. Kolovos, K., S. Tsivilis, and G. Kakali, *Study of clinker dopped with P and S compounds.* Journal of thermal analysis and calorimetry, 2004. **77**(3): p. 759-766.

110. Strunge, J., D. Knoefel, and I. Dreizler, *Influence of alkalis and sulfur on the properties of cement: I, Effect of the SO sub 3 content on the cement properties.* ZKG, Zement-Kalk-Gips, Edition A, 1985. **38**(3): p. 150-8.

111. Strunge, J., D. Knoefel, and I. Dreizler, *Influence of alkalis and sulfur on the properties of cement: III, Influence of alkalis and sulfate on the properties of*

cement, taking account of the alumina ratio and lime standard. ZKG, Zement-Kalk-Gips, Edition A, 1986. **39**(7): p. 380-6.

112. Gies, A., and Knöfel, D., *Influence of Alkalis or the Composition of Belite-Rich Cement and the Technological Properties of the Resulting Cements.* Cemenf and Concrefe Research, 1986. **16**(3): p. 411-422.

113. Gies, A., and Knöfel, D., *Influence of Sulfur on the Composition of Belite-Rich Cement Clinkers and the Technological Properties of the Resulting Cements.* Cement and Concrete Research, 1987. **17**: p. 317-328.

114. Gartner, E.M., *The Effects of Minor and Trace Elements on the Manufacture and Use of Portland Cement*. 1980, Portland Cement Association, Internal report: Skokie, Illinois.

115. Gartner, E.M. and F. Tang, *Formation and properties of high sulfur Portland cement clinkers.* Il Cemento, 1987. **84**.

116. Ghosh, S.N., *Cement and Concrete Science and Technology*. 1991: ABI Books Pvt. Limited.

117. Ha, T.-H., et al., *Effect of unburnt carbon on the corrosion performance of fly ash cement mortar.* Construction and Building Materials, 2005. **19**(7): p. 509-515.

118. Hornain, H., *The Distribution of Transition Elements and Their Influences on Some Properties of Clinker and Cement.* Revue des Materiaux de Construction, France, 1971. **671-672**: p. 203-218.

119. Weisweiler, W. and W. Krcmar, *Heavy metal balances of a cement kiln plant with a grate preheater.* ZKG International, Edition B, 1990. **43**(3): p. 149-52.

120. Moir, G.K., and Glasser, F. P., *Mineralizer, Modifiers and Activators in the Clinkering Process*, in *9th.International Congress of Chemistry of Cement*. 1992: Delhi, India. p. 125-152.

121. Odler, I. and S. Abdul-Maula, *Effect of Mineralizers on the Burning Process of Portland Cement Clinker, Part 1: Kinetics of the Process.* Zemenf-Kalk-Gips, Bauverlg GMBH/Maclean Hunter, 1980(3): p. 132-136.

122. Ifka, T., et al., *Evaluation of P 2 O 5 distribution inside the main clinker minerals by the application of EPMA method.* Cement and Concrete Research, 2014. **59**: p. 147-154.

123. Akstinat, M.H., and Rott, Chr., *Coulometric Determination of Low HalideConcentration in Inorganic Binders and Minerals Raw Materials.* Zement-Kalk-Gips, Bauverlag GMBH/Maclean Hunter, 1988(3): p. 138-143.

124. Saint-Jean, S.J., et al., *Chlorellestadite in the preheater system of cement kilns as an indicator of HCl formation.* Cement and concrete research, 2005. **35**(3): p. 431-437.

125. Klemm, W.A., I. Jawed, and K. Holub, *Effects of calcium fluoride mineralization on silicates and melt formation in portland cement clinker.* Cement and Concrete Research, 1979. **9**(4): p. 489-496.

126. Moir, G., et al., *Improvements in the Early Strength Properties of Portland Cement [and Discussion].* Philosophical Transactions of the Royal Society of London A: Mathematical, Physical and Engineering Sciences, 1983. **310**(1511): p. 127-138.

127. Kakali, G., V. Kasselouri, and G. Parissakis, *Investigation of the effect of Mo, Nb, W and Zr oxides on the formation of Portland cement clinker.* Cement and Concrete Research, 1990. **20**(1): p. 131-138.

128. Bogue, R.H., *Calculation of the Compounds in Portland Cement.* Ind. Eng. Chem. Anal. Ed., 1929. **1**(4): p. 192-197.

129. Taylor, H.F.W., *Modification of the Bogue calculation.* Advances in Cement Research, 1989. **2**(6): p. 73-77.

130. Stutzman, P., et al., *Uncertainty in Bogue-calculated phase composition of hydraulic cements.* Cement and Concrete Research, 2014. **61–62**(0): p. 40-48.

131. Barry, T. I., F. P. Glasser, *Calculations of Portland cement clinkering reactions.* Advances in Cement Research, 2000. **12**(1): p. 19-28.

132. Stutzman, P. and J. R. Clifton, *Specimen Preparation for Scanning Electron Microscopy.* Contribution of the National Institute of Standards and Technology, 1999.

133. Scrivener, K.L., *Backscattered electron imaging of cementitious microstructures: understanding and quantification.* Cement and Concrete Composites, 2004. **26**(8): p. 935-945.

134. Goldstein, J., I., Newbury, D. E., Echlin, P., Joy, D. C., Fiori, C., Lifshin, E., *Scanning electron microscopy and X-ray microanalysis,*. 1981, New York: Plenum Press.

135. Winter, N.B., *Scanning Electron Microscopy of Cement and Concrete*. 2012: WHD Microanalysis.

136. Svinning, K., S. K. Bremseth and Justnes, *X-ray diffraction studies on variations in microstructure in Portland clinker correlated to variations in production in the kiln.* World Cement, 1999. **10**: p. 80-86.

137. Regourd, M., (Barnes, P. ed.), *Crystal Chemistry of Portland cement phases, in Structure and performance of cement.* Applied Science Publishers, London and New York, 1983: p. 128-135.

138. Rietveld, H.M., *A profile refinement method for nuclear and magnetic structures,*. Journal of Applied Crystallography, 1969. **2**: p. 65-71.

139. Neubauer, J., H.-J. Kuzel and R. Siber, *Rietveld quantitative XRD analysis of Portland cement: Part II. Quantification of Synthetic and Technical Portland cement clinkers.* Proceedings of the 18th International Conference on cement microscopy, Houston, 1996: p. 100-111.

140. Neubauer, J., H. Pöllmann, and H. W. Meyer, *Quantitative X-ray analysis of OPC clinker by Rietveld refinement.* Proceedings of the 10th International Congress on the Chemistry of Cement, Gothenburg, 1997. **3**.

141. *Modern techniques used in the industry for quality control of cement.* European Cement Research Academy (ECRA) newsletter, 2014. **1**.

142. Scrivener, K., et al., *Quantitative study of Portland cement hydration by X-ray diffraction/Rietveld analysis and independent methods.* Cement and Concrete Research, 2004. **34**(9): p. 1541-1547.

143. Stutzman, P. and S. Leigh, *Phase composition Analysis of the NIST reference clinkers by optical microscopy and X-ray powder diffraction.* NIST Technical Note 1441, Washington, 2002.

144. *The Rietveld Method,* Available from:http://home.wxs.nl/~rietv025/, cited: 2015.

145. Reed, J.S., *Principles of ceramics processing.* 1995.

146. Maso, J., *Interfacial transition zone in concrete*. Vol. 11. 2004: CRC Press.

147. Taylor, H.F.W., C. Famy, and K. Scrivener, *Delayed ettringite formation.* Cement and concrete research, 2001. **31**(5): p. 683-693.

148. Comité Européene de Normalisation, *Cement–Part 1: Composition, specification and conformity criteria for common cements.* European Standard EN, 2000: p. 197-1.